Rift basins of the central LaHave Platform, offshore Nova Scotia

Mark E. Deptuck* and Brian Altheim

Canada-Nova Scotia Offshore Petroleum Board, 8th Floor TD Centre, 1791 Barrington Street, Halifax, Nova Scotia, B3J 3K9, Canada; *Corresponding author - mdeptuck@cnsopb.ns.ca

Abstract

This study provides an overview of the structure and fill of ten separate rift basins that underlie the central Scotian Shelf and Slope. All basins developed above decoupled continental crust, each flanked by important border faults that sole into multi-tiered mid-crustal shear zones that separate brittle upper crust from ductile lower to middle crust. Moderately stretched 25-30 km thick crust underpins the landward study area (proximal domain), thinning abruptly to 10-15 km thick in the seaward study area (necking domain). Individual rift basins range from <45 to >160 km long, are up to 40 km wide, and contain up to 6 km of strata. Basins are dominantly half-graben and are flanked mainly by landward-dipping border faults with opposing heavily eroded hinged margins; only two are true grabens. Four wells calibrate portions of the fill in two of these basins. Sambro I-29 penetrating a sharply truncated and incomplete lower synrift succession in the Emerald Graben, composed mainly of poorly dated mixed-grade red beds. Glooscap C-63, Moheida P-15, and Mohican I-100 penetrate an incomplete upper synrift succession in the Mohican Graben composed mainly of late Norian to Rhaetian (Weston et al. 2012) halite or red fine-grained dolomitic siliciclastics, or some combination of the two. One well (Glooscap C-63) also penetrated interpreted CAMP volcanics that, on the basis of seismic jump correlations, are present locally in six of the rift basins, heavily eroded along the postrift unconformity. This study also documents, for the first time, a potential pre-rift succession that underpins parts of the Oneida Graben.

1 Introduction and geological setting

Most of our knowledge about Nova Scotia's pre-Quaternary offshore geology comes from the extrapolation of onshore geology combined with the study of offshore reflection seismic profiles and borehole data collected for the purpose of hydrocarbon exploration. Bedrock encountered in a number of offshore wells is consistent with onshore Paleozoic rocks that make up mainland Nova Scotia, emplaced during late Paleozoic Appalachian compressional or transpressional tectonics as Pangea was assembled (Pe-Piper and Jansa 1999; Waldron et al. 2015). More recent reactivation of pre-existing fabrics within these basement rocks took place in the early Mesozoic as Pangea fragmented under a dominantly extensional to transtensional tectonic regime. This produced a series of rift basins strongly aligned with these Paleozoic fabrics (Figure 1). Triassic and Lower Jurassic strata exposed in cliffs around the edges of the Fundy Basin record this event (e.g. Olsen 1997; Leleu et al. 2009; Leleu and Hartley 2010). Lithospheric extension eventually gave way to seafloor spreading as oceanic crust accreted along the mid - Atlantic Ridge (Klitgord and Schouten 1986; Swanson 1986; Schlische et al. 2003).

Offshore borehole and reflection seismic data-sets acquired since the late 1960s provided the foundation for a number of regional studies describing the post-Paleozoic structural and stratigraphic development of Nova Scotia's Atlantic margin (e.g. McIver 1972; Jansa and Wade 1975; Given 1977; Holser et al. 1988; Welsink et al. 1989; Wade and MacLean 1990; Fensome et al. 2008; OETR 2011; Weston et al. 2012; Deptuck and Campbell 2012; Campbell et al. 2015; Deptuck and Kendell, 2017). Data coverage across the outer shelf and slope is seemingly widespread (Figure 2), but data quality is unevenly distributed. For example, 3D seismic data-sets are heavily biased towards the slope and in areas where hydrocarbons were discovered in the Sable Subbasin. Likewise, although wildcat exploration wells were widely distributed during the earliest exploration cycle in the 1970s, the discovery of the Venture gas and condensate field by Mobil and partners in 1979 caused drilling to shift almost exclusively to test deep rollover anticlines in the Sable Subbasin, geographically skewing much of the subsequent borehole calibration. As such,

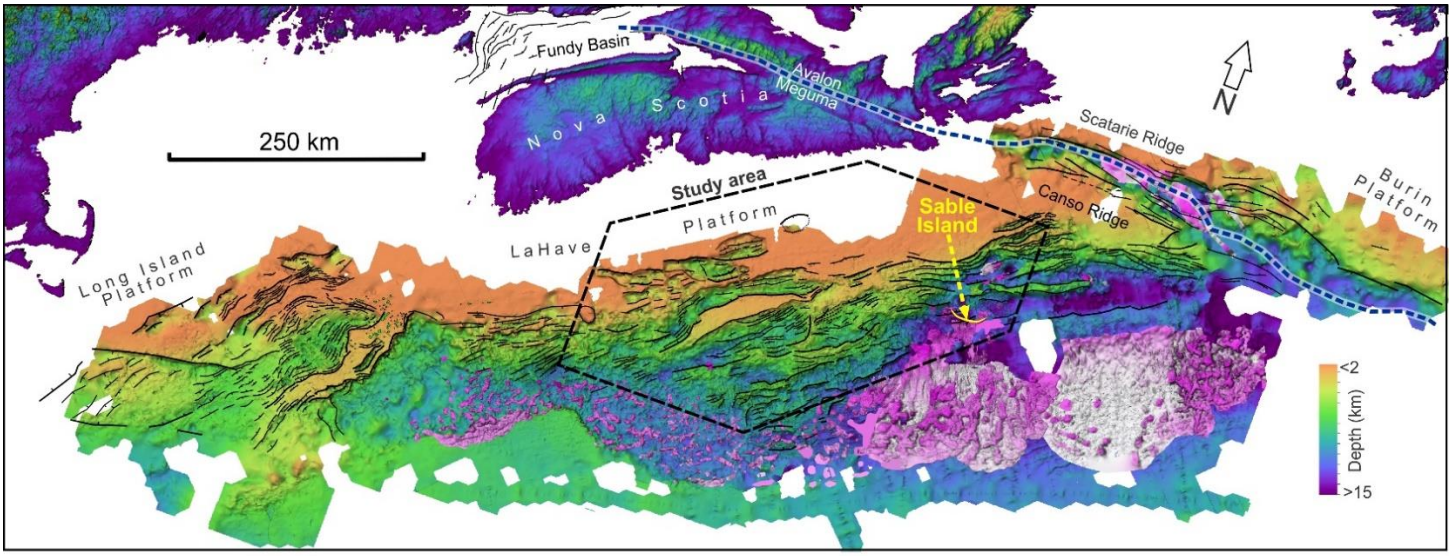

Figure 1 Map of the Scotian margin showing the top basement structure, overlain by basement faults (black) and allochthonous salt bodies (pink). Blue dashed line shows boundary between the Avalon and Meguma terranes, and the black dashed line shows the location of the study area on the central LaHave Platform. Land topography scaled from 0 m (blue) to 500 m (red). Gridded basement and top salt surfaces adapted from Deptuck and Kendell (2017). Faults in the Fundy Basin from Wade et al. (1996).

not all areas of the offshore have been studied equally, reflecting the anisotropy in data quality/availability and historical perceptions about hydrocarbon potential.

This study focuses on a 40 000 km^2 region of the central Lahave Platform that underpins the Scotian Shelf, mainly west of the more heavily explored Sable Subbasin (Figures 1, 2). There are three notable early Mesozoic geological features here:

(i) *Rift basins* - A series of poorly-calibrated continental to marginal marine synrift basins developed above Paleozoic crystalline basement in response to Middle Triassic to Early Jurassic lithospheric extension between Nova Scotia and Morocco;

(ii) *Carbonate Bank* - A widespread carbonate bank with a well-developed bank edge/reef margin and steep foreslope developed in the Middle to Late Jurassic as the western margin of the young Atlantic Ocean thermally subsided;

(iii) *Sable Delta* – An increase in siliciclastic influx in the latest Jurassic to mid-Cretaceous took place as river systems built out adjacent to and eventually across the carbonate bank, burying the bank edge in the eastern study area in the Tithonian and the western study area by the Albian.

Both the Jurassic carbonate bank (corresponding to the Abenaki Formation; Figure 3) and the uppermost Jurassic to mid-Cretaceous fluvial-deltaic clastics that eventually prograded over it (Missisauga and Logan Canyon formations; Figure 3) have been described in detail in a number of studies (e.g. Eliuk 1978; Welsink et al. 1989; Wade and MacLean 1990; Wierzbicki et al. 2002; Piper et al. 2004; Cummings and Arnott 2005; Kidston et al. 2005; Cummings et al. 2006; Deptuck 2008; OETR 2011; Piper et al. 2012; Qayyum et al. 2015), in part because these stratigraphic units contain known hydrocarbon-bearing reservoirs. In contrast, despite accounting for more than half the total stratigraphic thickness on the LaHave Platform (compare Figure 4a and 4b), relatively little work has been published on the Upper Triassic to Lower Jurassic synrift succession beneath the central Scotian Shelf. The stratigraphic succession in Figure 4a records the break-up of Pangea and early separation of Nova Scotia from Morocco, and as such is important for understanding how the early Atlantic Scotian margin developed. We are not aware of any detailed studies of the rift basins that underpin the central LaHave Platfrom beyond mapping of border faults by Wade and MacLean (1990) and cursory results presented by Welsink et al. (1989), Deptuck et al. (2015) and Deptuck and Kendell (2017). In part, this is a consequence of limited exploration interest in this region over the past three decades, and resulting dearth of good-quality reflection

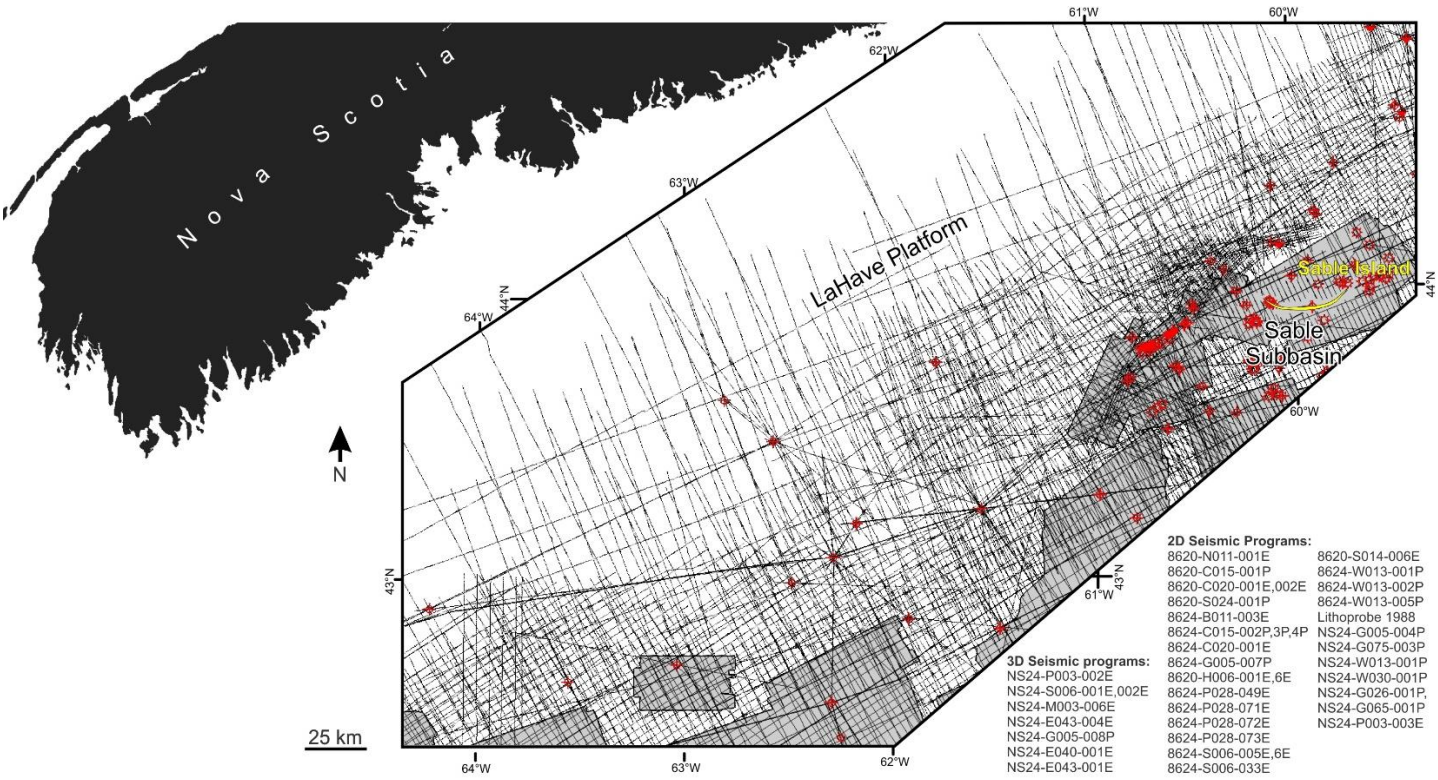

Figure 2 Map showing seismic data coverage across the study area. 3D seismic volumes shaded in grey. Tables show list of CNSOPB program numbers for seismic programs covering the LaHave Platform. Wells shown in red. The main study area is located west of the Sable Subbasin. Figure 6a identifies the key wells used in this study.

seismic profiles and wells to calibrate their fill.

To help bridge this gap, we have assembled and interpreted all available reflection seismic data-sets collected over the past five decades – including those archived only on paper or microfiche – in an attempt to build a robust multi-vintage data-set with the most complete coverage possible across the central LaHave Platform (Figure 2). Despite significant data-quality limitations, a number of seismic surfaces were confidently correlated across the study area, as were a large number of basement-involved faults, enabling us to produce a series of isopach maps calibrated to a handful of wells, and to establish a detailed fault framework for the study area. This study aims to address some of the basic, first-order questions about these rift basins. How many rift basins are there and how much sediment do they contain? What are their dimensions and structure? Are there regional variations in their structural style or patterns in their fill? The results provide insight into broad-scale pre-, syn-, and postrift structural and stratigraphic development of the central LaHave Platform and more generally help elucidate how the proximal margin evolved during lithospheric necking. These results can also be used as a starting point for evaluating the exploration potential (and challenges) of the platform's rift system.

2 Data-set and approach

To study the seismic stratigraphy of the central LaHave Platform, we compiled an extensive suite of analogue and digital 2D seismic surveys from more than 26 seismic programs collected between 1969 and 2001 (Figures 2, 3). The seismic database comprises more than 75 000 line kilometers of data. Some surveys are only available on paper or from microfiche, and were scanned and vectorized in-house and loaded into a digital workstation environment. Data quality varies substantially from barely useable to good. A mistie analysis was attempted, using a relatively modern 2D survey as a baseline reference (CNSOPB program number NS24-W30-1P), but some misties were unavoidable (generally smaller than 20 ms). Despite wide variations in data acquisition parameters, phase normalization was not attempted because of widely varying image quality and vectorization results. There were also several instances where errors in the navigation files were identified, and old shot-point maps and major geological features mapped on intersecting seismic profiles (like basement

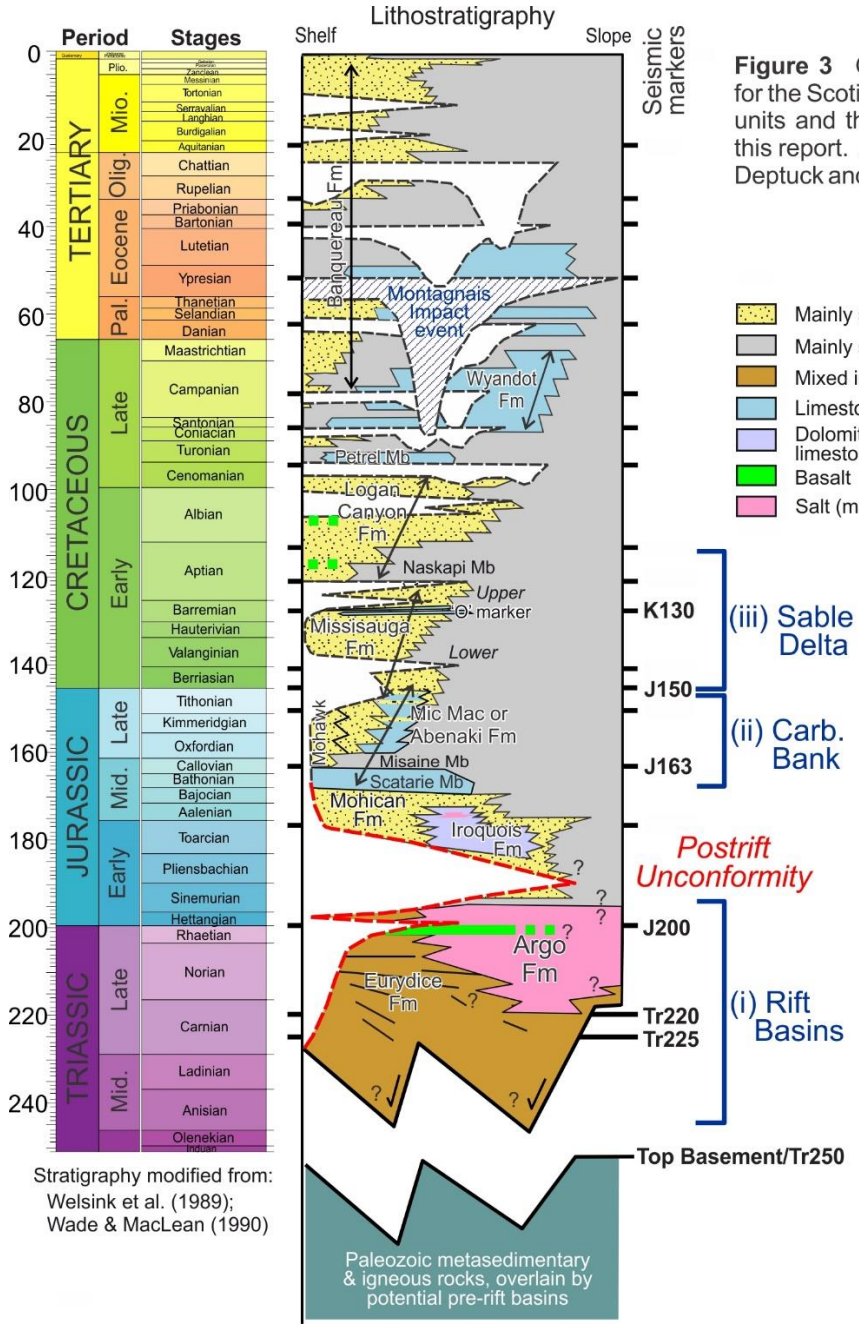

Figure 3 General litho-chronostratigraphic chart for the Scotian Basin, showing the lithostratigraphic units and the main seismic markers discussed in this report. Adapted from Weston et al. (2012) and Deptuck and Campbell (2012).

border faults, basement highs, the edge of the carbonate bank or the modern continental shelf edge) were used to reconcile such situations. It is possible that navigation inaccuracies remain on some profiles, but errors are likely to be less than 500 m.

Seismic interpretation was undertaken using Petrel™ software, with time-depth relationships derived from 20 wells using checkshot surveys to calibrate sonic logs and through generation of synthetic seismograms. Building on the seismic stratigraphic framework proposed in earlier work (e.g. Deptuck 2008; OETR 2011; Weston et al. 2012; Kendell et al. 2013; Deptuck et al. 2014), thirteen regional surfaces were correlated across the study area (Figure 2), and a detailed fault-framework was built in Petrel™. The most important basement-offsetting faults are shown in Figure 5. A four-layer velocity model (water column, seabed to J150, J150 to J163 and J163 to Top Basement) was built for conversion of interpreted surfaces into depth, using time-depth relationships from calibrated sonic logs in 17 of the wells (Figure 6a), and using an interval velocity of 4.5 km/s for

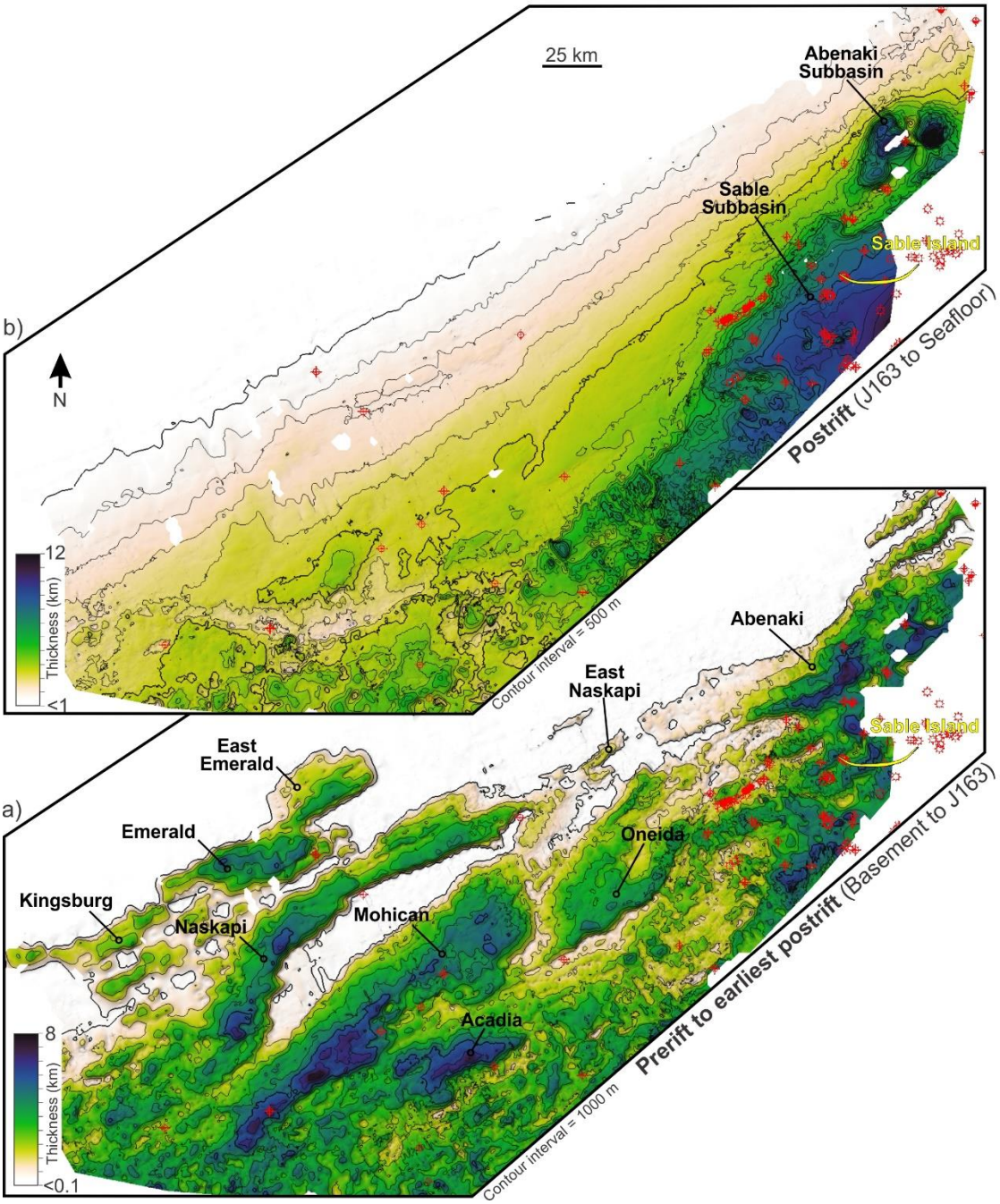

Figure 4 a) Isopach map between top basement and the Bathonian J163 marker, showing distribution of prerift to earliest postrift strata beneath the central Scotian Shelf and Slope. Isopach dominantly reflects the location of Triassic to earliest Jurassic synrift sedimentary basins; **b)** Isopach map between the J163 marker and the seafloor, showing substantially different distribution of postrift strata, where most sedimentation was focused in the Abenaki and Sable Subbasins. Most of the drilling activity has taken place in these younger sedimentary basins. Wells shown in red.

the sparsely penetrated Lower Jurassic and older successions below the J163 marker.

Most of the wells in Figures 2 and 4 strongly cluster along the eastern edge of the study area, near or in the proven Sable Subbasin. Nine wells are scattered above the LaHave Platform, west of the Sable Subbasin (Figure 6a). They are widely-spaced, and seven of them were spudded prior to 1978 during Nova Scotia's earliest offshore exploration cycle more than 40 years ago. All but four of these wells targeted Middle Jurassic or younger stratigraphic intervals.

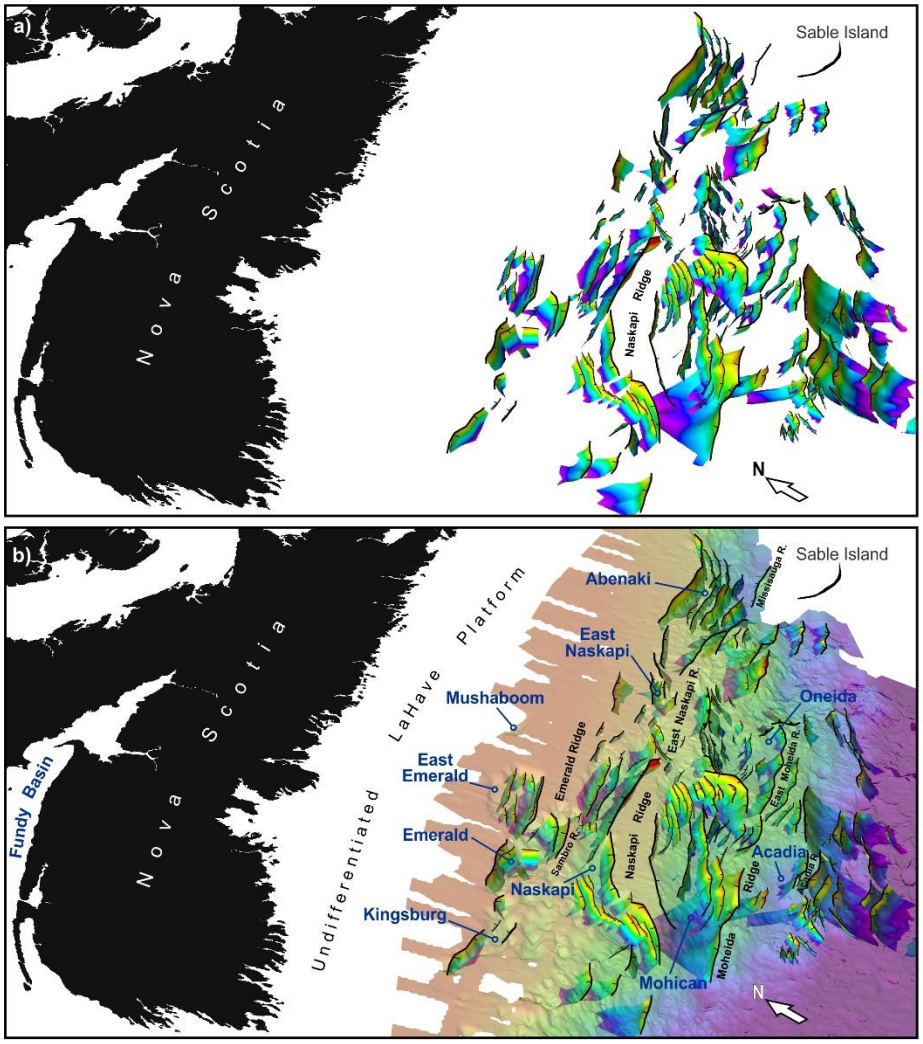

Figure 5 a) Perspective-view (from south-west) visualization of the basement fault framework built for this project. Many of the large border faults sole into mid-crustal shear zones. **b)** Annotated version of (a) showing transparent top basement surface. Grabens discussed in this report are labelled in blue. Basement highs are labelled in black.

3 Seismic surfaces and structure maps

We correlated thirteen regional to sub-regional seismic markers throughout the study area, as well as a number of more local markers. The most important markers for this study lie within Lower Cretaceous and older strata (Figure 3). Figures 7 through 12 show depth structure maps of these surfaces. The **Top Basement** marker is the deepest surface interpreted (Figures 1, 7a, b), corresponding to the top of Cambrian-Ordovician Meguma metasedimentary rocks and associated Devonian plutonic rocks that intrude them (calibrated at Naskapi N-30 and Ojibwa E-07, respectively) (Pe-Piper and Jansa 1999). It forms a moderate to high amplitude reflection where overlain by thin, young cover strata, but commonly produces little or no seismic reflection where overlain by older (pre-Middle Jurassic), higher impedance strata. In such areas, we carried "top basement" along the interpreted base of layered cover strata, guided in part by the fault framework shown in Figure 5. In some areas – particularly beneath the thickest parts of rift basins – the exact placement of this marker has a high degree of uncertainty.

In the central study area, a prominent angular unconformity (**Tr250**) separates an older prerift(?) layered and heavily folded stratigraphic succession from younger synrift strata. No wells penetrate Tr250 and the marker cannot be projected with confidence beyond the Oneida Graben (Figure 7a). The unconformity probably formed in the Late Paleozoic during the final assembly of Pangea (discussed later). We correlated three markers (Tr225, Tr220, and J200; Figure 3) through the fill of a number of Triassic rift basins that underpin the study area (Figures 5a, 7a). To produce more regionally extensive surfaces and thickness maps, each of these markers

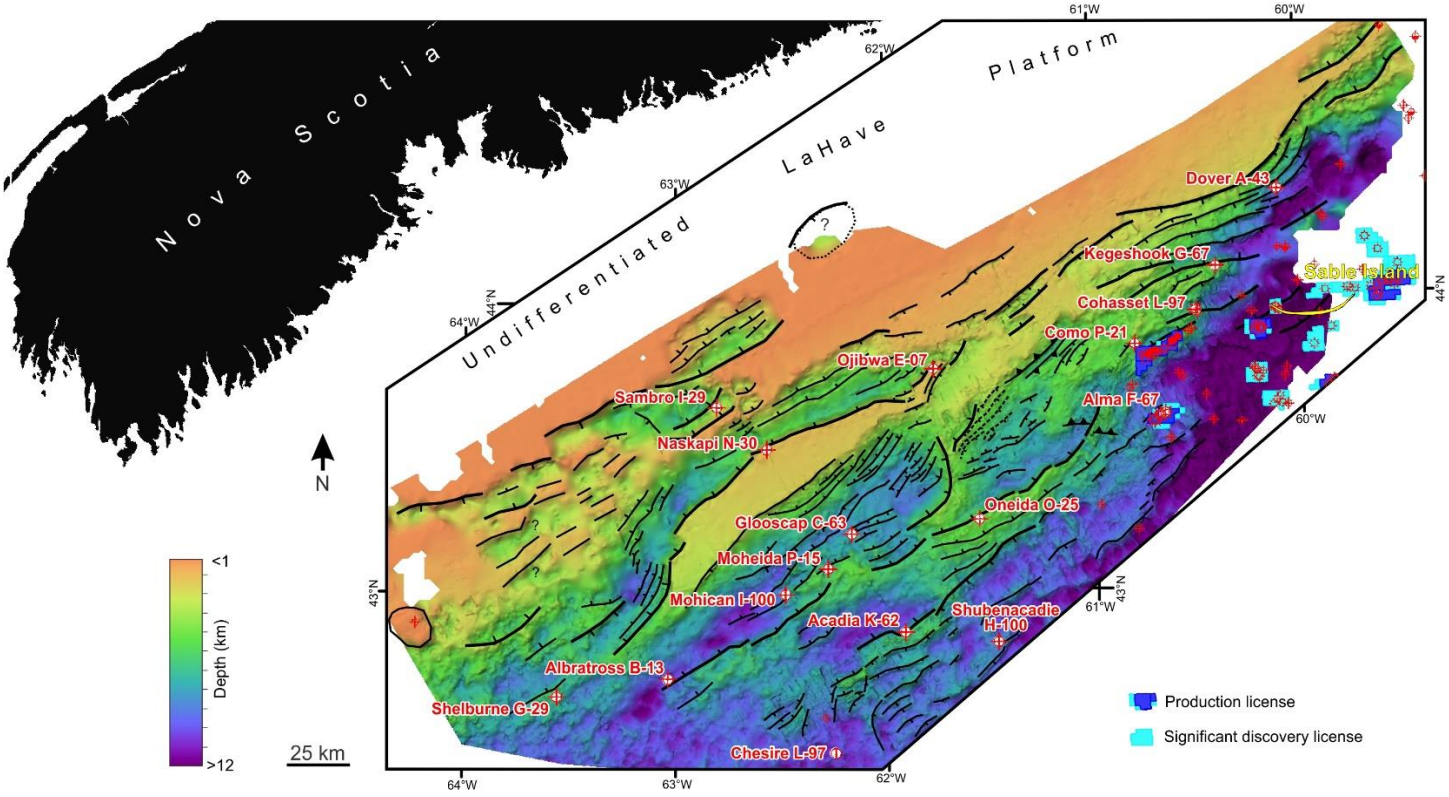

Figure 6a Top basement structure map showing location of key wells used for calibration and the generation of the velocity model in this study. Also shown are the production and significant discovery licences in the Sable Subbasin.

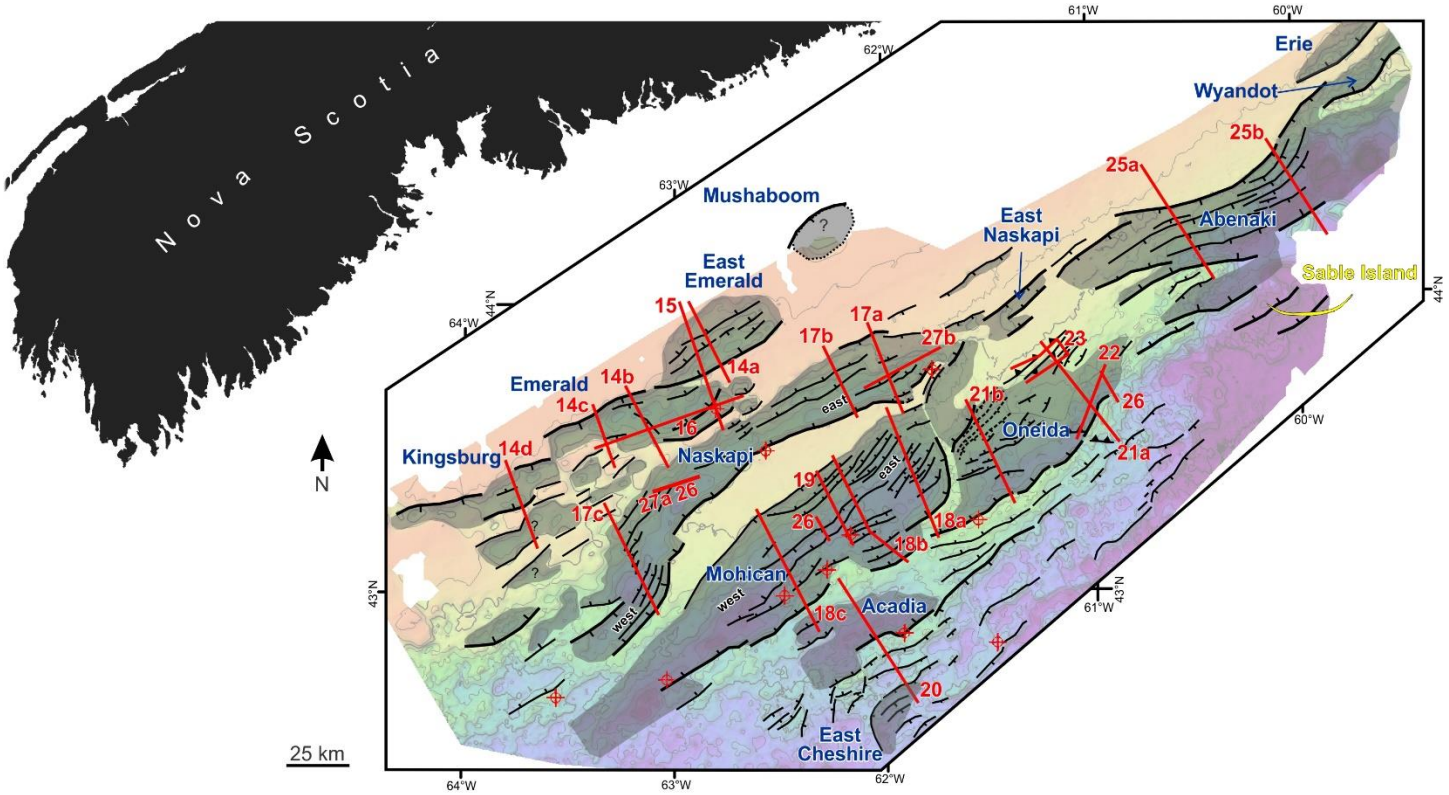

Figure 6b Map showing location of seismic profiles shown in this report.

was merged with the younger postrift unconformity that, at different locations, truncates them.

The **Tr225** marker (Figure 8) is a bright amplitude roughly mid-synrift reflection that separates the landward rift basins (East Emerald, Emerald, Kingsburg, Naskapi) into a higher amplitude faulted reflection series below from an overlying generally less reflective interval above. Tr225 could not be correlated with confidence into the distal parts of the Oneida and Mohican grabens, where reflection amplitude diminishes or seismic imaging deteriorates. The slightly shallower **Tr220** marker can be carried more widely across the seaward parts of the study area (within and seaward of the Oneida, Mohican, Acadia, and Abenaki grabens) where it corresponds to a faulted bright amplitude reflection (Figure 8). Erosion of the late synrift interval and loss of reflection character hinders correlation of this marker landward into the Naskapi Graben, however the marker appears to merge with or lie just above Tr225 in the easternmost Nakapi Graben (near the base of a distinctly lower amplitude later synrift interval). Both markers overlap in the landward parts of the Mohican and Oneida grabens, where they form separate diverging markers. In the Mohican Graben, Tr220 defines an approximate base to the Late Triassic primary salt layer, separating folded and more continuous mixed amplitude reflections above (corresponding to bedded salt or a lateral equivalent) from more heavily faulted mixed amplitude reflections below. The Tr220 marker becomes increasingly reflective in the western parts of the Mohican Graben, within the Acadia and Abenaki grabens, and moving into deeper water. It is possible that the marker corresponds to a volcanic or carbonate layer in these locations. No age calibration is available for either of these markers and their names are arbitrary.

The **J200** marker (Figure 9) corresponds to a strong peak-trough doublet reflection that is distinctive and shown at Glooscap C-63 to correspond to the reflection response from a 152 m thick basalt layer emplaced conformably above Late Triassic halite with interbeds of dolomitic shales and siltstones. The strong reflection produced by the basalt is concordant with underlying reflections, does not appear to cross-cut other events, and was jump correlated to the hanging wall in a number of grabens. It probably corresponds to the top of ~200 Ma CAMP-related basaltic lava flows, making it a very important time marker (Figure 3). If correct, J200 separates pre-CAMP strata below from post-CAMP strata above – and approximates a base-Jurassic marker. J200 is difficult to correlate east of the Oneida Graben. Instead, the top of the primary salt layer (a heavily deformed surface due to sediment loading and salt expulsion) was used as a proxy for the J200 surface in the easternmost study area (e.g. in the Abenaki Graben), where the basalt appears to be absent.

The J200 volcanic and the underlying/overlying synrift succession are widely eroded along a complex, time-transgressive surface referred to here and in previous work as the "**postrift unconformity**" (**PU**). In places, PU cuts the top basement, Tr250, Tr225, Tr220, and J200 surfaces, forming a clear angular unconformity (Figure 3). The amount of erosion of Lower Jurassic and older strata below this surface varies, as does the age of Jurassic strata that progressively onlap it. Outside of rift basins, this peneplain surface probably formed through the merger of a number of erosive surfaces that formed before rifting (e.g. erosion of elevated Appalachian topography), in response to the onset of rifting (e.g. local clastics supplied during denudation of the relief immediately adjacent to rift basins), or immediately after continental break-up (e.g. as remnant topography, perhaps influenced by basin inversion, continued to evolve and shed sediment).

The magnitude of erosion along PU generally decreases moving seaward, particularly within the hanging walls of more distal rift basins where the greatest rift accommodation developed and the least amount of post-rift exhumation took place (see also Post and Coleman 2015). In basins like the Oneida Graben (described later), correlation of the PU is difficult as several potential candidate surfaces (both erosive and other discordances like onlap surfaces) splay off the main angular unconformity towards the hanging-wall border fault. We chose to carry the PU marker 'shallow', where it coincides with an onlap surface for interpreted earliest postrift (post-Pliensbachian?) strata. The absence of clear erosion combined with the subtle character of onlapping strata above it, reduces the correlation confidence of PU where rift and earliest postrift accommodation were greatest in these distal rift basins. The overlying early postrift (upper Bathonian or lower Callovian) J163 marker was correlated with more confi-

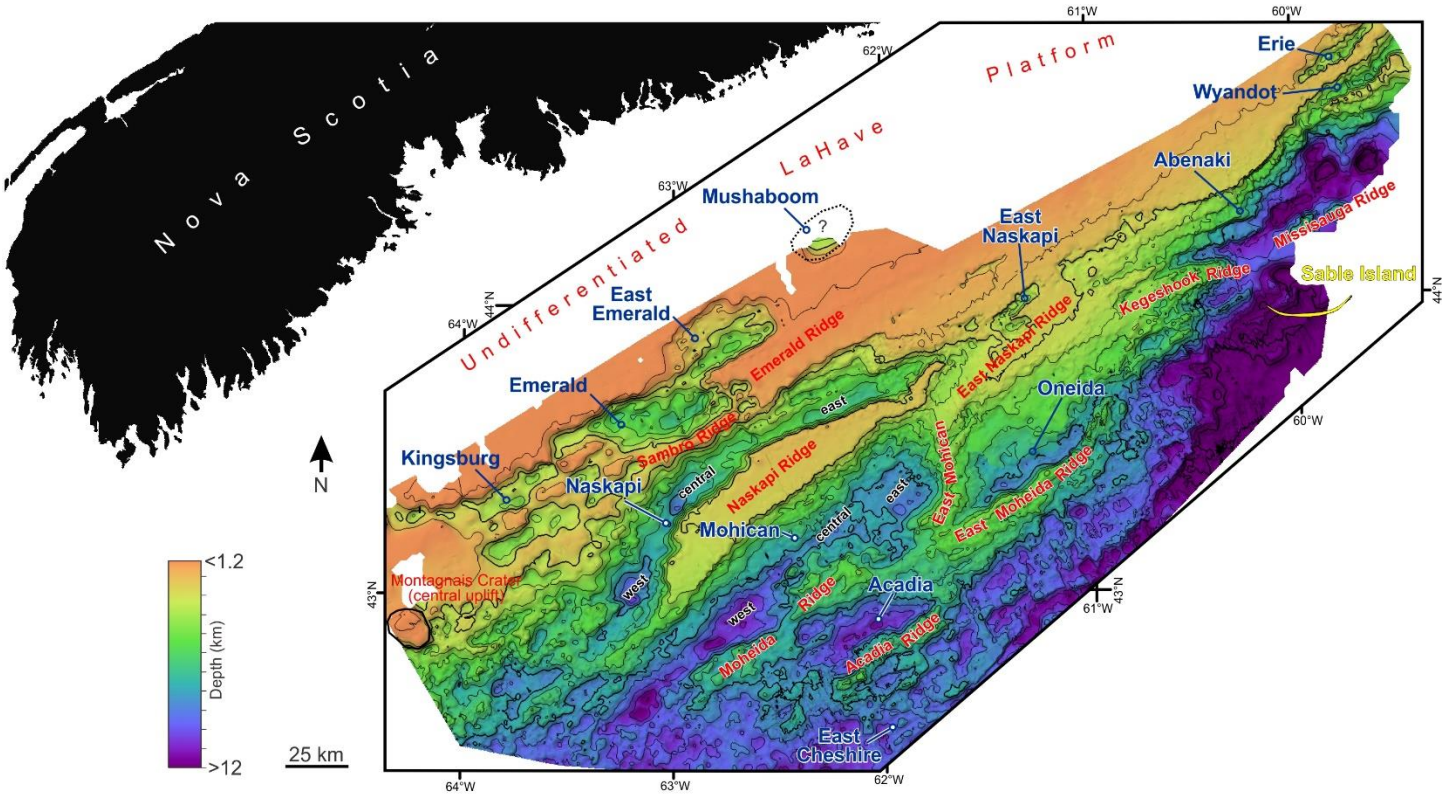

Figure 7a Top basement depth structure map, correlated above the Tr250 unconformity, showing the base of the synrift succession. Synrift grabens shown in blue; positive relief basement elements shown in red. See text for details.

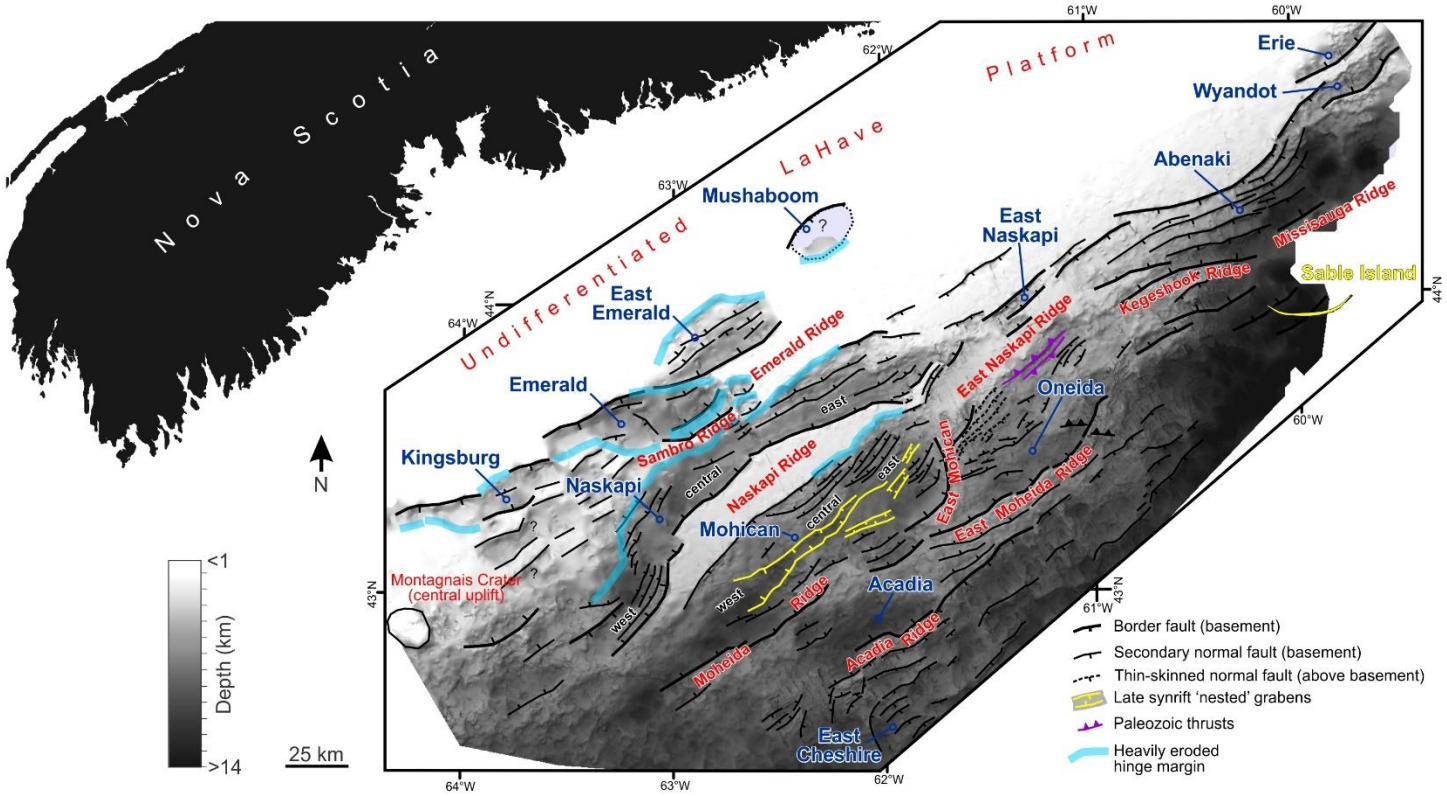

Figure 7b Map of study area showing the top basement depth structure map overlain by the main synrift structural elements that define the central LaHave Platform rift system. Synrift grabens shown in blue; positive relief basement elements shown in red. See text for details.

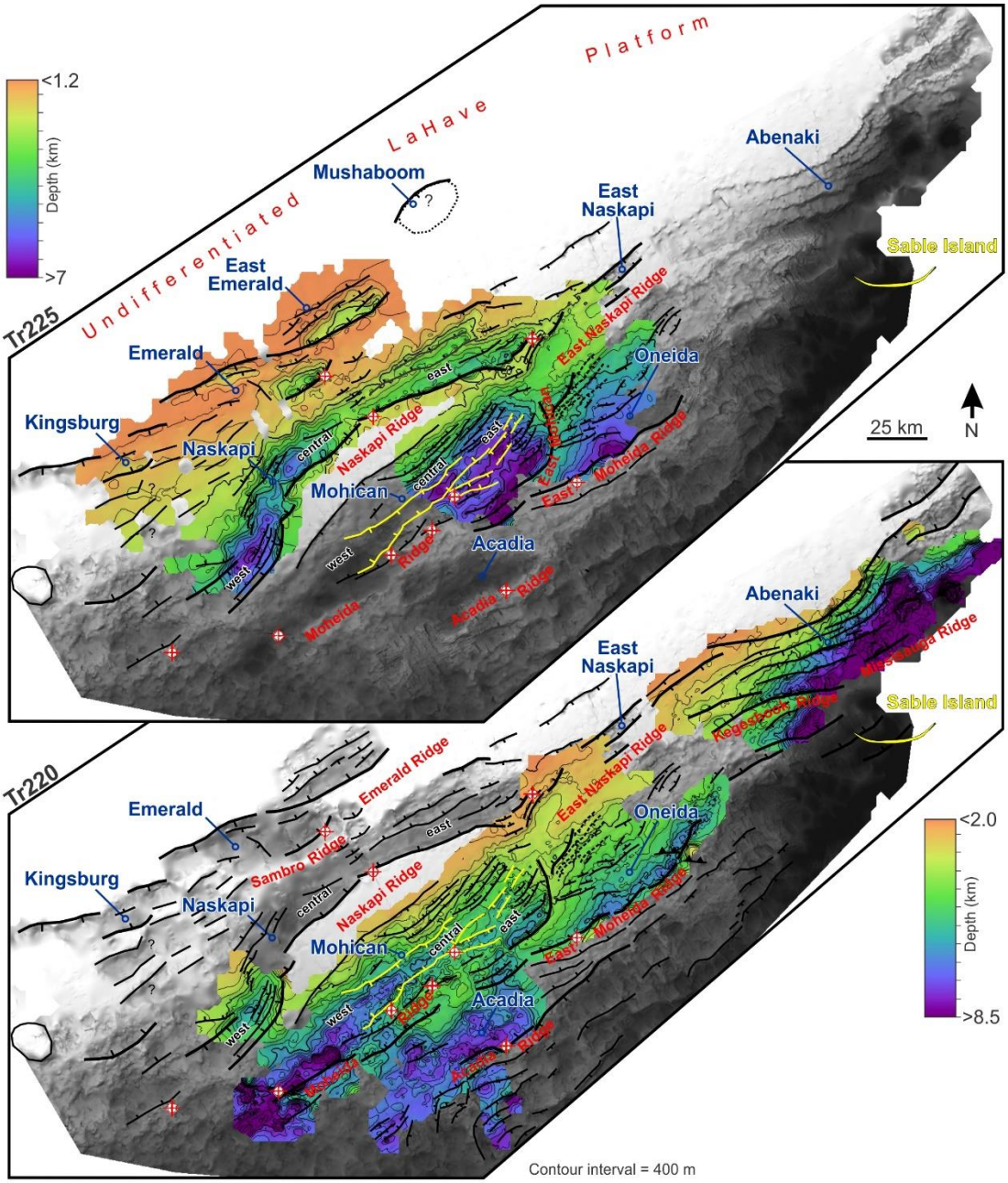

Figure 8 Structure maps of the Tr225 (top) and Tr220 (bottom) markers, correlated through the landward and seaward rift basins, respectively. Underlying greyscale grid is the top basement surface. Tr220 is a slightly younger mid-synrift marker. There is no age calibration for either of these markers. See text for details, and Figure 7b for legend.

dence, and as such is a more accurate surface for generating regional thickness maps.

The **J163** marker (Figure 10) is the first seismic marker that can be correlated regionally above PU. It corresponds to a strong peak immediately inboard the carbonate bank edge, where it commonly forms a downlap surface for subtle overlying clinoforms within the Misaine Member (Abenaki Formation) (Figure 3). The marker is more difficult to correlate landward, where it undergoes several phase shifts likely produced by a combination of lithological changes and tuning effects from stratigraphic thinning of overlying and underlying post-rift strata that onlap the PU. Variations in phase and processing between different vintage seismic programs exacerbate difficulties in marker correlation, but despite these challenges, the J163 surface was correlated with a moderate to high degree of confidence. A number of wells penetrate the marker where it corresponds mainly to the impedance contrast between Misaine shale and hard Scatarie oolitic limestone. The top surface lies with-

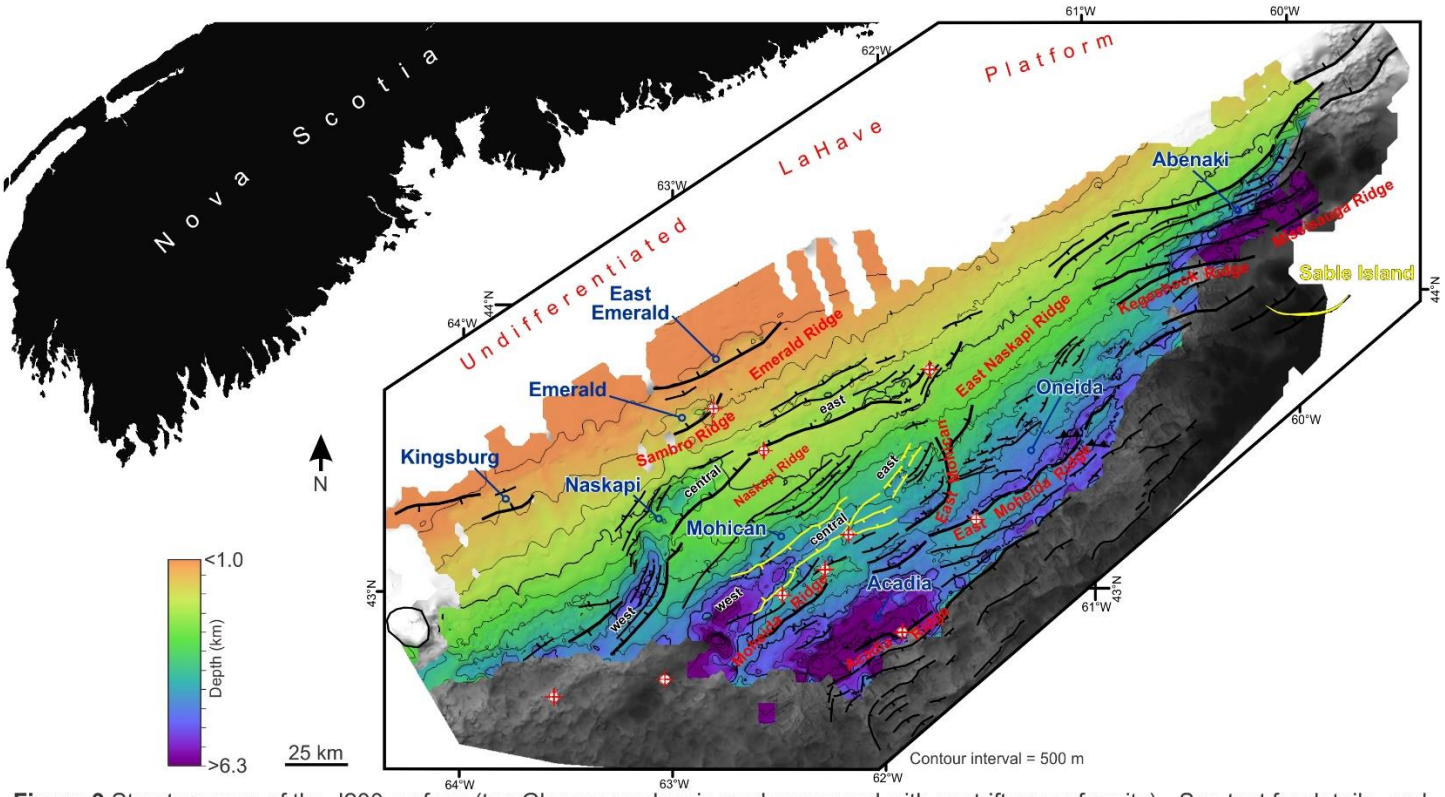

Figure 9 Structure map of the J200 surface (top Glooscap volcanic marker merged with postrift unconformity). See text for details, and Figure 7b for legend.

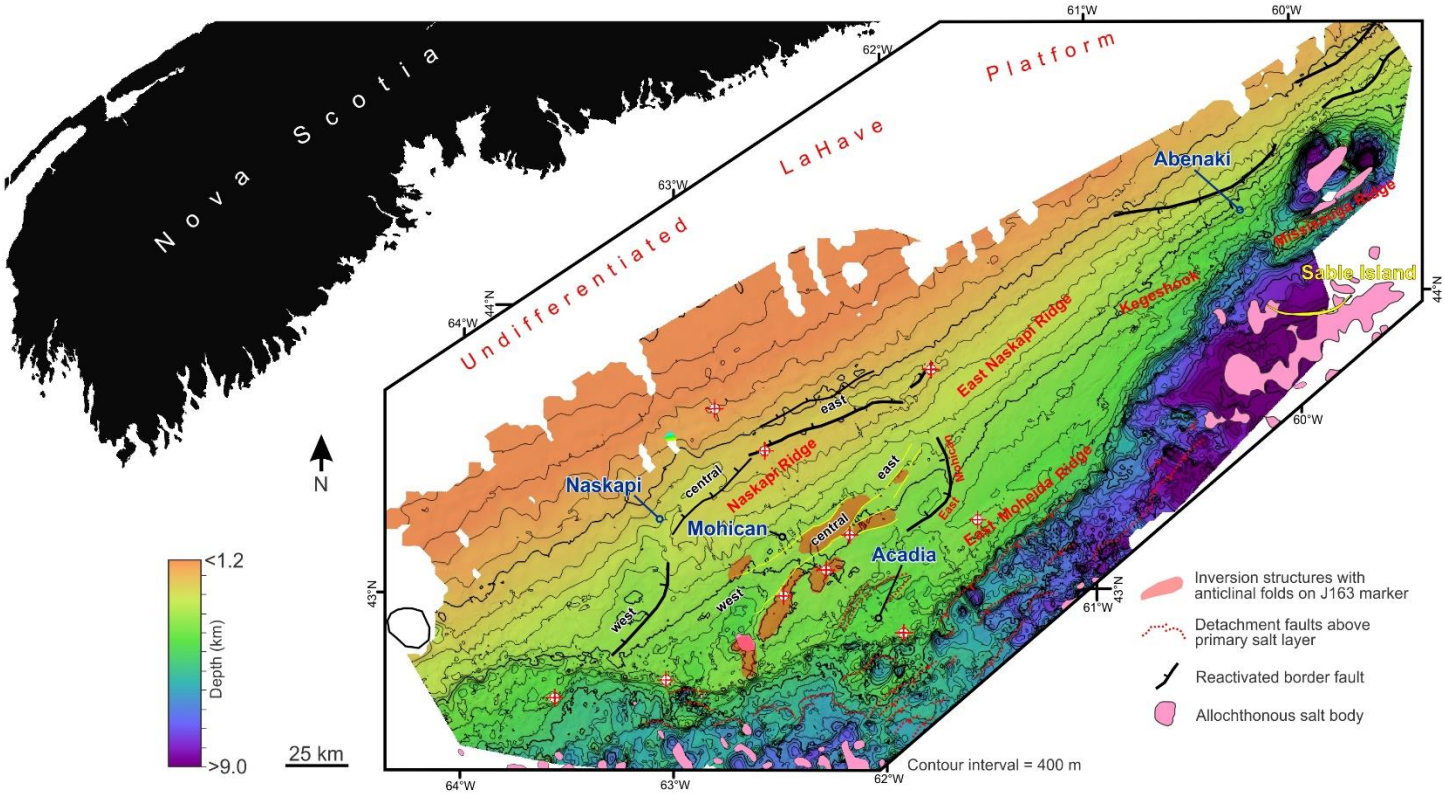

Figure 10 Structure map of the J163 surface. Note the continued subsidence above the central and western parts of the Naskapi and Mohican grabens, as well as the Acadia and Abenaki grabens. A series of prominent to subtle inversion folds are present between the axis and southern margin of the Mohican Graben. Relatively few basement faults are active, but Early to Middle Jurassic cover strata show widespread detachment above the primary salt layer (red dashed faults) in the seaward direction. See text for details. Allochthonous salt bodies from Deptuck and Kendell (2017).

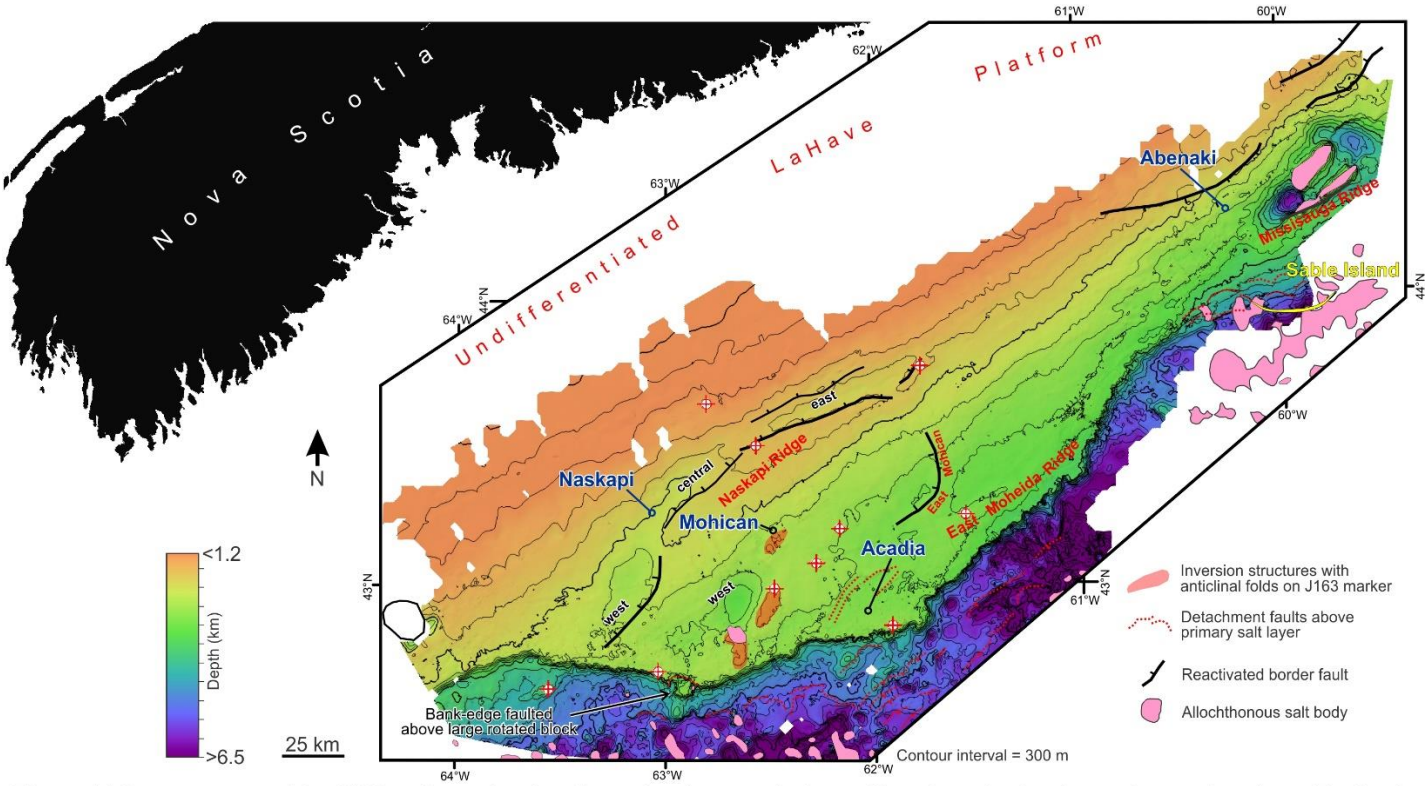

Figure 11 Structure map of the J150 surface, showing rimmed carbonate platform with a sharp bank edge and steep foreslope. The bank edge is less sharp to the east where there was increased siliciclastic input. Note continued subsidence above the central and western parts of the Naskapi and Mohican grabens, and eastern parts of the Abenaki Graben. Relatively few basement faults offset J150, but the outer bank edge detaches above thin-skinned listric faults in the Acadia Graben and a large heavily rotated fragment of the carbonate bank has detached above salt at the mouth of the Mohican Graben. Further seaward there is widespread evidence for detachment of Middle to Upper Jurassic cover strata above the primary salt layer (red dashed faults). Allochthonous salt bodies from Deptuck and Kendell (2017).

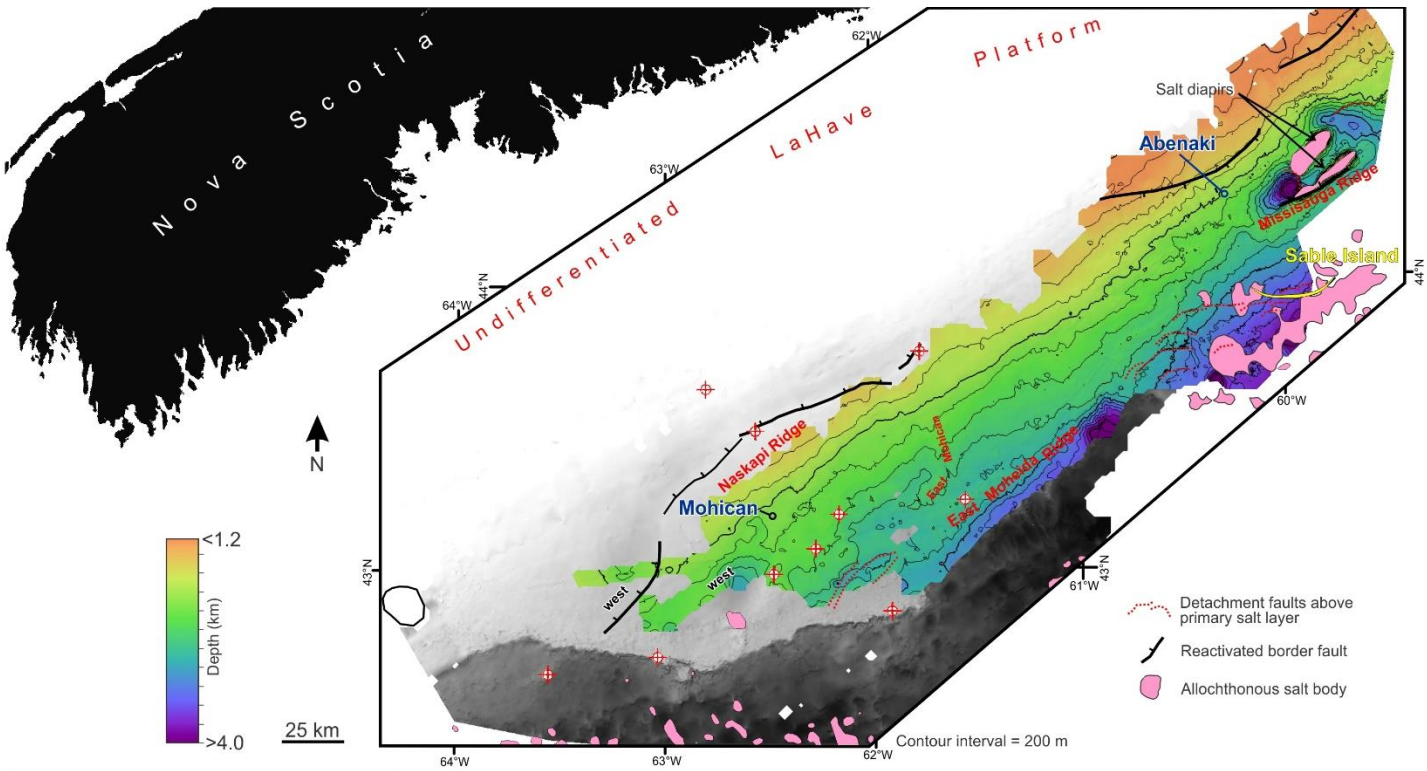

Figure 12 Structure map of the K130 surface, corresponding to the Barremian O-marker that caps Lower to mid Missisauga Formation fluvial-deltaic clastics in the eastern study area, and the top of the Roseway Unit in the western study area (where carbonates continued to accumulate into the Early Cretaceous). Underlying greyscale image is the J150 marker. Surface is offset across a number of listric faults that sole into the primary salt layer in the eastern study area near Sable Island. Allochthonous salt bodies from Deptuck and Kendell (2017).

in upper Bathonian or lower Callovian strata (Weston et al. 2012), and hence J163 is an early postrift marker (Figure 3).

The **J150** marker (Figure 11) is a strong but variable reflection that approximates the top of the Jurassic Abenaki carbonate bank. Like J163, there is no single J150 reflection as the marker merges or diverges both along strike and progressing from the bank edge towards the inner bank. Increased Late Jurassic clastic input from the east in the eastern study area places the J150 surface above siliciclastics of the lowermost Missisauga Formation, where it is difficult to correlate; it lies above carbonates of the Abenaki Formation in the western study area. J150 is a Tithonian marker (Weston et al. 2012) (Figure 3).

The **K130** marker (Figure 12) is a strong peak to trough reflection that defines the top of the lower part of the Missisauga Formation in the eastern study area. Here the reflector is an Hauteriavian oolitic limestone referred to as the O-marker (Wade and MacLean 1990; Weston et al. 2012; Figure 3). In the western study area the K130 marker merges with a peak above a very strong trough corresponding to a marker in the upper parts of the Roseway Unit – a lithologically mixed but condensed lateral equivalent of the Missisauga Formation that developed in areas further removed from siliciclastic sediment input (Wade and MacLean 1990).

4 Pre- and synrift basins of the LaHave Platform

Ten separate rift basins and one candidate prerift basin (described separately) were identified and mapped in the study area (Figures 4, 7; Table 1). Individual rift basins range from <45 to >160 km long and up to 40 km wide, containing as much as 6 km of strata. Figure 13 shows a scaled cross-sectional comparison between type seismic sections across each rift basin. Seven of these basins are restricted to the platform, whereas the axes of the remaining three plunge off the platform either to the southwest (Mohican, Acadia) or to the northeast (Abenaki).

Prominent, heavily eroded and flat-topped basement highs flank both sides of the six landward-most rift basins (Mushaboom, East Emerald, Emerald, Kingsburg, Naskapi, East Naskapi). The same style of basement highs flank two additional rift basins (Mohican and Oneida), but on their landward side only, with much more complicated segmented basement elements composed of rotated fault blocks overlain by synrift strata flanking their seaward sides. One rift basin (Acadia) is flanked on both sides by the latter. Rift basins in the study area are commonly interconnected across synthetic, convergent and divergent accommodation/ transfer zones (*sensu* Morley et al. 1990). Strike-slip offsets mark the boundaries between some rift basins, but more commonly there are intricate fault arrays, flexures (relay zones), and changes in basement topography that, along with changes in bulk sediment thickness, mark the transition from one rift basin to another, without an obvious sharp transfer fault.

In terms of their broad-scale structural style, eight of the ten rift basins are classified as predominantly half graben structures. Their hinged (flexural) margins are heavily eroded, with the opposing border fault margin having increased accommodation and preserving the thickest and youngest graben fill. Landward-dipping (antithetic; towards the northwest) border faults flank five basins (East Emerald, Naskapi, Mohican, Acadia, and Oneida), with a seaward-dipping fault (synthetic; towards the southeast) flanking just one (Mushaboom). Two form hybrids (Kingsburg and Emerald) with border faults (and opposing eroded hinged margins) switching from the landward to the seaward side in the same rift basin. Only two of the basins (Abenaki and East Naskapi) are classified as true grabens with opposing border fault margins over most of their lengths.

In terms of their finer-scale structure and fill, six basins contain numerous internal secondary faults that show a significant amount of mid to late synrift normal slip, and at least four experienced some degree of late synrift to early postrift inversion (Nakapi, Emerald, Mohican and Oneida). Two rift basins are flanked also on one side (Naskapi to the south and Abenaki to the north) by border faults that were recently reactivated, offsetting Late Cretaceous or even younger strata, with strike-slip movement indicated by young transpressional folds. Seismic facies consistent with the Late Triassic salt penetrated at Glooscap C-63 (Mohican Graben) were identified in segments of eight of these rift basins, three of which (Mohican, Acadia, and Abenaki) also contain salt diapirs along their seaward-plunging peripheries. CAMP-related volcanics (also calibrated at Glooscap C-63) were

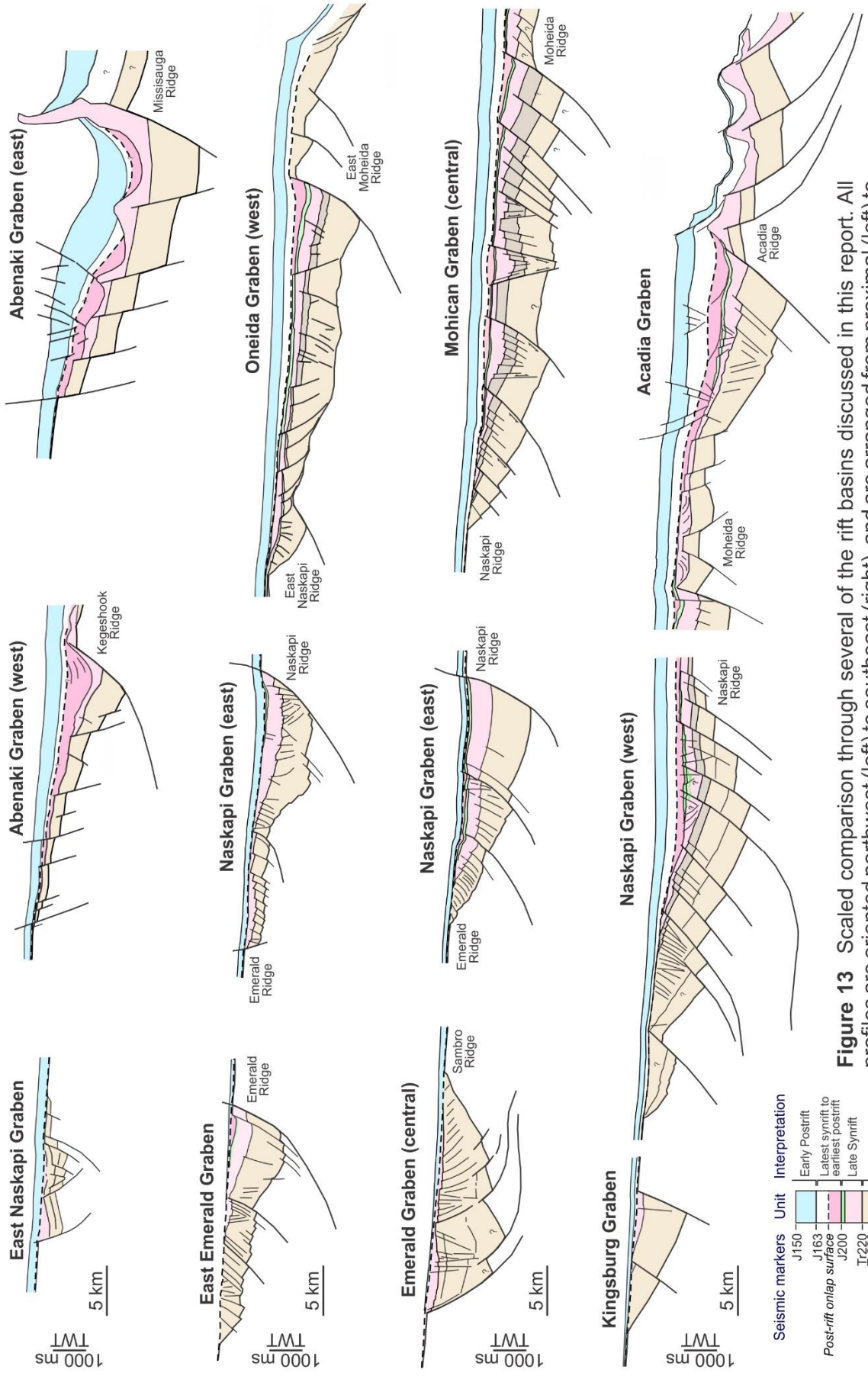

Figure 13 Scaled comparison through several of the rift basins discussed in this report. All profiles are oriented northwest (left) to southeast (right), and are arranged from proximal (left) to distal (right) and generally from the eastern study area (top) to the western study area (bottom). Vertical exaggeration is roughly 1.5:1 at 4.5 km/s.

Table 1 – Rift basins of the central LaHave Platform

Rift Basin Name	*Length*	*Width (max)*	*Thickness (max)*[1]	*Style (border fault dip direction)*	*Structural domain*[2]	*Landward (L)/seaward (S) basement elements*	*Indications of inversion (timing)*	*Data-quality/ interp. confidence*
1. Mushaboom	*<??*	*?*	>?	Half graben (SE)	Proximal	Undiff. LaHave Platform (L, S)	?	Very Low*
2. East Emerald	46 km	25 km	1.9s (twt)/ 4.5 km	Half graben (NW)	Proximal	Undiff. LaHave Platform (L), Emerald Ridge (S)	Minor reverse faults	Low to Moderate
3. Emerald	73 km	25 km	2.05s (twt)/ 4.6 km*	Overlapping convergent half-graben (NW and SE)**	Proximal	Undiff. LaHave Platform (L), Sambro Ridge (S)	Folded/truncated strata above Sambro rider block (late synrift to early postrift?)	Low to Moderate
4. Kingsburg*	68 km	15 km	1.5s (twt)/ 3.3 km	Half graben (NW and SE)*	Proximal	Undiff. LaHave Platform (L), unnamed (S)	?	Very Low
5. Naskapi	168 km	26 km	2.0s (twt)/ 4.5 km	Half graben (NW)*	-	-	-	-
East	79 km	26 km	-	-	Proximal	Emerald Ridge (L), Naskapi Ridge (S)	Minor folding and reverse motion along secondary faults (late synrift to early postrift); late transpressional folds along border fault (post-Cretaceous)	Moderate to High
Central	51 km	20 km	-	-	Proximal	Sambro Ridge (L), Naskapi Ridge (S)		Moderate
West	58 km	25 km	-	-	Proximal to Necking	Unnamed Ridge (L), Naskapi Ridge (S)		Low
6. Mohican	145 km	46 km	2.25s (twt)/ 5.0 km	Half graben (NW)	-	-		-
East	*	*	*	-	Proximal	Naskapi Ridge (L), Moheida/ East Moheida ridges (S)	Subtle inversion above 'nested grabens' (early postrift)	Moderate to High
Central	*	*	*	-	Proximal	Naskapi Ridge (L), Moheida Ridge (S)*	Clear inversion folds above 'nested grabens' (early postrift)	Moderate
West	*	*	*	-	Necking	Naskapi Ridge (L), Moheida Ridge (S)*	Clear reverser faults and inversion-related folds (early postrift)	Low to Moderate
7. Acadia	52 km	19 km	2.1s (twt)/ 4.7 km	Half graben (NW)	Necking	Moheida Ridge (L), Acadia Ridge (S)	None recognized	Low to Moderate
8. Oneida	95 km	40 km	1.8s (twt)/ 4.0 km	Half graben (NW)	Proximal to Necking	East Naskapi Ridge (L), East Moheida Ridge (S)	Inversion folds and reverse faults (late synrift or early postrift); post-inversion angular unc.	Low to High
9. East Naskapi	35 km	13 km	1.0s (twt)/ 2.3 km	Graben	Proximal	Undiff. LaHave Platform (L), East Naskapi Ridge (S)	?	Low to Moderate
10. Abenaki	120 km	35 km	>1.5s (twt)/ 3.4 km	Graben*	Proximal to Necking	Undiff. LaHave Platform (L), Kegeshook/Missisauga ridges (S)	Uncertain; masked by salt tectonics?	Low to Moderate

Rift Basin Name	*Salt-bearing*[3]	*Salt deformation style*	*CAMP? (LC/XC)*[4]	*Well calibration*	*Oldest strata penetrated*	*Probable age of strata above PU*	*Comments*
1. Mushaboom	?	-	?	No	-		*Partially imaged on only one profile (seaward part; hinged-margin)
2. East Emerald	Probable	Folded	LC	No	-		
3. Emerald	Probable	Folded	LC	Sambro I-29	M.(?) or U. Triassic?	U. Jurassic? or Lower Cretac. ***highly condensed	*Position of top basement highly uncertain; **although the total thickness below Tr225 shows one depocenter, shallower intervals indicate Emerald Graben comprises two separated half-grabens with opposing border faults
4. Kingsburg	No	-	None identified	No	-		*Overall structure really a series of alternating slightly laterally offset landward and seaward verging half grabens; heavily eroded and top basement correlated with low confidence
5. Naskapi	Probable	-	-	No	-		*Segmented into three left-stepping depocentres
East	?		LC	-	-		
Central	Probable	Folded	LC	-	-		
West	?		LC, XC	-	-		
6. Mohican	Yes	-	-	Yes	-		*Boundaries between the East, Central, and West segments only loosely defined
East	Probable	Folded	LC	No	-		
Central	Yes	Folded	LC	Glooscap C-63 Mohican I-100 Moheida P-15	Late Norian to Rhaetian** U. Triassic U. Triassic	Late Bathonian or older** " "	*Top basement correlated with low to moderate degree of confidence **Weston et al. (2012)
West	Yes	Diapiric and detached cover strata	LC, XC	No			*Top basement correlated with low degree of confidence; some folding potentially related to an igneous intrusion beneath salt layer
7. Acadia	Yes	Diapiric and detached cover strata	LC, XC	Acadia K-62	Bajocian?	Bajocian?	
8. Oneida	Probable	Folded	LC, XC	Oneida 0-25	Bajocian?	Bajocian or older?	*Underpinned by Ojibwa pre-rift basin
9. East Naskapi	No	-	None identified				
10. Abenaki	Yes	Diapiric and detached cover strata	None identified	Cohasset L-97	Bajocian*	Bajocian or older	*Weston et al. (2012)

*, ** notes

1. Maximum thickness between basement and postrift unconformity or correlative conformity; depth converted using velocity of 4.5 km/s

2. Based on terminology of Sutra et al. (2013) and Chenin et al. (2017)

3. Direct calibration or based on similarity of seismic facies to the layered salt penetrated at Glooscap C-63

4. On the basis of similar reflections seismic character of basalts penetrated at Glooscap C-63; LC – layer conformable (implying lava flows); XC – cross cutting (implying intrusive igneous sills or dykes)

correlated into six of these grabens, where they are best preserved on the hanging walls adjacent to border faults and large displacement secondary faults where accommodation was greatest. Four of the rift basins (Naskapi, Mohican, Acadia, and Abenaki) contain significantly expanded intervals of late synrift to earliest postrift fill (accommodated at least in part by salt expulsion), and one basin (Oneida) contains a clear prerift stratigraphic succession beneath synrift strata. We describe the structure of each rift basin in more detail below and in Table 1.

East Emerald Graben

The East Emerald Graben (Figure 14a) is the most proximal of the studied rift basins of the central LaHave Platform rift zone (note that the Mushaboom Graben is actually located further landward, but it is only partially crossed by one seismic profile, and cannot be mapped; Figure 7). It forms a 46 km long and up to 25 km wide northeast-trending half graben, with a maximum preserved fill of 1900 ms (or 4.2 km at 4.5 km/s) (Table 1). Seismic quality is fair to poor; no strike lines are available and no wells penetrate its fill. Flanking the half graben to the northwest are elevated and heavily eroded basement rocks of the undifferentiated LaHave Platform, and to the southeast the Emerald Ridge. The main border fault dips landward (towards the northwest), with the thickest and youngest preserved basin fill skewed towards the Emerald Ridge (Figure 14a). The hinged (landward) margin is heavily eroded, exposing older rift-basin strata along the prominent postrift unconformity.

Two or three important secondary normal faults offset basement and the overlying graben fill on the hanging wall, each with between 150 and 250 ms of maximum throw. The density of smaller-scale landward-dipping normal faults generally increases towards the northwestern half of the graben, where the flexed basement shallows towards the undifferentiated LaHave Platform. Three profiles also show what appear to be high angle reverse faults, but these cannot be correlated between the widely spaced profiles in the existing dataset, so their orientations are unknown. They imply that the East Emerald Graben experienced at least a small degree of compression or transpression during the synrift or early postrift phase.

Emerald Graben

The Emerald Graben (Figure 14b and 14c) is located southwest of the East Emerald Graben, forming a left-stepping and partly overlapping basin with a complex structure (Figures 4, 7). Seismic quality is fair to poor and one well – Sambro I-29 – calibrates its deeper fill above a rider block along its southeastern margin (Figure 15; discussed in a later section). Emerald Graben is 73 km long and up to 25 km wide, with a maximum preserved fill of 2050 ms (or roughly 4.6 km at 4.5 km/s) (Table 1). Its southern boundary is the Sambro Ridge that branches off the Emerald Ridge. Its northern boundary is the undifferentiated LaHave Platform. Where the axes of the Emerald and East Emerald grabens overlap, the Emerald Ridge separates them. Here, the postrift unconformity exhumed older synrift strata along the basin's hinged margin, and a dense array of low-angle normal faults offsets synrift strata, soling above the top basement surface (see Figure 15).

The structure of the Emerald Graben varies along strike and is more complex than the East Emerald Graben. Seaward-dipping (towards the southeast) border faults flank the western part of the graben, whereas two main landward-dipping (towards the northwest) border faults flank its eastern part. This produces an overlapping convergent geometry (*sensu* Morley et al. 1990) with a complexly faulted intra-basin high in the overlapping region between the opposing border faults (see also work by Paul and Mitra 2013). Heavily eroded hinged margins lie opposite to each (one landward and one seaward of the corresponding border faults) (Figure 5). The maximum preserved sediment fill skews towards its northern border fault in the west, and towards its southern border faults in the east, forming two distinct depocentres offset from each other by roughly 5-10 km (Figure 6a).

The western part of the Emerald Graben narrows abruptly from 25 km to less than 10 km wide in part because of enhanced erosion of both the hinged and border fault margins beneath the postrift unconformity (Figure 14c). Less than 1200 ms of mainly early synrift strata (2.7 km at 4.5 km/s) are preserved here. A sharp left-stepping offset in the LaHave Platform defines the southwestern most limit of the Emerald Graben.

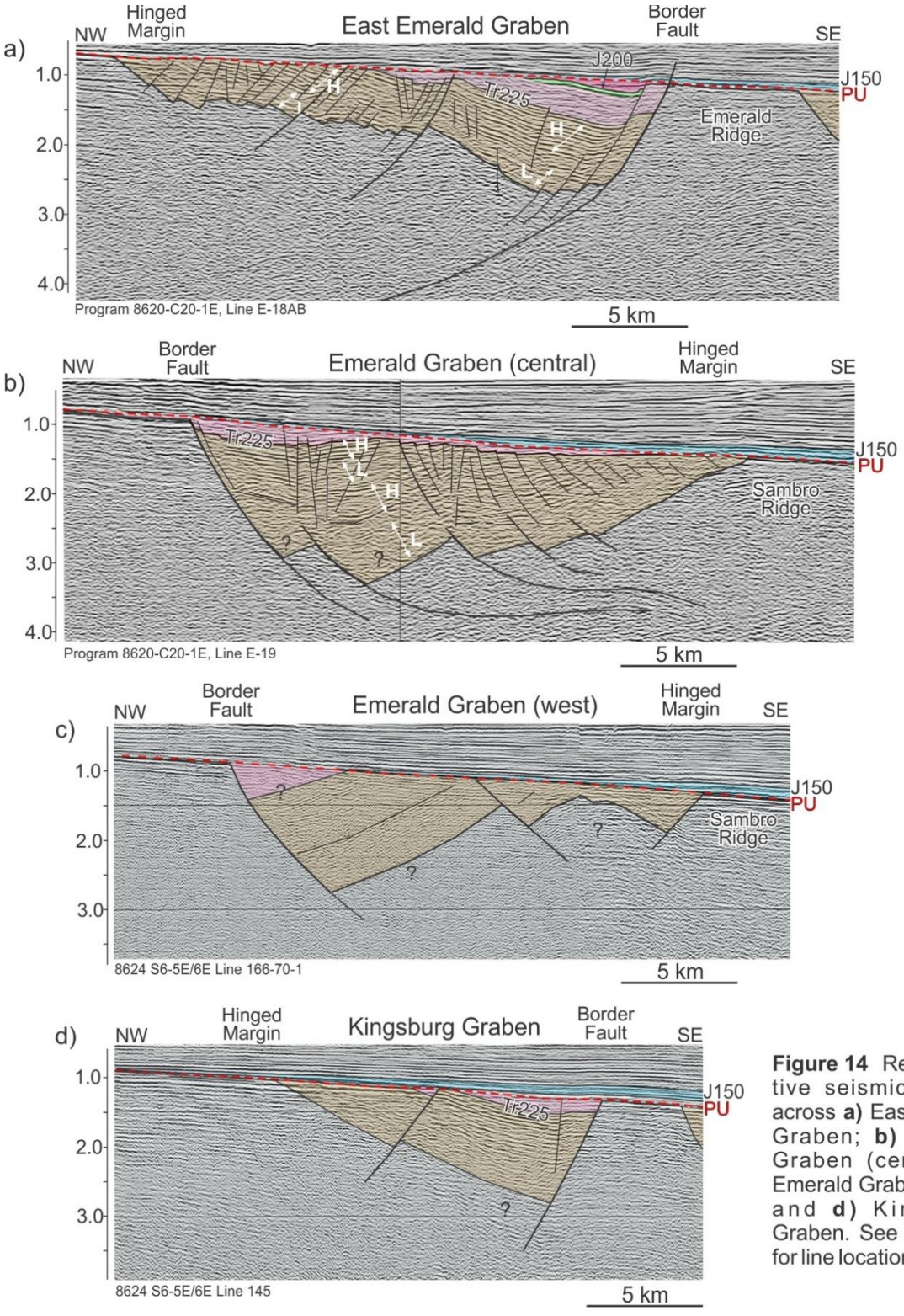

Figure 14 Representative seismic profiles across **a)** East Emerald Graben; **b)** Emerald Graben (central); **c)** Emerald Graben (west); and **d)** Kingsburg Graben. See Figure 6b for line location.

The Emerald Graben also thins abruptly to the east approaching the Emerald Ridge, but its structure is more complex. Here, its two southern border faults, separated from each other by a prominent 4-7 km wide rider block (referred to as the 'Sambro rider block'; Figures 15 and 16), as well as the Sambro Ridge, terminate sharply and are offset by roughly 3-4 km toward the northwest relative to the edge of the Emerald Ridge (Figure 7). As such, the eastern limit of the graben probably coincides with a northwest-trending lateral transfer fault with strike-slip displacement. The folded and more strongly tilted early synrift strata at the Sambro I-29 well location,

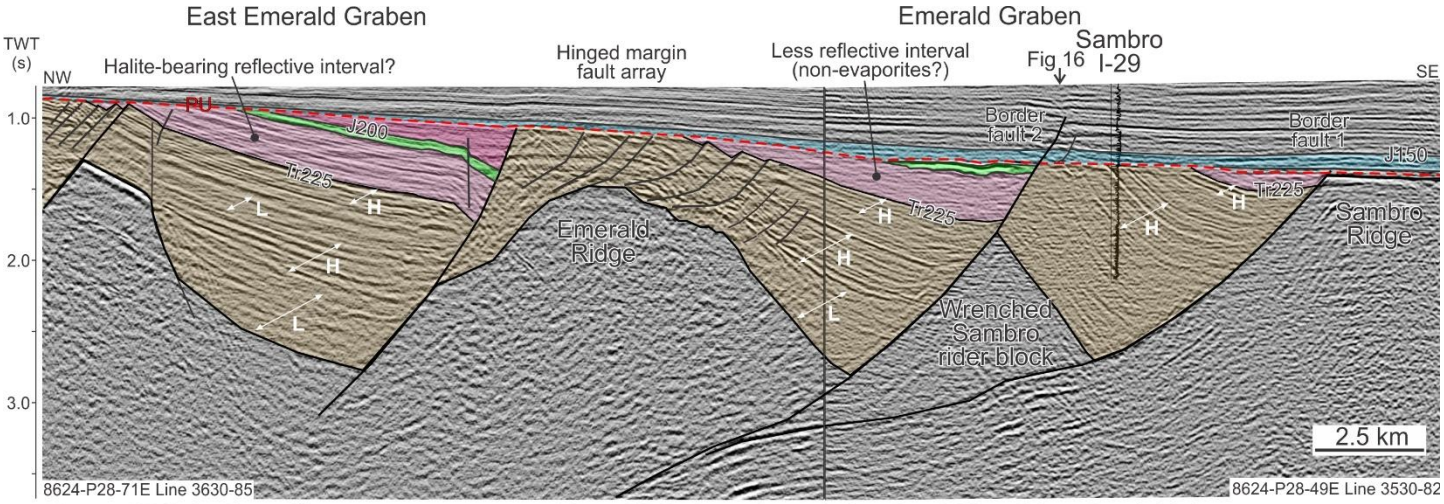

Figure 15 Seismic profile across easternmost Emerald Graben, through Sambro I-29 well location (which penetrates more strongly tilted and folded early synrift strata above a rider block). Profile also crosses the western part of East Emerald Graben. See Figure 6b for line location.

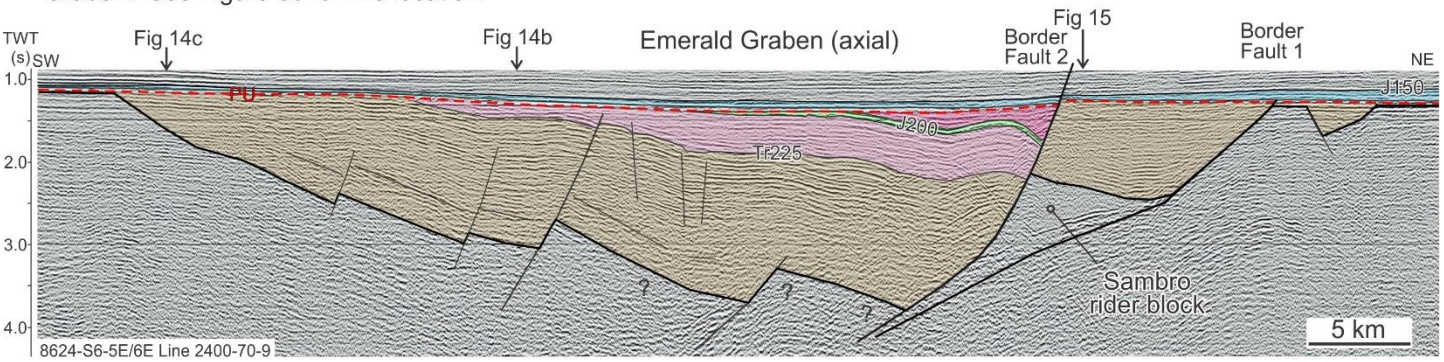

Figure 16 Profile sub-parallel to the axis of the Emerald Graben, crossing its southern border faults. Note that younger synrift strata are preserved only adjacent to border fault 2. See text for details and Figure 6b for location.

and their abrupt truncation along the PU, is unique in the study area. Combined with the roughly 30° northward rotation of the Sambro rider block compared to the Sambro Ridge, it is possible that the Sambro rider block underwent wrenching during strike-slip deformation, with transpression deforming the eastern parts of the rider block and its synrift cover into a positive relief structure that was subsequently heavily eroded. Younger synrift strata appear only to have been accommodated (or preserved) adjacent to the more northerly border fault ('border fault 2' in Figures 15 and 16).

Kingsburg Graben

The Kingsburg Graben is a narrow northeast-trending half graben located southwest of the Emerald Graben (Figure 14d). Seismic quality here is poor to very poor, coverage is sparse, and mapping results are tentative. No wells penetrate the fill of this graben. The Kingsburg Graben is roughly 68 km long and up to 15 km wide, containing as much as 1500 ms of fill (or roughly 3.3 km at 4.5 km/s). Its landward boundary is the LaHave Platform, offset sharply 10 km or so to the south compared to the Emerald Graben. A number of discontinuous and laterally offset (generally by < 5km) unnamed basement elements define its seaward boundary, and together with alternations between landward-dipping and seaward-dipping border faults, separate the Kingsburg Graben into three segments (Figure 7). This narrow graben narrows further still to the southwest, were it is barely discernable and no more than 8 km wide, heavily eroded along the postrift unconformity.

A number of other small, poorly constrained rift basins are recognized south of the Kingsburg Graben, but these cannot be confidently mapped with the existing dataset, and are not considered further.

Naskapi Graben

With its northeast-oriented axis stretching more than 168 km, a width generally less than 26 km, and up 2000 ms (roughly 4.5 km) of fill, the Naskapi Graben is a long, narrow, and deep half graben (Figures 4, 7, 17; Table 1). Its southern boundary is the prominent, heavily eroded and flat-topped Naskapi Ridge. Its northern boundary consists of a heavily eroded hinged margin (e.g. Figure 17b) flanked by different basement elements along strike. Although it is the longest graben in the study area, it is segmented into three left-stepping depocentres, each separated by sills generated by more elevated basement topography and changes in border fault orientation across interpreted transfer zones (e.g. Figures 7a, 8, 9). The eastern segment is flanked to the north by the Emerald Ridge. The central segment is flanked to the north by the Sambro Ridge, and the western segment is flanked to the north by a series of poorly imaged and unnamed basement elements located south of the Kingsburg Graben. Seismic quality is mixed, and both the quality and coverage diminishes from the eastern towards the western graben segments. No wells penetrate the fill of the Naskapi Graben.

In its eastern reach, where data density is highest, the graben consists of one main landward-dipping (northwest) border fault that separates the hanging wall from the Naskapi Ridge, and two to three large-offset landward-dipping secondary faults offsetting its hinged margin (Figures 7b, 17a, b). These secondary faults largely parallel to the main border fault and continue along strike for ~50 km, with up to 470 ms (~1 km) of normal slip displacement to the northwest. Abrupt variations is sediment thickness, folding, and local reverse offset across some of the secondary faults implies they may have experienced a component of strike-slip displacement during rifting. Local hanging wall folds and minor inversion also implies the main border fault experienced similar displacement, but at a much later time (in the Late Cretaceous) (Figure 12).

The eastern segment of the Naskapi Graben broadens to the northeast from just 13 km wide to more than 26 km wide, before narrowing again near its eastern termination. Total fill thins both to the southwest and to the northeast, with the thickest fill centered adjacent to its southern border fault; secondary thicks are preserved on the hanging wall adjacent to large offset secondary faults (Figure 4a). Where the graben is widest, a steep seaward (southeast) dipping normal fault with up to 450 ms (or roughly 1 km) of throw also offsets the hinged margin, reducing its flexure and diminishing the amount of erosion beneath the postrift unconformity (compare the hinged margins in Figure 17a and 17b). An intricate array of finer-scale synrift faults is also present along the hinged margin, with fault density increasing approaching the Emerald Ridge (Figures 17a, b). The eastern termination of the Naskapi Graben coincides with the narrow, eastern tip of the Naskapi Ridge, which is heavily faulted and has a more northerly orientation. Here, it separates faults that dip landward from those that dip seaward in what appears to be an important accommodation/transfer zone. The easternmost fill of the Naskapi Graben thins but is continuous above a low-relief relay ramp or sag located between the eastern edge of the Naskapi Graben and the East Naskapi Graben (Figure 7a). This is important because it enables direct correlation of strata from the eastern Naskapi Graben, across the relay ramp, and into the landward parts of both the Oneida and Mohican grabens (a useful observation as it enables comparison of the stratigraphy between different rift basins - discussed later).

The boundary between the Naskapi Graben's eastern and central segments coincides with a change in graben trajectory and total sediment thickness, as well as offsets along its southern border fault and secondary faults (Figures 4a, 7). That the boundary between the Naskapi Graben's eastern and central segments coincides with the eastern edge of the Emerald Graben and the western edge of the East Emerald Graben to the north, implies that they share a common genesis, perhaps forming along an important northwest-trending accommodation zone or synrift strike-slip fault zone.

The overall structure of the central reach is similar to that of the eastern reach, with the exception that some of the secondary faults trend oblique to the more northerly trajectory of its southern border fault. The axis of the central reach plunges towards the southwest, where graben fill thickens before thinning again approaching the graben's western reach. The boundary between the central and western reaches is topographically elevated

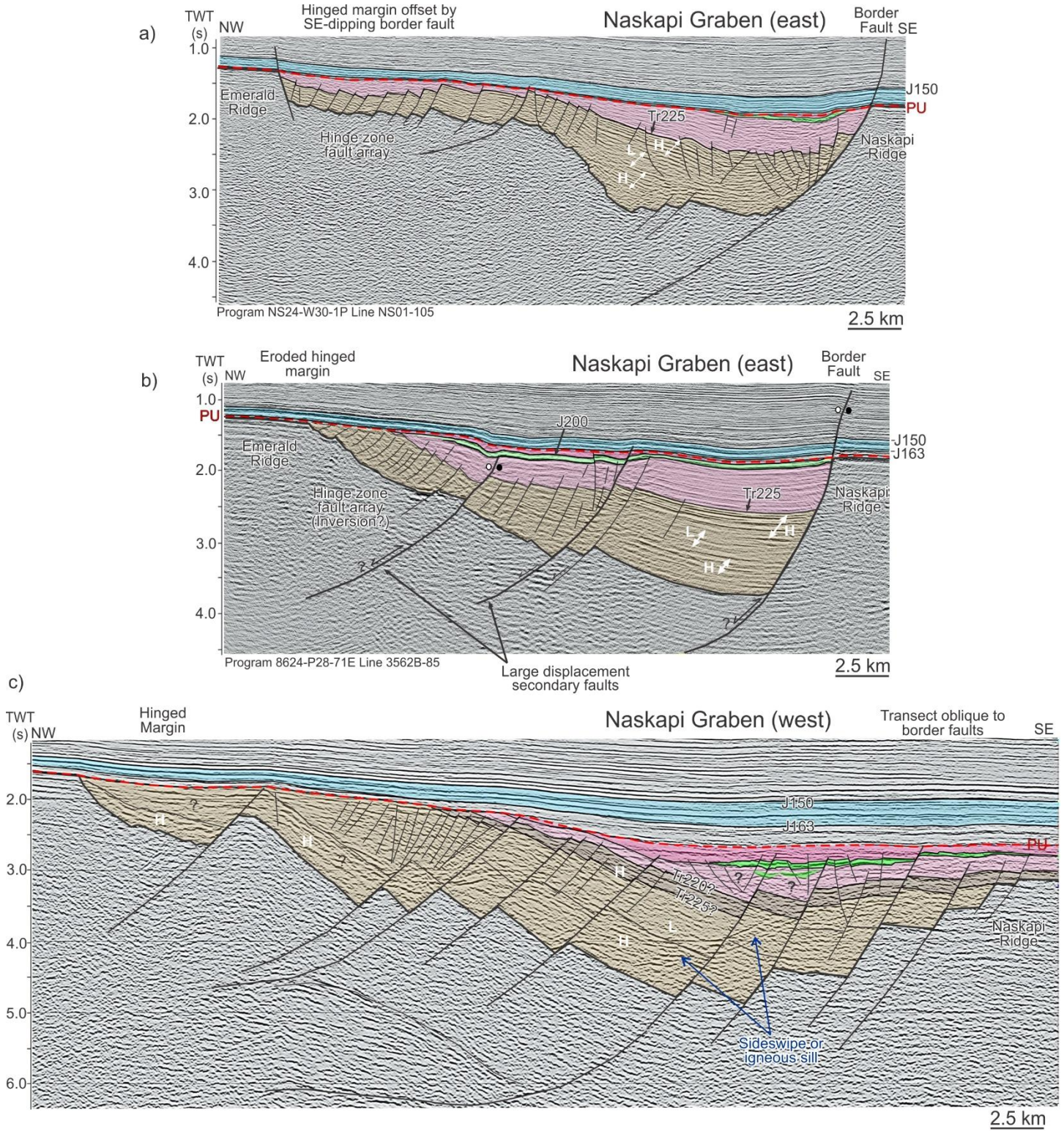

Figure 17 **a)** Profile across the eastern reach of the Naskapi Graben, across a dense hanging wall fault array (potential negative flower structure?). **b)** Profile across eastern Naskapi Graben with a heavily eroded hinge zone and potentially inverted. **c)** Profile across the poorly imaged western reach of the Naskapi Graben (interpretation has a high degree of uncertainty). Profile located oblique to the graben axis. See Figure 6b for location.

and complexly faulted (see for example the Tr225 and J200 structure maps in figures 8 and 9). Strata thicken again down the axis of the western segment. Unlike the central and eastern reaches, four or five arcuate northwest-dipping border faults define the seaward margin of the western reach. These faults substantially narrowed the width of the Naskapi Ridge, which appears to have foundered across a number of 2-3 km wide rider

blocks that step down towards the northwest (Figure 17c). The trajectory of these faults (and the rider blocks between them) is rotated roughly 30 degrees to the north compared to the trend of the normal faults in the central reach, matching the more northerly arcuate edge of the Naskapi Ridge here. The southwestern limit of the Naskapi Graben appears to pass into a series of smaller fault-bound grabens with trajectories similar to its central segment, but seismic imaging is poor across its western reach, and consequently its westward termination is poorly constrained.

Mohican Graben

The Mohican Graben tracks parallel to and seaward of the Naskapi Graben (Figures 4a, 7). Its overall structure is that of a half graben, with a complex network of segmented, generally landward-dipping (towards the northwest) border faults defining its southern margin and the heavily eroded Naskapi Ridge defining its northern hinged margin (Figures 5, 18). At more than 145 km long, it is second in length only to the Naskapi Graben, though with a maximum width of 46 km it is much wider. The graben contains up to 2250 ms of synrift fill (or roughly 5 km at 4.5 km/s) (Table 1). Seismic coverage is good across much of the graben, with data quality ranging from very poor to good. There is a notable lack of data coverage along the seaward part of its central reach, and data quality is particularly poor along its deeply buried southwestern parts where salt expulsion and postrift inversion took place. The top basement surface is difficult to correlate beneath its deepest parts, and the interpretation is therefore tentative. Three wells calibrate the graben's uppermost fill: Glooscap C-63, Moheida P-15, and Mohican I-100. Glooscap C-63 is the most notable (Figure 19) encountering a 152 m extrusive basalt layer (top surface corresponding to our J200 surface) above 441 m of interbedded Late Triassic halite and dolomitic shale deposited above the Tr220 surface (discussed in more detail later). No wells penetrate its deeper fill.

Overall, the Mohican Graben plunges to the southwest. Like the Naskapi Graben, it can be separated (though more loosely) into an eastern, central, and western reach (Figure 7) that largely reflect lateral changes in its width caused by seaward or landward shifts in the location of its main border faults and associated elevated basement elements. Its eastern reach terminates along the north-south oriented East Mohican Ridge, which separates it from the slightly overlapping Oneida Graben (Figure 7). This ridge curves 45° to the southwest such that it also defines the seaward edge of the eastern Mohican Graben. The main northwest dipping border fault tracks along the ridge, and several additional landward-dipping (to the northwest) secondary normal faults parallel it, offsetting both deep and shallow intervals of synrift strata by up to 200 ms (Figure 18a). All of these northeast-trending faults curve northwards as they approach, and terminate against, the East Mohican Ridge (Figures 5, 7).

The Mohican Graben's central segment is structurally similar to the eastern segment (Figure 18b), except that its seaward border fault has shifted further southeast where it tracks along the Moheida Ridge. This increases basin width by roughly 10 km (compare Figures 18a and 18b). The basin appears to narrow to 23 km, prior to widening again to 30 km in its western reach, probably reflecting sharp offsets in the Moheida Ridge that defines its southern margin. The Moheida Ridge, however, is a cryptic basement element composed of a number of faulted basement blocks, and correlation of the "top basement" surface across the ridge is difficult (two alternate basement interpretations shown in Figure 18c). In several locations, intervals of synrift strata from the Mohican Graben proper correlate clearly into the strata above the Moheida Ridge (e.g. Figures 18b, 18c, 20) implying that to some extent its relief is a relatively young feature. The ridge could be a product of early postrift inversion or late synrift migration of the most active border faults towards the axial parts of the basin (leaving older synrift successions above the new 'footwall', as sedimentation was focused above the new hangingwall where younger rift accommodation was greatest; see Dart et al. 1995), or, some combination of the two.

The overall structure of its western reach is still that of a half graben flanked by landward-dipping border faults, but a steep seaward-dipping (towards the southeast) normal fault with up to 500 ms (roughly 1.1 km) of total throw also offsets the hinge margin adjacent to the Naskapi Ridge (Figure 18c). Increased synrift accommodation across this fault reduces the magnitude of erosion beneath the postrift unconformity here. Evidence for widespread inversion increases in the

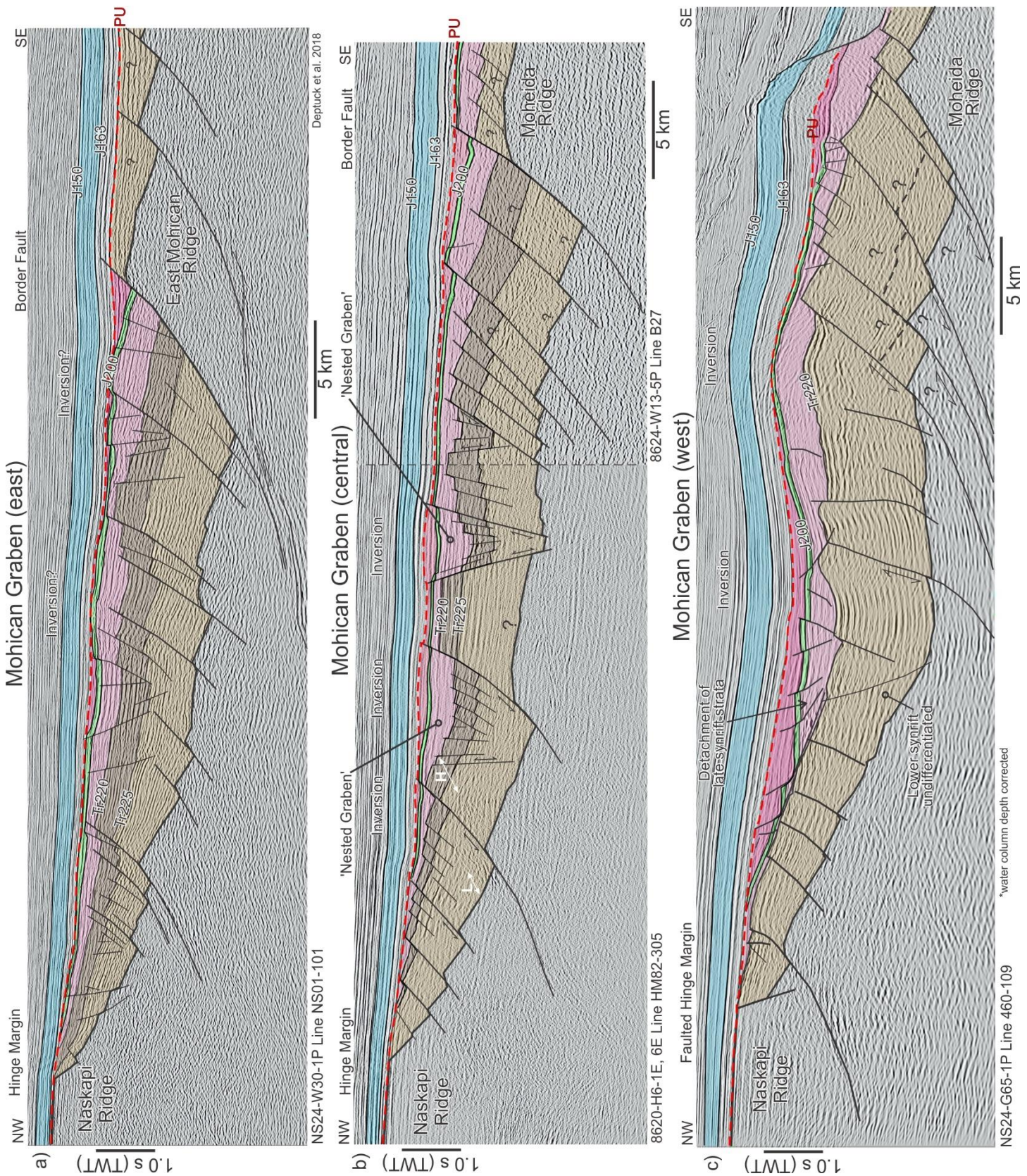
a)
NW
Hinge Margin
Mohican Graben (east)
Border Fault
SE
Inversion?
Inversion?
J-150
J-163
J200
PU
Tr226
Tr225
Naskapi Ridge
East Mohican Ridge
1.0 s (TWT)
5 km
NS24-W30-1P Line NS01-101
Deptuck et al. 2018
b)
NW
Hinge Margin
'Nested Graben'
Mohican Graben (central)
'Nested Graben'
Border Fault
SE
Inversion
Inversion
Inversion
J-150
J-163
J200
PU
Tr220
Tr225
Naskapi Ridge
Moheida Ridge
1.0 s (TWT)
5 km
8620-H6-1E, 6E Line HM82-305
8624-W13-5P Line B27
c)
NW
Faulted Hinge Margin
Mohican Graben (west)
SE
Inversion
Inversion
Detachment of late-synrift-strata
J-150
J-163
J200
PU
Tr220
Naskapi Ridge
Lower synrift undifferentiated
Moheida Ridge
1.0 s (TWT)
5 km
NS24-G65-1P Line 460-109
*water column depth corrected

⇦ **Figure 18** Representative seismic profiles across the a) eastern, b) central, and c) western Mohican Graben. See Figure 6b for line location.

southwestern part of the graben, and a number of steeply dipping faults appear to have been reactivated in the Jurassic as reverse faults (Figure 18c). There is also strong evidence for detachment of cover strata above the primary salt layer in the southwestern reaches of the Mohican Graben.

'Nested' axial grabens – Deviating from the dominantly landward-dipping normal faults that offset strata in the Mohican Graben are four northeast-trending grabens bound by opposing steeply inclined normal faults (referred to here as 'nested grabens'). These narrow grabens occupy the axial parts of the western, central and eastern Mohican Graben, and appear to be products of late synrift extension (post-Tr220, and especially post-J200 strata thicken along their axes). The largest of these nested grabens is roughly 60 km long and broadens from 8 km wide in the central reach to more than 12 km wide in the western reach of the Mohican Graben (yellow faults in Figures 7b). A second 20 km long and 7 km wide nested graben branches off of this graben in the central reach (both nested grabens are crossed in Figure 18b), and two additional laterally offset nested grabens occupy the eastern reach (ranging from 3-6 km wide, with a combined length of 17 km). These apparent late synrift grabens are floored by fault arrays composed of numerous steeply inclined small-scale normal faults that cut pre-Tr220 strata. The J200 marker is faulted downward along the steep opposing normal faults that border these narrow grabens, commonly folded into elongate synclines with northeast-oriented fold axes. It is not clear if both of their bounding faults offset basement.

Clear inversion structures nucleate above or adjacent to these grabens, with subtle folding along the J163 surface implying that inversion of these late-synrift grabens took place during the early postrift, probably in the Middle Jurassic (Figures 10, 18b). Several additional inversion structures are present in the seaward parts of the central reach, adjacent to southwest dipping growth faults. They also appear to have formed in the Jurassic.

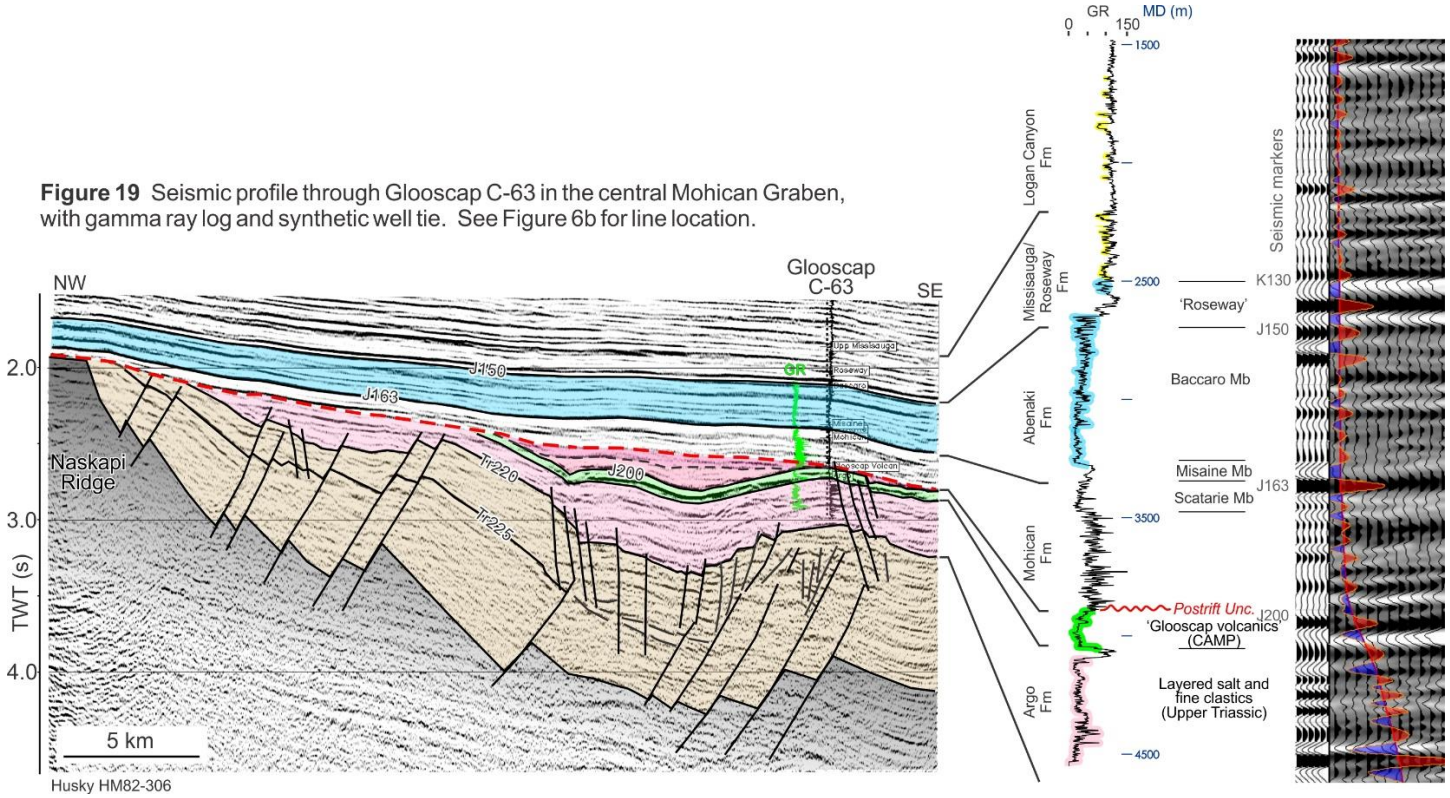

Figure 19 Seismic profile through Glooscap C-63 in the central Mohican Graben, with gamma ray log and synthetic well tie. See Figure 6b for line location.

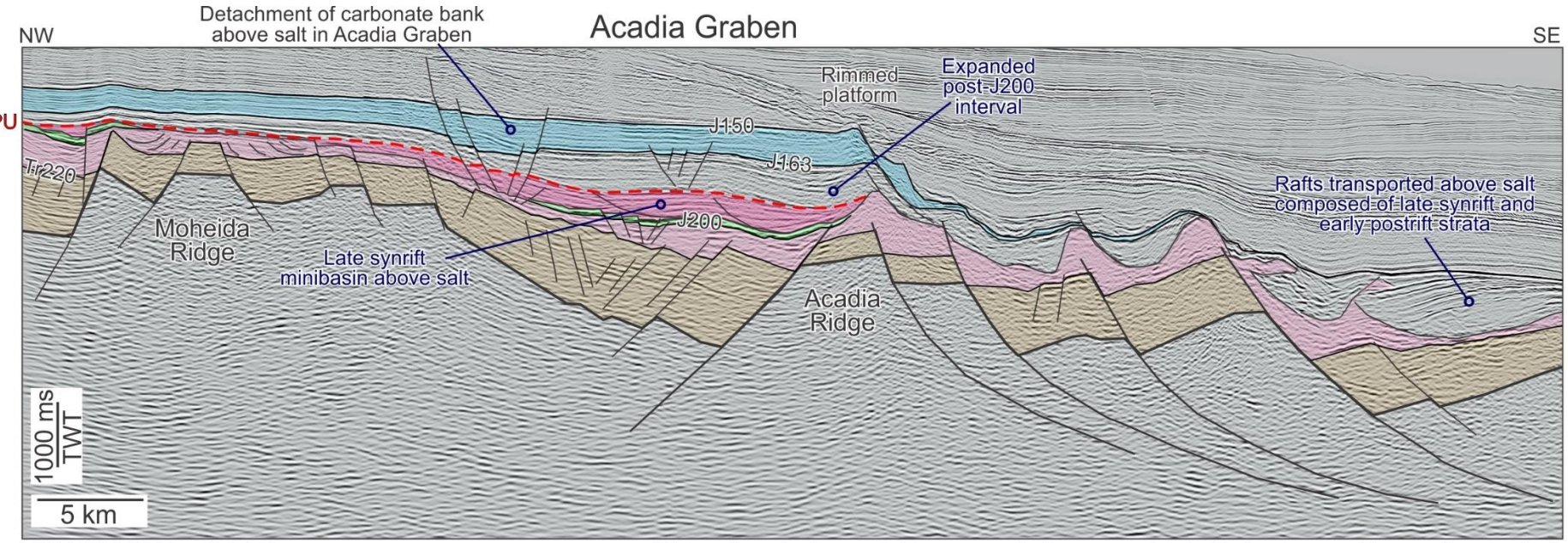

Figure 20 Representative seismic profile across the Acadia Graben, showing the increased impact of salt on both late synrift and early postrift strata. J200 basalt marker also appears to have been transported above the salt, but commonly is discontinuous and not easily correlated on the slope. Note that the Acadia Ridge is an important structural element that commonly separates dominantly northwest dipping faults landward of it from southeast dipping faults seaward of it. See Figure 6b for line location.

Acadia Graben

The Acadia Graben is the most distal rift basin of the central LaHave Platform rift zone evaluated in this study (Figures 4a, 7). It is roughly 52 km long and up to 19 km wide. Like the Mohican Graben, correlation of the top basement surface beneath the graben is very difficult, but it could contain as much as 2100 ms of syn-rift strata (or roughly 4.7 km at 4.5 km/s). Seismic quality is fair to good and no wells calibrate its fill. Its overall structure is a half graben, with the hinged margin located along the heavily faulted Moheida Ridge (Figure 20). The half graben is flanked to the southeast by three sharply offset landward-dipping (towards the northwest) border faults located adjacent to the laterally segmented Acadia Ridge. The Acadia Ridge is an important basement element that separates northwest-dipping faults (landward side) from dominantly southeast-dipping very large displacement basement faults (seaward side). The ridge also coincides with the seaward nose of the overlying Abenaki carbonate bank edge. The Acadia Graben landward of this ridge plunges to the southwest, offset abruptly along strike by two transfer zones that coincide with offsets in the Acadia Ridge. Its lower fill is poorly-imaged, but like the Mohican Graben there is clear evidence that cover strata, including the overlying carbonate bank, detach above a the post-Tr220 salt-bearing succession that overlies faulted lower synrift strata. Salt pillows are also present seaward of the Acadia Ridge, separating rafts composed of latest synrift to early postrift cover strata (Figure 20).

Oneida Graben

The roughly 95 km long and up to 40 km wide Oneida Graben contains as much as 1800 ms (or roughly 4 km at 4.5 km/s) of complexly faulted and folded synrift fill (Figures 4a, 7). As such, it is smaller and contains less fill than the Mohican Graben to its west. Seismic quality is mixed, and there are more imaging issues (mainly ringing) here that may be related to thicker or more heavily faulted intervals of CAMP-related volcanics. There are also some indications of igneous intrusions (sills) that produce reflections that cross-cut stratigraphic layers. No wells calibrate its fill.

Overall, the Oneida Graben is a half-graben (Figure 21). Its southern margin comprises a number of slightly offset landward-dipping border faults that separate the thickest hanging wall graben fill to the north from the heavily faulted East Moheida Ridge to its south. Its northern hinged margin steps off the East Naskapi Ridge, and with the exception of the Abenaki Graben to its east, synrift strata adjacent to it are less intensely eroded than in other grabens. The East Mohican Ridge defines the western margin of the Oneida Graben, approaching which synrift strata both thin and are increasingly eroded along the postrift unconformity. Its southwestern extremity is narrow – just 10 km wide – where it overlaps with the easternmost parts of the Mohican Graben. The eastern half of the graben is also quite narrow – just 15 km wide – where it is sandwiched between a broadly domed basement element to the north and the East Moheida Ridge to the south (Figure 21a). Its eastern margin shows a general thinning of synrift strata but is not sharply defined (Figure 4a). Unlike the Mohican and Acadia grabens, the Oneida Graben does not plunge into deeper water along the Scotian Slope, and instead remains on the platform.

The structure of the East Moheida Ridge along its southern margin is quite similar to the Moheida Ridge that flanks the Mohican Graben, being composed of a number of rotated basement blocks with overlying intervals of synrift strata. Younger synrift strata all along the East Moheida Ridge are tightly folded into elongated hangingwall synclines that parallel the border faults (Figure 9). As in the Mohican Graben, these folds may be inversion-related. A particularly clear inversion structure is imaged where the East Moheida Ridge bends roughly 35° northward, mid-way along the axis of the Oneida Graben (Figure 22). Here, at least two crustal-scale northeast-dipping faults cut perpendicular across the ridge (striking northwest; Figure 7b). The synrift succession adjacent to the fault is clearly inverted, and synkinematic strata at the fault tips, as well as the timing of a prominent angular unconformity, indicate inversion took place in the Early Jurassic. These northwest-trending faults pass into deep crustal shear zones, and their tips, as well as the bend in the Moheida Ridge, align closely along strike with the nose of a broad basement arch beneath the eastern Oneida Graben. These elements align to form a northwest-trending lineament that appears to have strongly controlled the thickness of the Oneida Graben fill, as well as the prerift Ojibwa Basin (described below) that underlies it. Thus, the latest synrift or earliest postrift inversion structure in Figure 22 may reflect reactivation of an older pre-existing

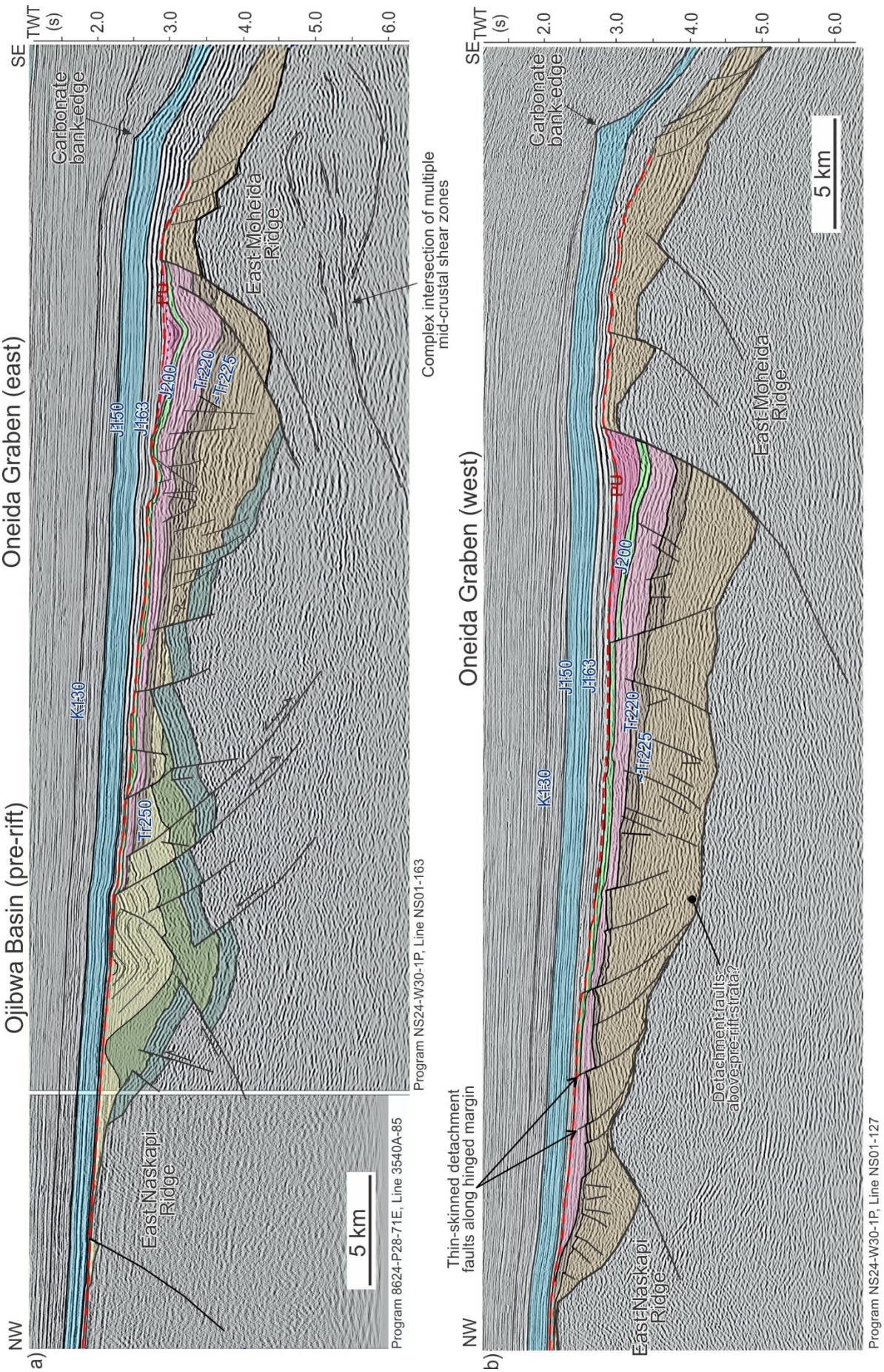

Figure 21 Representative seismic profiles across **a)** eastern Oneida Graben and **b)** western Oneida Graben. See Figure 6b for line location.

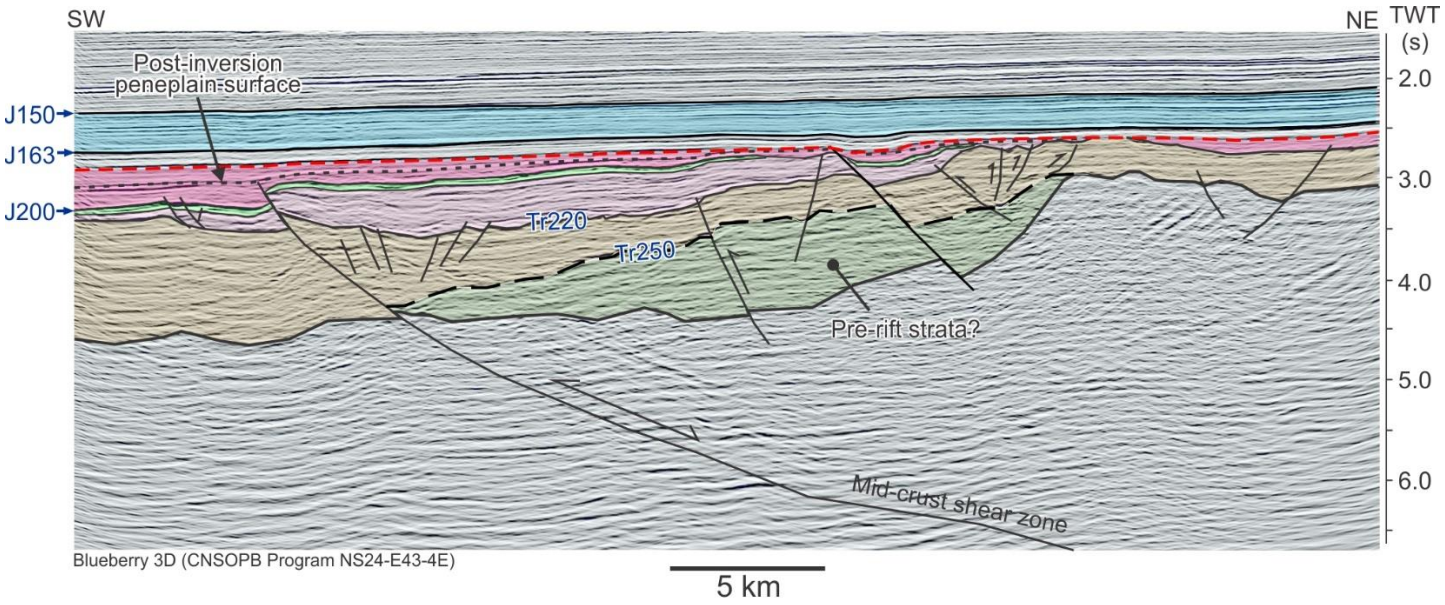

Figure 22 Seismic profile across inversion structure in the eastern Oneida Graben. A prominent angular unconformity (not seen in this line orientation) truncates folded strata along the hanging wall of the Oneida Graben, indicating the inversion probably took place in the Early Jurassic, and appears to have formed through reactivation of an older crustal shear zone. See text for details. Line location shown in Figure 6b.

northwest-trending crustal lineament tracking through the Oneida Graben.

Oneida Graben's northern hinged margin is dominated by seaward-dipping, thin-skinned detachment faults that step off the East Naskapi Ridge (Figures 7b, 21b). Many of these listric faults do not appear to be basement-involved; rather, they detach above an unusually reflective basement marker, or within an interpreted prerift succession, producing landward-rotated synrift blocks. This style of hinge-margin listric faulting appears to be unique to the Oneida Graben in the study area, though similar thin-skinned faults may offset synrift strata on the slope seaward of the study area.

Ojibwa Basin (prerift succession?)

A variably folded and thrusted older stratigraphic succession underlies the Tr250 unconformity beneath parts of the Oneida Graben and the East Naskapi Ridge to its north (Figures 21a and 23). This pre-Tr250 succession was deformed by compressional tectonism, and we interpret it as the eroded remnants of a prerift extensional or transtensional basin, later inverted during Paleozoic orogenesis during the final stages of Pangea assembly (see discussion). The prominent Tr250 angular unconformity separates this older succession from overlying synrift strata, merging with the postrift unconformity above the East Naskapi Ridge.

Thickness maps between Tr250 and basement reveal these deformed strata are thickest in two slightly offset northeast-elongated regions, collectively referred to here as the *Ojibwa Basin* (Figure 24). The first is a 40 km long by 18 km wide region beneath the northeastern Oneida Graben and East Naskapi Ridge. Here, convergent structures (mainly thrusts in the deeper section and folds in the shallower section) dominate the basin structure, with some structures reactivated as southeast-dipping extensional faults during Triassic rifting (Figure 21a). The northeast-southwest orientation of thrust faults indicate a northwest-southeast compression direction. Total maximum thickness is about 1600 ms (roughly 3.4 km at 4.5 km/s). The second depocenter is a 36 km long by 10 km wide more broadly folded region beneath the central Oneida Graben, containing up to 1100 ms of strata that are sharply truncated from above by the Tr250 unconformity.

Abenaki Graben

The Abenaki Graben is the eastern most rift basin examined in this study (Figure 4a). Overall its structure is that of a true graben constrained by large-offset extensional faults on both its northern and southern boundaries (Figure 25). The graben is at least 120 km long and up to 35 km wide, with an east-northeast oriented axis along which its floor deepens as it plunges off the platform. Seismic quality is mixed but coverage is

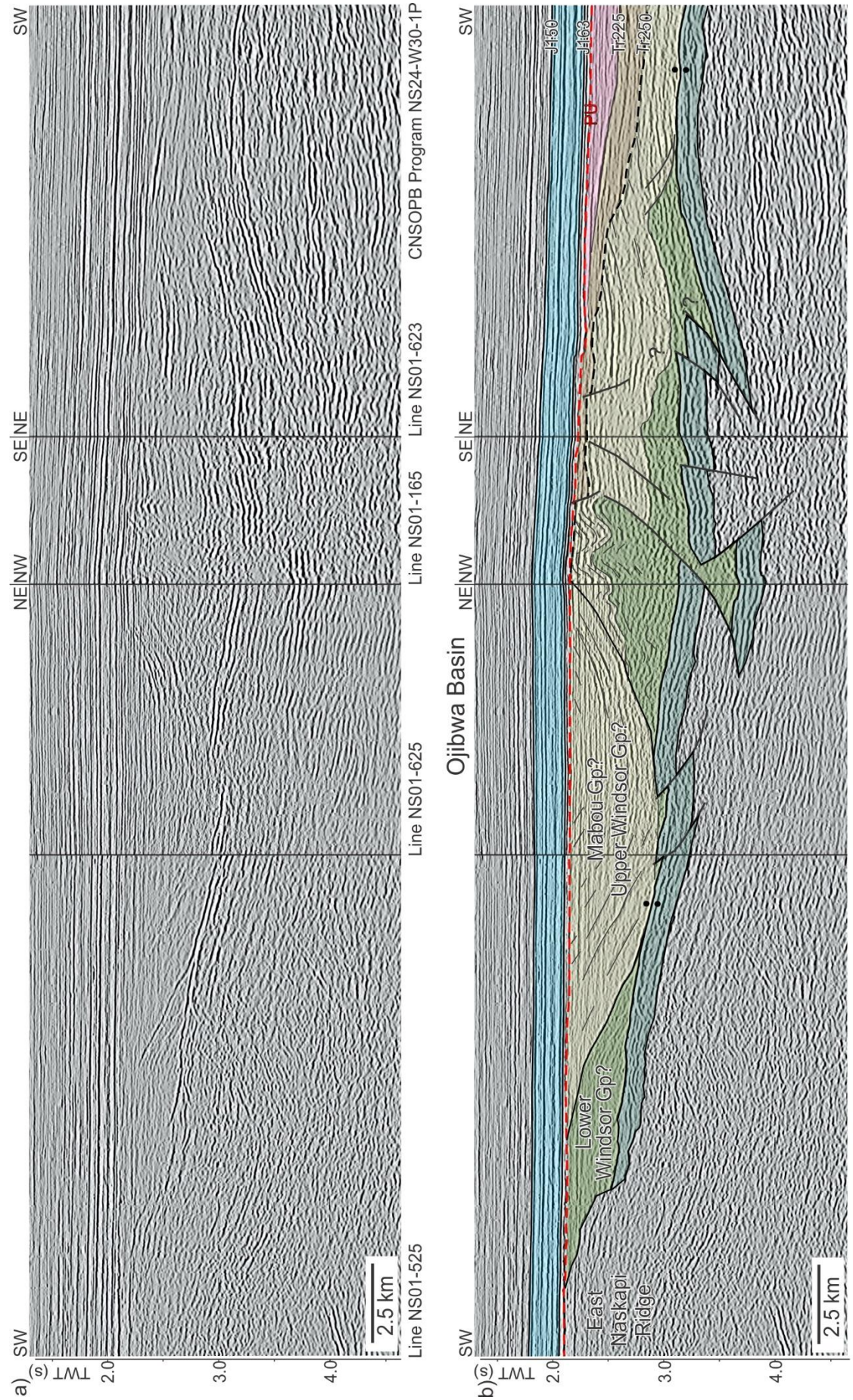

Figure 23 Composite seismic section through the Ojibwa Basin - an interpreted Early Carboniferous prerift basin that underlies the Oneida Graben and the East Naskapi Ridge. Prerift strata were probably folded during the final assembly of Pangea during Appalachian orogenesis, and eroded along the Tr250 angular unconformity. Some structures were reactivated as extensional faults during Triassic lithospheric extension. See Figure 6b for location.

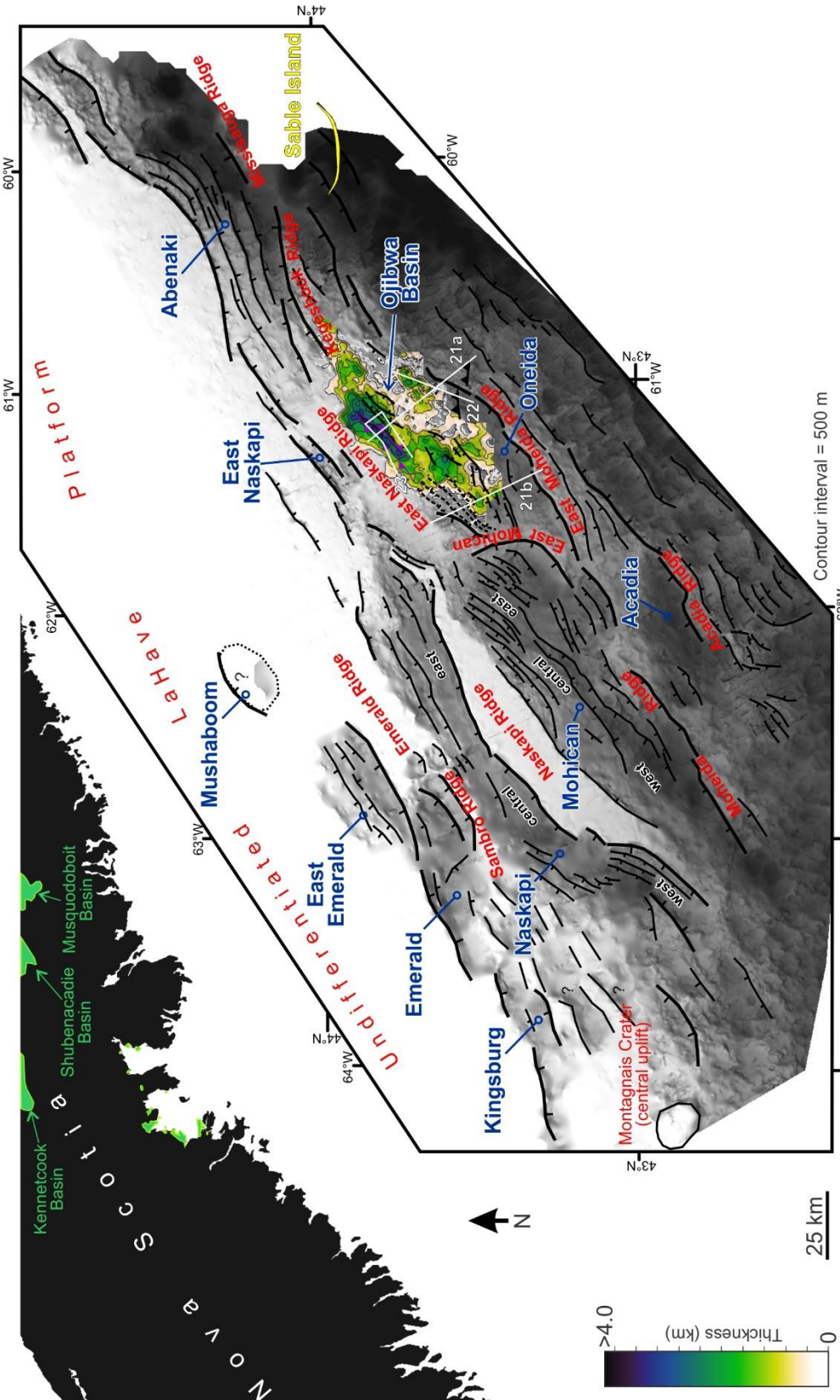

Figure 24 Isopach map between basement and the Tr250 unconformity, showing the thickness distribution of the *Ojibwa Basin* - an interpreted Late Paleozoic prerift basin that underlies the Oneida Graben and the East Naskapi Ridge. Early Carboniferous Windsor Group rocks exposed on mainland Nova Scotia shown in green. Exposures along the shores of Mahone Bay and St. Margarets Bay from Giles (1981); southwest reaches of the Kennetcook, Shubenacadie, and Musquodoboit basins from Boehner (1984). See text for details.

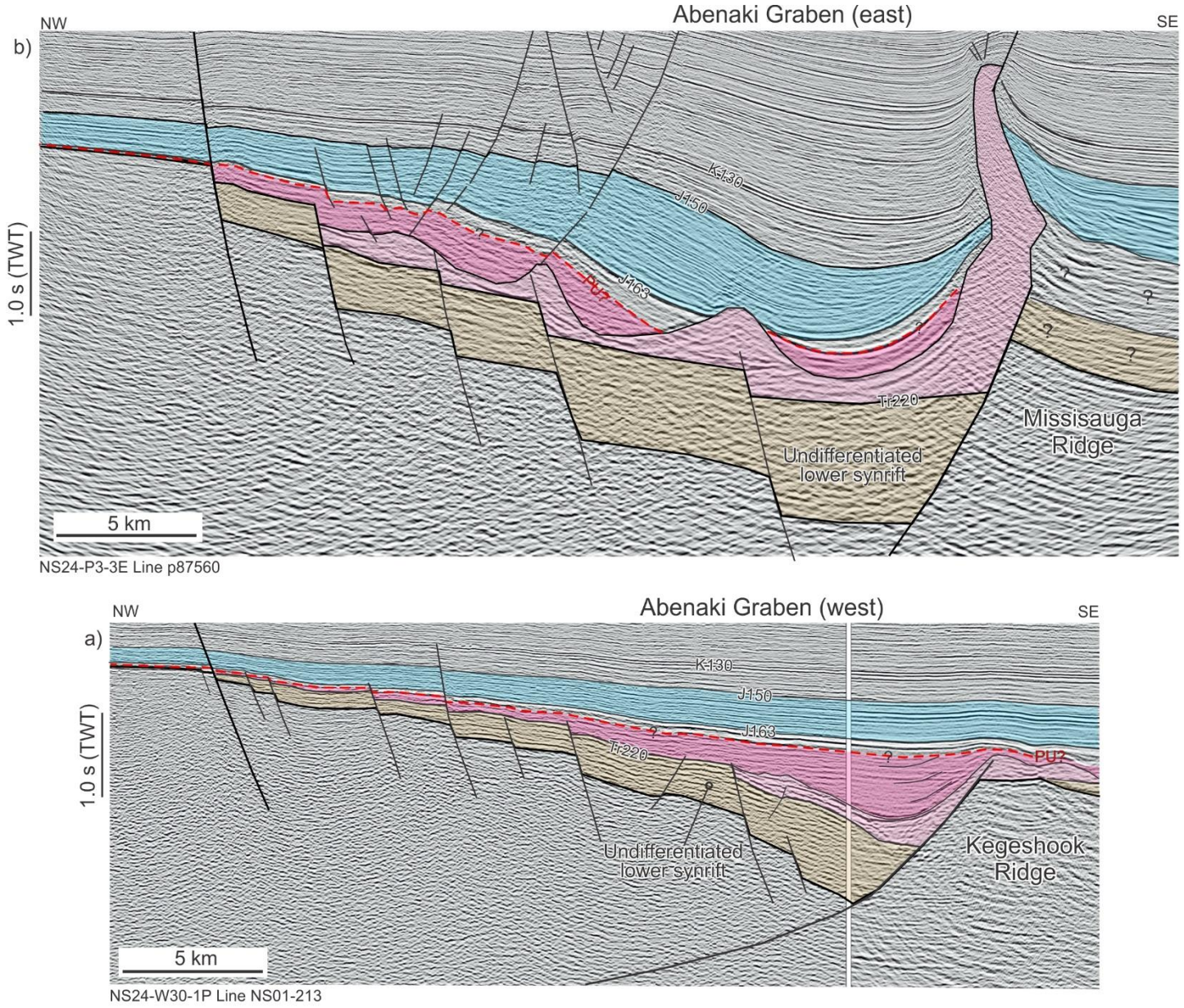

Figure 25 Representative seismic profiles through the **a)** western and **b)** eastern parts of the Abenaki Graben. Note the increased thickness of early postrift strata in the eastern parts of the graben, where Upper Jurassic strata have an increased siliciclastic component. The postrift unconformity cannot be identified in the Abenaki Graben, and its interpretation is subjective. See Figure 6b for line location.

generally good, and aside from Iroquois J-17 that penetrated the flank of a salt diapir expelled from the graben, no wells calibrate its synrift fill.

Its southern landward-dipping border fault has three splays – one that branches off the East Naskapi Ridge, a second with greater throw flanking the Kegeshook Ridge, and a third poorly constrained fault that flanks the Missisauga Ridge, just east of the study area (Figures 5, 7b). Like the graben floor, the crest of the Kegeshook Ridge plunges abruptly towards the east. The graben is flanked to the northwest by elevated and heavily eroded undifferentiated basement rocks of the LaHave Platform. The northern border fault along the platform is steep, and sharply offsets the first of a series of down-to-the-basin stepping normal faults on its northern side (Figure 25). The axis of each of these stair-step fault blocks plunges to the east, and correspondingly the throw across these faults generally increases to the east. Each block varies in width from 2 to 6 km, and is veneered with synrift strata that thickens above each successive fault blocks stepping down towards its southern landward-dipping border faults. Graben fill also thickens to the

east (Figure 4a). Like the main landward-dipping border fault of the Naskapi Graben, the northern seaward-dipping border fault of the Abenaki Graben was active in the Late Cretaceous or even more recently. Very young inversion folds – nearly reaching the seabed – indicate this fault experienced a component of recent strike-slip motion (Figure 12).

Unlike the hinged margins of half-grabens on the platform further west, older synrift strata within the Abenaki Graben do not display significant erosion along the postrift unconformity. The lack of any angular discordance makes the unconformity more difficult to identify here (Figure 25). This may reflect the increased accommodation created along both margins of the Abenaki Graben throughout its development, and the absence of a prominent flexed hinge margin preventing exhumation of older synrift strata. Its maximum synrift fill is difficult to determine since there is no postrift unconformity, the J200 basalt marker is absent, and the primary salt layer that once occupied its upper fill has been largely expelled. Still, the thickest parts of its faults blocks, along its axis, are more than 1500 ms thick (or roughly 3.4 km at 4.5 km/s).

5 Rift basin fill, seismic stratigraphy & calibration

Jump correlation of seismic markers, combined with direct correlation of the Tr225 and Tr220 markers from the eastern parts of the Naskapi Graben, into the landward parts of both the Oneida and Mohican grabens, enables us to tentatively subdivide these rift basins into three intervals (Figures 13, 26, 27):

(i) *early synrift* (basement/Tr250 to Tr225/Tr220);
(ii) *late synrift* (Tr225/Tr220 to J200);
(iii) *latest synrift to earliest postrift* (J200 to J163)

Two additional intervals capture sedimentation mainly after the rift basins had filled:

(iv) *early postrift* (J163 to J150);
(v) *early postrift* (J150 to K130)

The resulting thickness maps (Figures 28 through 32) provide insight into the temporal and spatial distribution of sediments. Regional patterns in seismic reflection character, calibrated to a small number of well ties, further constrains the stratigraphic development of rift basins on the central LaHave Platform. The change from rifting and associated extension-driven accommodation localized along border faults (i, ii), to accommodation driven by postrift thermal subsidence (iv, v), takes place between the J200 and J163 markers (iii). Note that basin inversion, salt tectonics, the time-transgressive nature of the postrift unconformity, as well as the inability to correlate the postrift unconformity into the thickest parts of distal rift basins with confidence, make it impossible to precisely separate synrift from earliest postrift strata.

Early synrift (Basement to Tr225; Basement to Tr220)

The early synrift fault-bound interval – represented by two separate thickness maps in Figure 28, is the thickest of the three synrift intervals discussed here and likely records the most time. Sediments are widely distributed in all of the rift basins on the central LaHave Platform. The early fill in each generally thins in the landward direction reflecting a combination of true stratigraphic thinning onto the hinged margin (e.g. Figures 15, 17a, 18, 21, 23a, 27), and erosion beneath the postrift unconformity (particularly in more landward rift basins; e.g. Figures 14, 17b, 17c).

The thickest deposits – exceeding 1500 ms (or roughly 3.4 km at 4.5 km/s) – are found centered above the floors of the Emerald, central and western Naskapi, Mohican, Acadia and eastern Abenaki grabens (Figure 28). The increased thickness in the eastern Mohican Graben between Figures 28a and 28b reflects the increased separation between the diverging Tr225 and Tr220 markers moving down the axis of the Mohican Graben. This indicates that rift accommodation increased towards the southwest stepping off the East Naskapi and East Mohican ridges at this time. The early synrift succession is anomalously thick in the central Emerald Graben, indicating perhaps the basement marker was correlated too deep here, an older prerift succession is present at the base of the fill, or, that there was simply more rift subsidence. On some seismic profiles in the Oneida Graben there is no angular unconformity capping the prerift succession, and without it the interval cannot convincingly be separated from locally conformably synrift strata. Such could be the case in the Emerald Graben. The early synrift interval is also anomalously thin in parts of the central Mohican Graben where basin

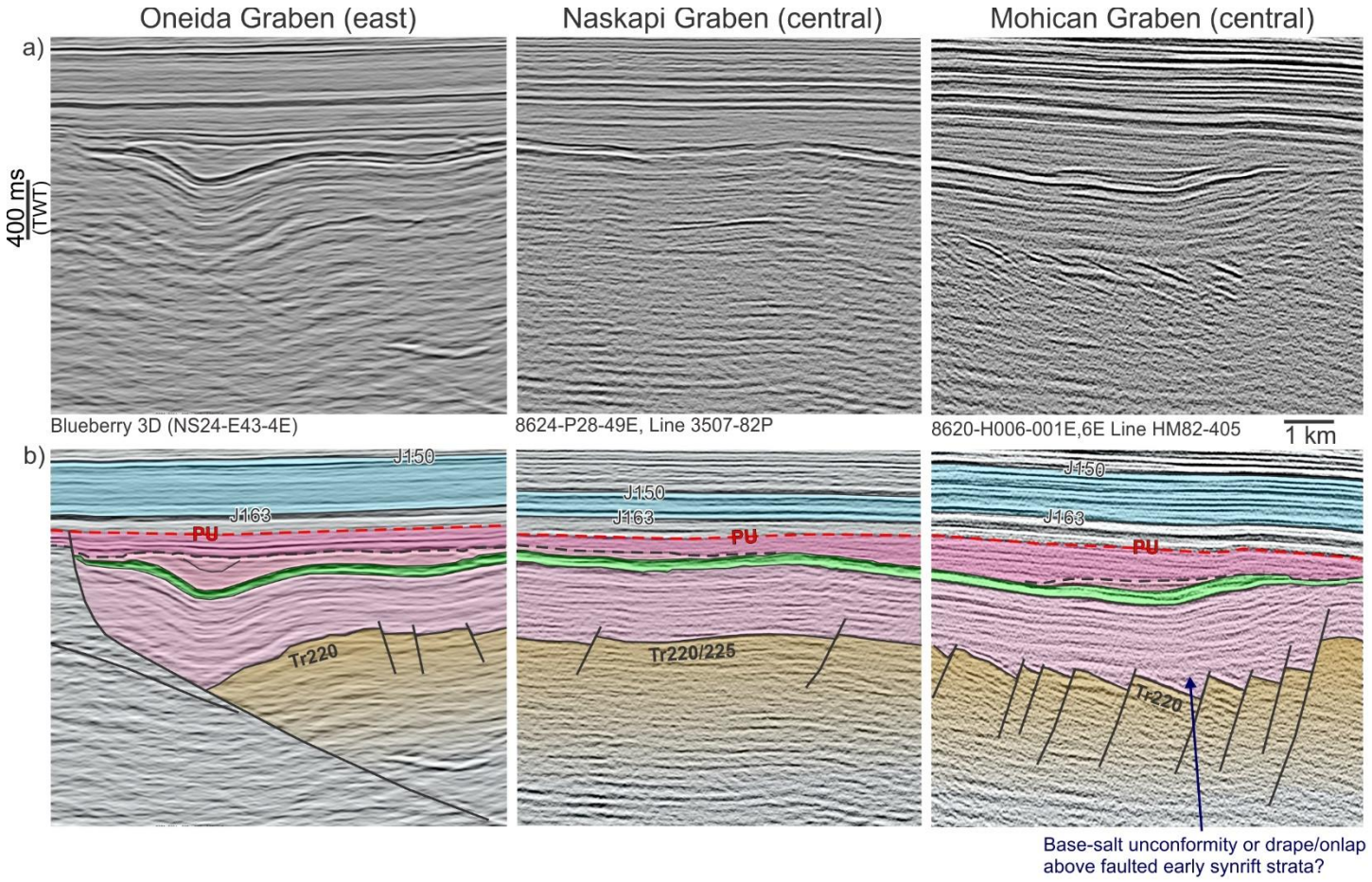

Figure 26 a) Uninterpreted and **b)** interpreted profiles across the eastern Oneida Graben, central Naskapi Graben, and central Mohican Graben, showing the remarkably similar seismic stratigraphic expression of synrift to early postrift strata, enabling jump correlations from one graben to another. Black dashed line corresponds to a late synrift unconformity; in the Oneida Graben it corresponds to a peneplain surface that truncates folded late synrift strata in the hanging wall. See Figure 6b for line location.

inversion took place (Figure 28b). The thinner succession here could be an artefact of miscorrelating the top basement surface across complex basement blocks that underlie the Moheida Ridge.

A closer look at the pre-Tr225/220 interval shows clustering of stronger and weaker reflections into three or four separate sub-intervals (e.g. Figures 14, 15, 17; labeled H for high, and L for low). These higher order variations in the stratigraphy cannot be widely correlated with the current dataset, and it is not clear what causes the variations in reflectivity. Sambro I-29 appears to sample the middle section of the early synrift interval, providing the *only* calibration of this succession anywhere on the Scotian margin (Figure 15). The abrupt thinning of the early synrift succession above the 'Sambro rider block' (Figure 28a) reflects prominent erosion along the postrift unconformity. The borehole encountered 1580 m of predominantly red mixed siliciclastics of probable Triassic age (note that no reliable biostratigraphy is available for this well). The steeply dipping reflections at the well location are poorly imaged, but the borehole does appear to go through an interval of brighter amplitude reflections immediately below the postrift unconformity (albeit less bright than those in the adjacent fault block) (Figure 15).

The upper 776 m of synrift strata at Sambro I-29 comprise interbedded shales, siltstones, and fine-grained sandstone that produce higher impedance contrasts on our synthetic tie, matching well with the slightly elevated reflection amplitude over the same interval on the seismic section. The interval contains numerous 4 to ~ 12 m thick sandstone beds with total porosity values from cores ranging from 20 to 24% and permeabilities up to 32 mD, with one 83 m thick conglomerate-rich interval with red clay matrix having little porosity or permeability (S. Rhyno, pers. comm. 2018). The dominantly shale to siltstone interval, with poorly developed sandstone beds in the bottom 804 m

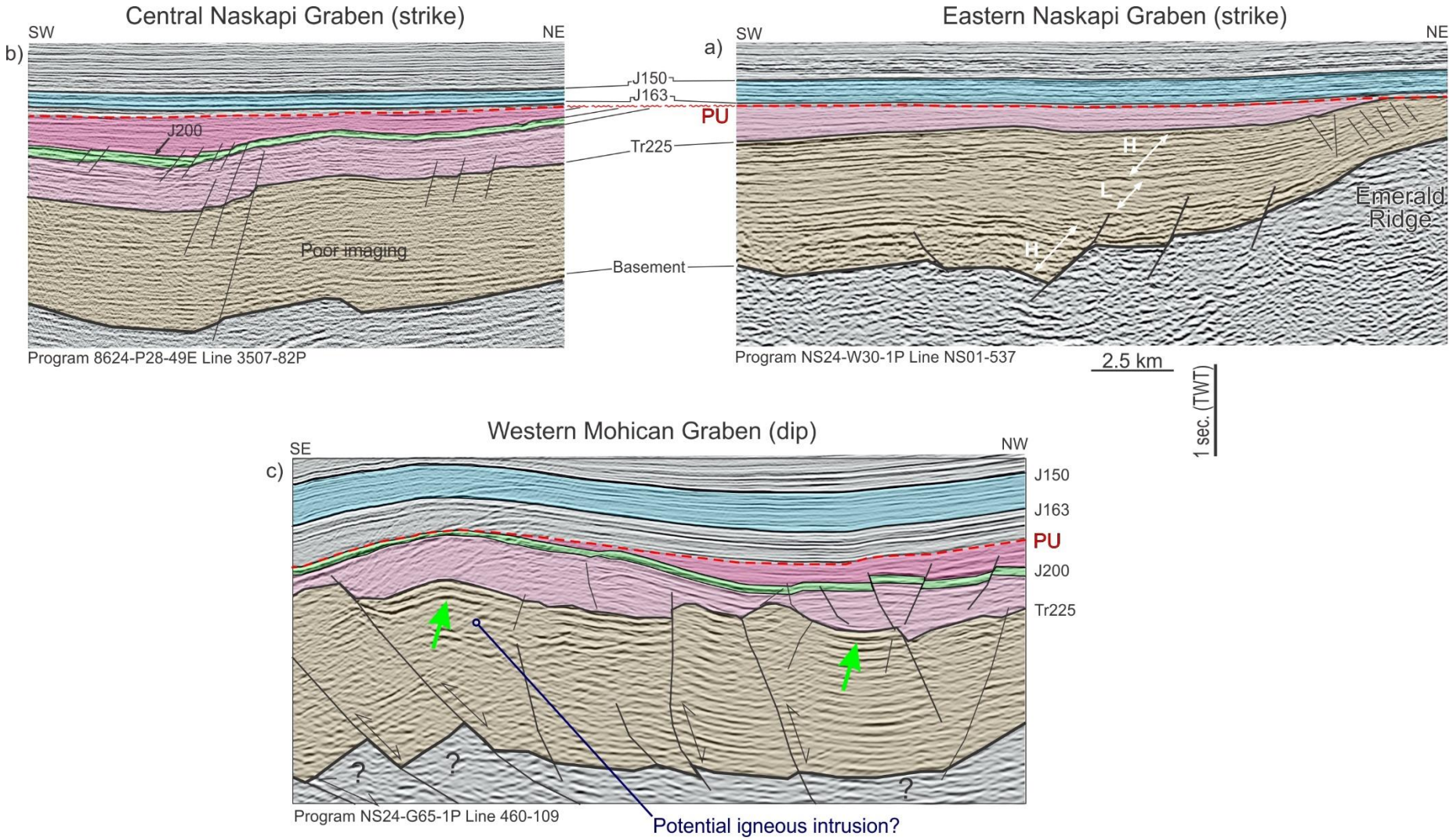

Figure 27 Axial profiles down **a)** eastern Naskapi Graben and **b)** central Naskapi Graben, and **c)** dip section across the western Mohican Graben, showing the subtle change in seismic facies between Tr225 and J200; based on calibration of this interval in the Mohican Graben (at Glooscap C-63), the increased continuity and reflectivity below the CAMP basalts is interpreted to correspond to an increase in interbedded evaporites (halite). See also Figure 26 for comparisons to the Mohican and Oneida grabens. Note the increased preservation of latest synrift and earliest postrift strata in the southwest plunging axes of both the Naskapi and Mohican grabens where more synrift and early postrift accommodation space developed. Also note the increased reflectivity of the Tr225 marker beneath the salt in the western Mohican Graben, which could indicate an increase in igenous activity (pre-salt extrusives or post-salt intrusive bodies) approaching areas of thinner continental crust beneath the present day slope (Deptuck 2018). See Figure 6b for line location.

of the well produce low impedance contrasts on our synthetic tie and coincide with a generally poorly imaged but low(?) reflectivity interval on seismic profiles. As such, at least some of the elevated reflection amplitudes in the early synrift succession coincide with higher net-to-gross intervals containing thicker sandstone and minor conglomerates. It is possible that some reflective intervals are produced by carbonates or carbonate-cemented sandstones, or perhaps even early synrift volcanics.

Late synrift (Tr220 to J200; Tr225 to J200)

The fault-bound late synrift interval – represented by two separate thickness maps in Figure 29 – is substantially thinner than the early synrift interval and probably records far less time; its distribution is also more localized, particularly in the northern rift basins. Here, the thickest deposits strongly skew towards the border faults of each rift basin, largely reflecting erosion along the postrift unconformity (Figure 29a). However, where the overlying J200 basalt marker is present, generally nearest the border fault or adjacent to large offset secondary faults where post-J200 rift-related accommodation was greatest, the late synrift succession has a relatively consistent thickness ranging from 600 to 850 ms (roughly 1.3 to 1.9 km thick at 4.5 km/s). Whereas landward truncation along the PU makes it impossible to determine whether there is stratigraphic thinning of the late synrift succession above the hinged margins of proximal rift basins like Emerald and East Emerald (e.g. Figures 14-16), the succession shows clear growth towards border faults in medial rift basins like Naskapi (e.g. Figure17b), indicating that slip along the border faults accommodated sedimentation (i.e. the late synrift succession in syn-tectonic).

The Emerald Graben forms two distinct basins at this time – with the thickest strata localized adjacent to its seaward-dipping border fault in the west, and its landward dipping border fault in the east (Figure 29a). Also, there appears to be very little to no preservation of late synrift strata in the region between the Kingsburg Graben (to the north) and the western Naskapi Graben (to the south), where numerous localized depocenters were present in the early synrift interval (compare Figure 28a and 29a). This could indicate this area was more widely elevated and eroded during the later stages of rifting, or that rift accommodation ceased here during the late synrift period.

The late synrift interval between Tr225 and J200 is by far the thickest in the eastern half of the Mohican Graben (Figure 29a), but this again reflects enhanced growth between the Tr225 and Tr220 seismic markers in the Mohican Graben at this time. Figure 29b shows the more modest thickness between the T220 and Tr200 markers seaward of the Naskapi Graben. Here, the succession is calibrated at Glooscap C-63 that encountered a 152 m thick interval of tholeiitic basaltic volcanics (Wade and MacLean 1990; Pe-Piper et al. 1992) above 441 m of Late Triassic halite (late Norian to Rhaetian; Weston et al. 2012) interbedded with meter-scale dolomite, red dolomitic shale and siltstone (Figure 19). The basalt marker ("Glooscap volcanic") produces the strong J200 seismic reflection, and interlayering between halite and finer grained sediments together produces a more reflective response on the synthetic tie, matching well with the distinctly layered appearance of this interval in the Mohican and Oneida grabens (Figure 26).

Overall, the interval thins as it onlaps the hinged margins of both grabens (e.g. Figure 21), and onlaps or drapes areas of increased accommodation above more heavily faulted older (pre-Tr220) synrift strata (e.g. Figures 18b and 19). On some profiles, its lower boundary may correspond to an unconformity that truncates more heavily faulted lower synrift strata (e.g. right side profile in Figure 26). In the Oneida Graben the late synrift interval is generally thickest above the hanging wall adjacent to the East Moheida Ridge, where both the salt and the overlying basalt marker are tightly folded and locally thrust upwards into inversion structures (e.g. Figure 22). In the Mohican Graben, it is locally thicker along the smaller scale "nested grabens" that formed along the basin axis, as well as along the main border faults adjacent to the Moheida Ridge. A similar interval with a distinctly layered and folded appearance resembling the salt-bearing succession at Glooscap C-63 is also recognized further landward, for example in the central parts of the Naskapi Graben (Figures 26, 27), the eastern part of the Emerald Graben, and on some profiles that cross the East Emerald Graben (see Figures 15 and 16).

Moheida P-15 – located 16 km southwest of Glooscap C-63 – sampled 255 m of generally finer grained but

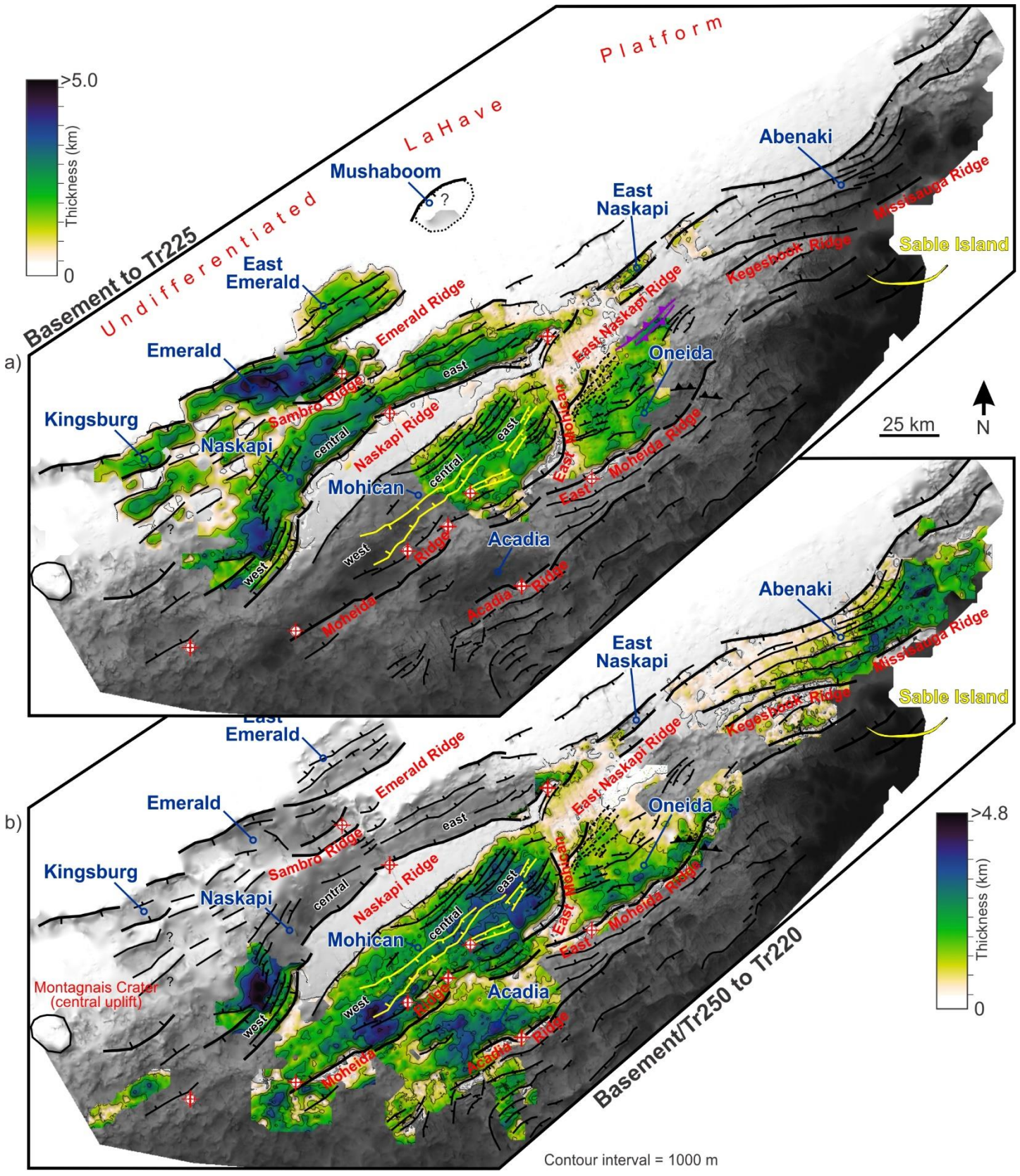

Figure 28 Isopach maps of the Basement to Tr225 interval (top) and the Basement/Tr250 to Tr220 interval (bottom), showing the *early synrift* fill correlated through the landward and seaward rift basins, respectively. Only Sambro I-29 in the Emerald Graben calibrates this interval. See text for details, and Figure 7b for legend.

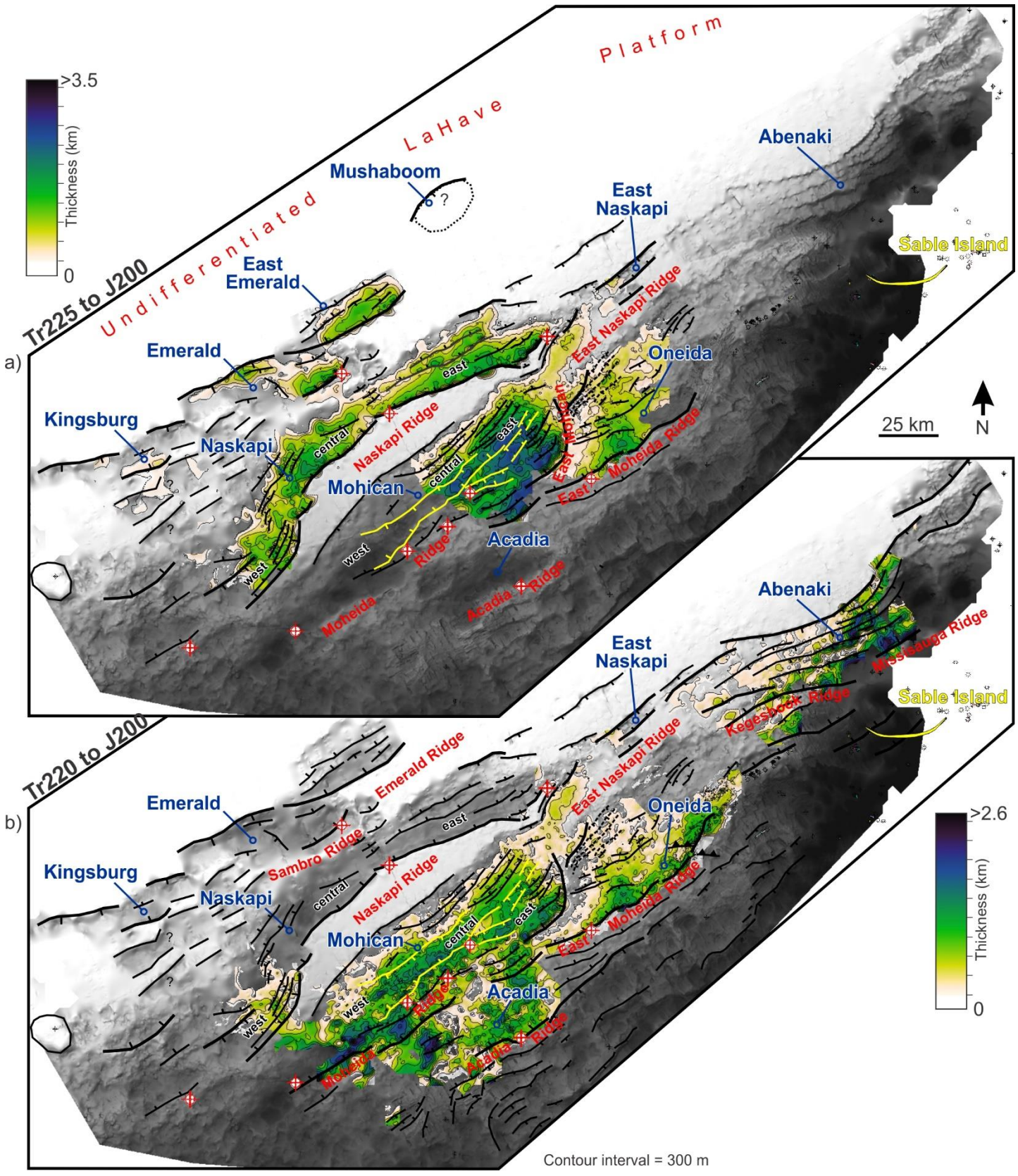

Figure 29 Isopach maps of the Tr225 to J200 interval (top) and Tr220 to J200 interval (bottom), showing the *late synrift* fill correlated through the landward and seaward rift basins, respectively. Both maps show area of potential Late Triassic salt deposition, calibrated below the J200 surface at Glooscap C-63 in the Mohican Graben. See text for details, and Figure 7b for legend.

heterolithic red beds (dolomitic shale, siltstone and poorly developed fine-grained sandstone) in a thinner, slightly less seismically layered late synrift interval that was folded above the Moheida Ridge (eroded from above by the postrift unconformity). The lack of evaporites at this location indicates lithofacies of the late synrift interval change over relatively short distances, perhaps in response to subtle variations in accommodation. It is possible Moheida P-15 was topographically elevated at the time of deposition compared to Glooscap C-63. The layered seismic facies produced by the evaporite-bearing succession at Glooscap C-63 also pass into a slightly less reflective interval with more discontinuous reflections in the northeast parts of the Mohican Graben, northwestern parts of the Oneida Graben, and eastern parts of the Naskapi Graben. A lithofacies transition to a more proximal shoreline setting with finer-grained siliciclastic strata lacking evaporites could account for this change.

The seismic facies of salt-bearing strata is increasingly incoherent moving down the plunging axes of the Mohican, Acadia and Abenaki grabens that step off the main platform (Figure 27). This may indicate that fewer finer grained clastic or dolomitic layers were laid down as salt accumulated in the deeper parts of rift basins (underpin by more strongly stretched crust), or could be a product of increased salt deformation and resulting degraded seismic imaging. In these areas, there is strong evidence for thin-skinned detachment of this salt-bearing succession above more heavily faulted older synrift strata. In some cases the salt has been mobilized in response to latest synrift or early postrift sediment loading, forming salt pillows and diapirs (e.g. Figures 18c, 20, 25).

Latest synrift to earliest postrift (J200 to J163)

Figure 30 shows the thickness of latest synrift to earliest postrift strata in the study area. Preserved strata are very thin and localized in landward areas like Kingsburg, Emerald and East Emerald, as well as the eastern Naskapi Graben. Here, strata are generally less than 300 ms thick and are present only along synclinal folds above the J200 marker immediately adjacent to border faults, or in the case of the eastern Naskapi Graben also adjacent to large offset secondary faults along its hinged margin. Outside these narrow fingers of increased accommodation/ preservation, the succession was removed entirely by the postrift unconformity, in turn overlain by Middle to Upper Jurassic coarse-grained lithologies of the Mic Mac and Mohawk formations (Figure 3) that form the lateral equivalent of the carbonate-dominated Abenaki Formation that aggraded above the J163 marker (described in the following section). The J200 to J163 succession thickens substantially stepping off the main platform, moving seaward and in particular down the southwest-plunging axes of the Naskapi, Mohican, and Acadia grabens, and down the east- to northeast-plunging axis of the Abenaki Graben. Here, up to 2 km of latest synrift to earliest postrift strata accumulated (Figure 30).

In the central and western parts of the Naskapi Graben, the succession is thickest where it is preserved in narrow fault-bound depocentres (e.g. Figure 27), thinning between the two graben segments (Figure 30). Here the succession appears to onlap the J200 marker, but in some places this could be an artefact caused by seismic ringing. In the Mohican Graben, strata are thickest along the main border faults of its central and western reach, and also above the folded J200 marker that was faulted downward along the axes of the narrow nested grabens found within the Mohican Graben (Figure 18b). These narrow grabens subsequently became the locus of inversion.

The J200 to J163 succession also thickens along a segmented longitudinal fold located adjacent to the main border fault in the Oneida Graben, forming a long and narrow depocentre (Figures 9 and 21). Improved seismic imaging in the small Blueberry 3D seismic survey (CNSOPB seismic program NS24-E43-4E), shows that this succession can be separated into three parts (as shown in Figure 26). A lower unit conformably overlies the J200 marker and, along with underlying pre-J200 strata, is deformed into a segmented hanginwall longitudinal fold located immediately adjacent to the East Moheida Ridge. A prominent angular unconformity truncates these strata. That the unconformity is offset across the border fault of the Oneida Graben indicates that basement extension continued after the folded interval was peneplained. A draping to onlapping middle interval overlies the angular unconformity, thickening above the hangingwall towards the border faults. The postrift unconformity (as we have correlated it; see earlier section) separates this middle draping to onlapping

interval from a generally landward thinning wedge of strata that onlap the postrift unconformity.

It is not always possible to distinguish these separate units, and no wells calibrate the deeper, older parts of the expanded succession in Figure 30 (lower or the middle units described above). This is because wells like Glooscap C-63, Moheida P-15 or Mohican I-100 were drilled above topographic highs where the lower units are cut out at the well location (e.g. Figure 19). In contrast, the upper parts of the expanded interval in Figure 30 (above the postrift unconformity) correspond to the platformal oolitic and bioclastic limestones of the Scatarie Member and underlying dolostones, tight sandstones and nodular to massive anhydrites of the Iroquois and Mohican formations (Figure 3) that have been penetrated and partly cored in a number of wells (e.g. Moheida P-15, Mohican I-100, Glooscap C-63, and Oneida O-35). Basement faults rarely offset the Iroquois and younger units, and hence deposition of these units occurred after lithospheric extension largely ended in the study area (i.e. Iroquois sedimentation was post-tectonic, at least in the study area; sensu Sutra et al. 2013). Therefore, the base of the poorly dated Iroquois Formation (which cannot be widely correlated on seismic profiles) approximates our postrift unconformity and likely closely corresponds to the end of lithospheric extension on the LaHave Platform.

In the westernmost part of the Mohican Graben, the eastern part of the Abenaki Graben, and above the Acadia Graben, distinguishing latest synrift from earliest postrift strata is further complicated where salt was expelled beneath minibasins that likely began to form in the late synrift, but continued to develop after lithospheric extension ended (e.g. Figures 18c, 20, 25).

Early postrift (J163 to J150 and J150 to K130)

Figure 31 shows the thickness of early postrift strata between the J163 and J150 markers. Numerous wells calibrate this Callovian to Tithonian interval deposited during a period dominated by carbonate sedimentation as the Abenaki Formation aggraded to form a broad carbonate bank with a well-developed bank edge/reef front and steep foreslope (Figure 11). Its heavily scalloped seaward edge parallels and directly overlies the East Moheida and Acadia ridges, but cuts obliquely across the Moheida and Naskapi ridges as well as the mouths of the Mohican and Naskapi grabens. The thickness distribution of sediment during this period was much more uniform than in any of the underlying successions. Overall, it forms a landward thinning wedge, with wells like Naskapi N-30, Ojibwa E-07, and Sambro I-29 showing that the interval becomes increasingly siliciclastic-rich in the landward direction where the Abenaki Formation passes laterally into the Mic Mac or Mohawk formations (Wade and MacLean, 1990).

The carbonate bank thickens above the western reaches of the Acadia, Mohican, and to a lesser extent the Naskapi grabens, and this likely reflects more rapid subsidence causing elevated carbonate aggradation rates above areas of continued salt expulsion. Thin-skinned faults locally offset both the J163 and J150 markers above the Acadia Graben in particular, soling into the primary salt layer (e.g. Figure 20). A slight increase in thickness of this interval takes place above the Oneida Graben, but a substantial increase in thickness exists in the easternmost study area above the Abenaki Graben (Figure 31). Here, the increase in clastic supply, particularly in the latter part of the interval (post Kimmeridgian), is believed to be linked at least in part to development of the Avalon Uplift (Jansa & Wade, 1975) affecting the region northeast of the study area, and redirected river systems westward, towards the Abenaki Graben (Deptuck et al. 2014; Deptuck and Kendell, 2017). The succession here was accommodated largely through the expulsion of late synrift salt, which must have been quite thick in the Abenaki Graben.

The overlying J150 to K130 interval (Figure 32) marks the beginning of a westward expansion of the fluvial-deltaic systems supplying siliciclastic to the eastern study area (corresponding to the lower to middle part of the Missisauga Formation; Figure 3), eventually blanketing the carbonate bank in the Lower and mid Cretaceous. This siliciclastic-dominated succession thickens substantially into the Abenaki and Sable Subbasins, where widespread salt expulsion took place. Deposits thin to the southwest, above the platform, where the interval corresponds to a condensed mix of carbonates and clastics forming the basal part of the Roseway Unit (Wade and MacLean 1990) that developed in areas further removed from siliciclastic sediment input (Figure 32).

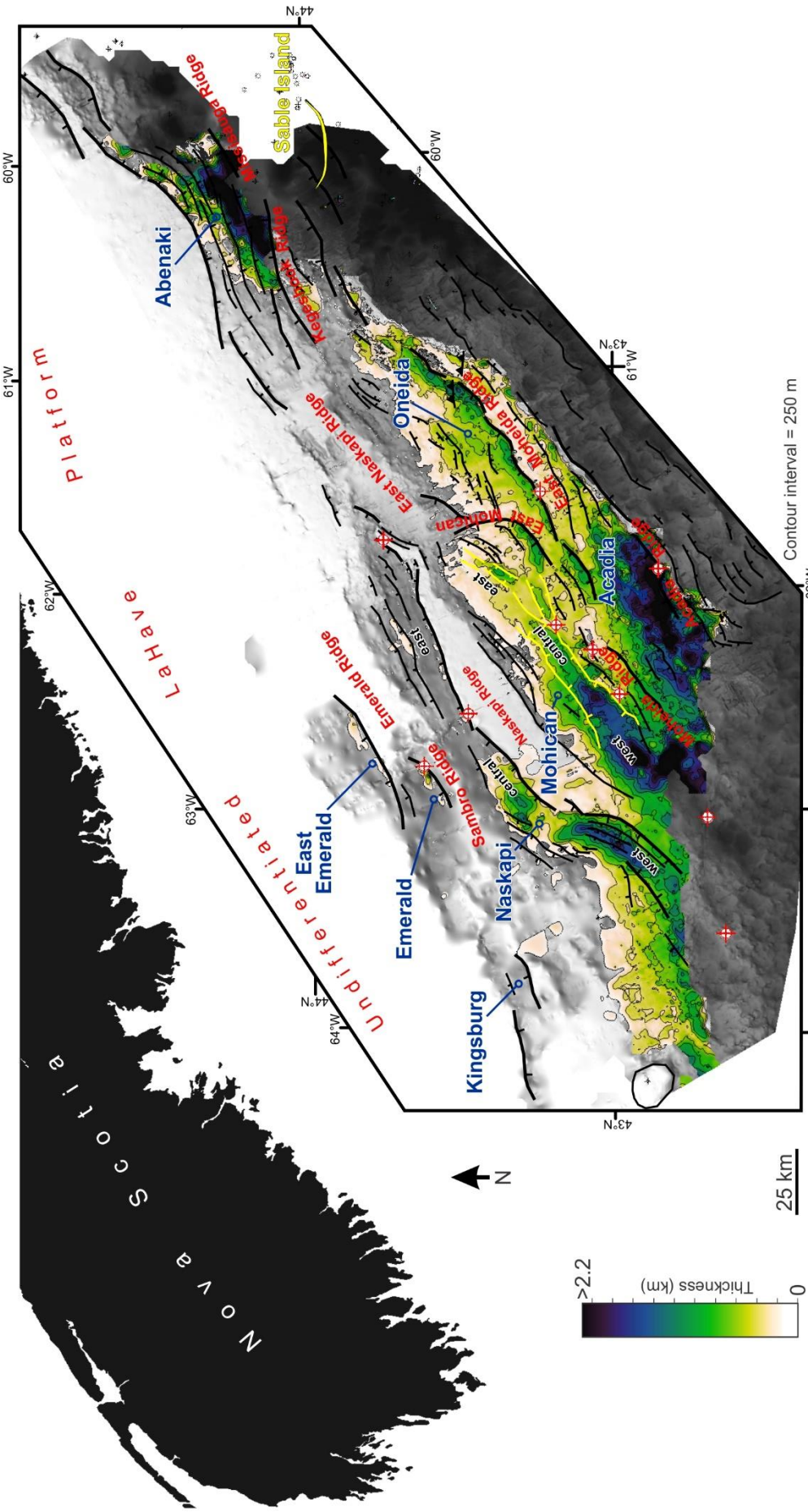

Figure 30 Isopach map between J200 and J163, showing *latest synrift to earliest postrift* strata deposited mainly in the western parts of the Naskapi, Mohican, and Acadia grabens, as well as in the Oneida and Abenaki grabens. See text for details, and Figure 7b for legend.

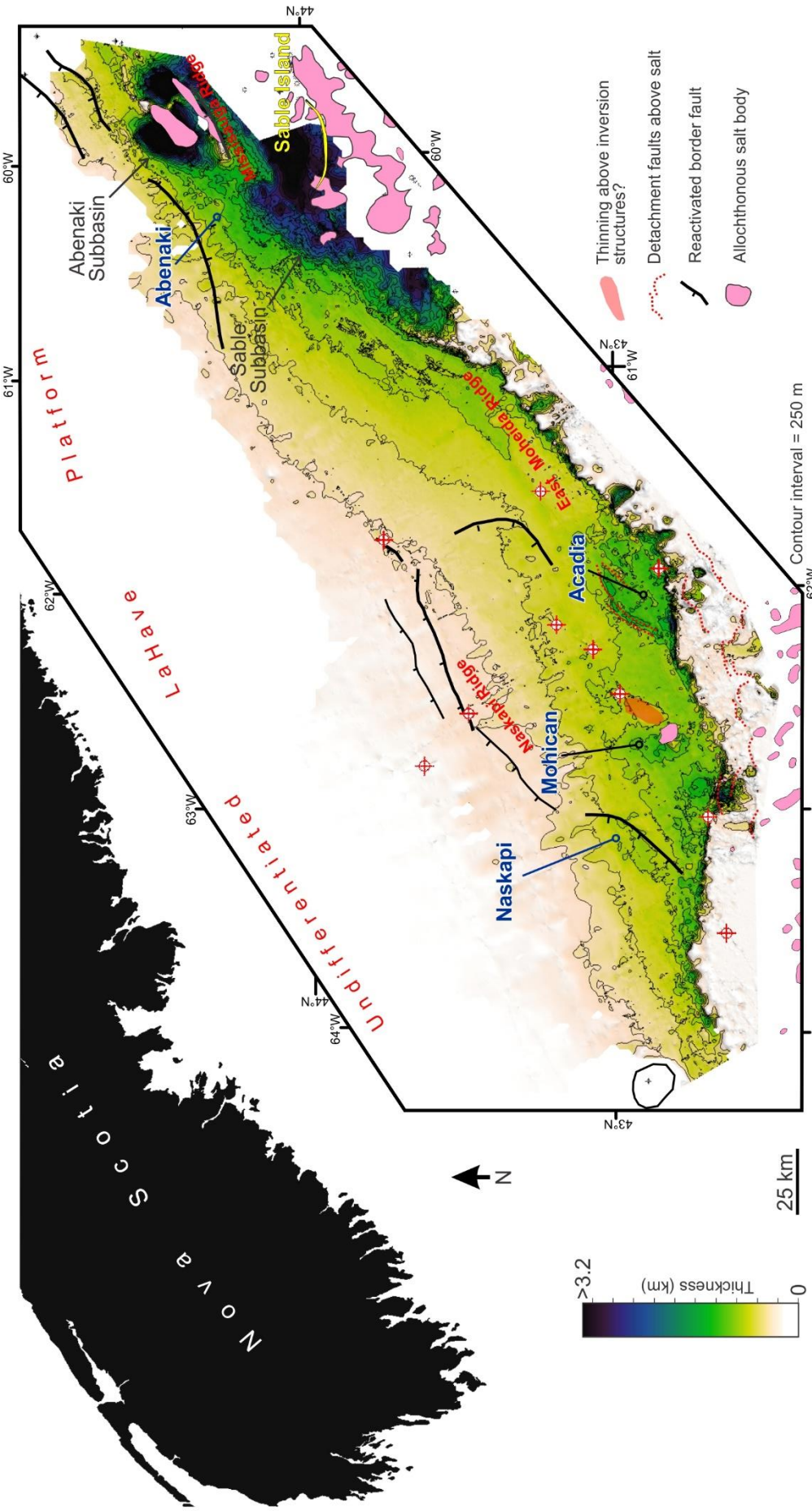

Figure 31 Isopach map between J163 and J150, showing *early postrift* strata deposited mainly in a rimmed carbonated platform in the west, and ramp margin with increased Middle and Late Jurassic clastic input in the east. Some of the thickness increase in the western parts of the Naskapi, Mohican, and Acadia grabens probably reflects increased subsidence here associated with salt expulsion. Location of the Sable and Abenaki subbasins described by Wade and MacLean (1990) and many others also shown. Allochthonous salt bodies from Deptuck and Kendell (2017).

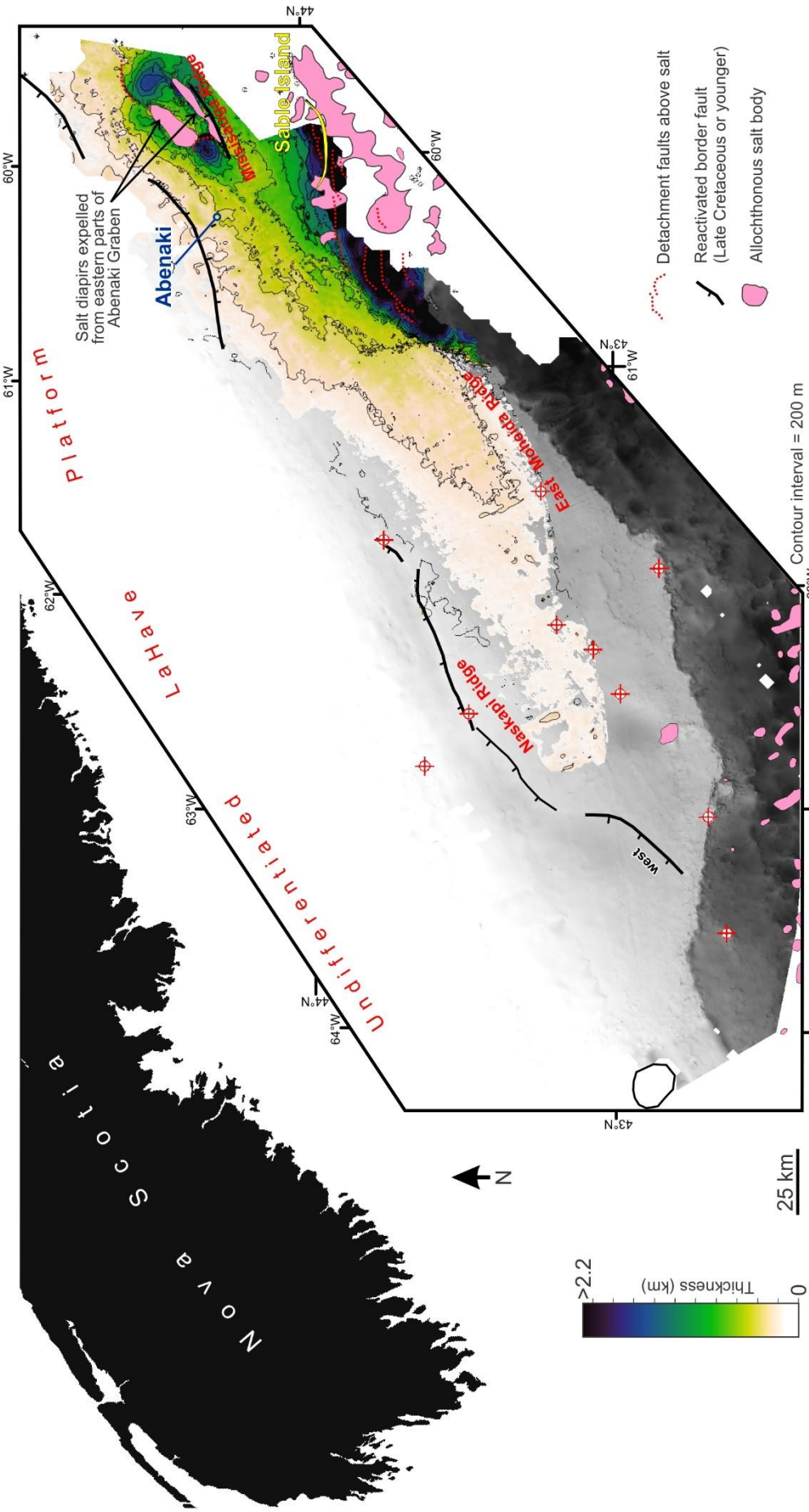

Figure 32 Isopach map between the J150 and K130 markers, showing the thickness distribution Lower to mid Missisauga Formation fluvial-deltaic clastics below the O-marker in the eastern study area, with thinning to the west where the succession contains more carbonates (distal from the main clastic source of the Sable Delta). Underlying greyscale image is the J150 marker. Allochthonous salt bodies from Deptuck and Kendell (2017).

6 Discussion

Prerift stratigraphy and deformation

MacLean and Wade (1992) speculated that prerift strata could floor some rift basins like the Orpheus Graben located northeast of the study area, but poor seismic imaging hindered their interpretations. The fill of the Oneida Graben is better imaged on seismic profiles, and provides the first glimpse into potential prerift sedimentary successions on the LaHave Platform (the Ojibwa Basin described earlier). Although there are hints on arbitrary lines that a similar succession may floor other rift basins, none of the available data is unequivocal. Likewise, no wells penetrate strata of the Ojibwa Basin, so we can only speculate about their age. Three scenarios are possible:

(i) Mid Paleozoic basin – eroded remnant of a Silurian (?) to early Devonian extensional or transtensional basin, later compressed during the Acadian Orogeny.

(ii) Late Paleozoic basin – eroded remnant of Latest Devonian to Late Carboniferous extensional or transtensional basin deformed by dextral transpression during the final assembly of Pangea (Alleghenian). Onshore examples of such basins are well documented above Meguma basement on mainland Nova Scotia (e.g. Kennetcook, Shubenacadie and Musquodoboit basins; Boehner 1984; Waldron et al. 2010; 2015)

(iii) Earliest synrift basin fill – the interval beneath the Tr250 unconformity is not a prerift succession, but rather an early synrift succession. In this scenario the Tr250 unconformity would represent a tectonic event separating early synrift (Late Permian to early Middle Triassic) from mid synrift strata. In the Fundy Basin, the (Late?) Permian Honeycomb Point Formation could be analogous (Olsen 1997; Sues and Olsen 2015).

The age of the strata in the Ojibwa Basin, and its subsequent shortening, is important both for academic reasons and for its implication on exploration potential. If the basin formed in the Silurian or Early Devonian, it implies extensional or transtensional forces existed within the Meguma block prior to final docking. It therefore could be related to the time-equivalent extension and rifting as the Meguma block separated from Gondwana (MacDonald et al. 2002; Pollock et al. 2012), with shortening produced during Acadian or later orogenesis. It is possible rocks of this age could contain organic-rich Silurian shales that are widespread in North Africa including Morocco (Lüning et al. 2000). Conversely, if it formed in the Late Devonian and earliest Carboniferous, the Ojibwa Basin would be contemporaneous with transtensional basins filled with Late Devonian to Late Carboniferous strata known further north, on mainland Nova Scotia and the large offshore Magdalen and Sydney basins. Deformation would then reflect dextral transpression during final docking of the Meguma Terrane during the final assembly of Pangea (Waldron et al. 2015). This scenario has implications for petroleum systems on the LaHave Platform. For example, Early Mississippian Horton Group fluvial-lacustrine successions have known source and reservoir rocks, and hydrocarbon occurrences, throughout Atlantic Canada, including production of oil and gas in onshore New Brunswick. If, instead, the strata in the Ojibwa Basin are related to the early Atlantic rift, it implies an earlier period of sedimentation and extreme inversion separates the early synrift succession from subsequent synrift strata.

The completely different tectonics - with dominantly compressional structures - argues against scenario (iii); we do not believe this is an early synrift succession. Likewise, Silurian to Early Devonian volcanic and sedimentary rocks in Nova Scotia (e.g. White Rock and Torbrook formations) are variably metamorphosed (e.g. MacDonald et al. 2002), and it is unlikely these rocks would produce a significantly different seismic reflection response than Meguma basement itself. The highly reflective and thrusted floor of the Ojibwa Basin is overlain by intervals of more heavily deformed strata with a more chaotic reflection character. These in turn are overlain by a layered but folded upper succession (Figures 21 and 24). Together, the succession strongly resembles the reflection seismic character of Late Paleozoic strata in both the Kennetcook Basin onshore Nova Scotia (Waldron et al. 2010) and known Late Paleozoic basins on the southern Grand Banks (Pascucci et al. 1999). Combined with the similarity in the dimensions and orientation of the Ojibwa Basin to the onshore Late Paleozoic Shubenacadie and

Musquodoboit basins (Boehner 1984), and exposures of Windsor Group rocks along the south shore of Nova Scotia, 200 km to the northwest (Giles 1981) (Figure 25), scenario (ii) is most likely to be correct.

The highly reflective basement below the Ojibwa Basin (Figures 21 and 24) could have been produced by a lower volcanic interval similar to the Late Devonian Fountain Lake Group, or alternatively could correspond to the base of the Windsor Group, known to produce a strong reflection (Waldron et al., 2010). The overlying more chaotic interval, with abrupt changes in thickness, would then correspond to an Early Carboniferous lower Windsor Group succession dominated by mobile halite salt (Ryan and Giles 2017). This in turn passes upwards into a folded layered succession that might correspond to mixed evaporites, mudstones, and limestones equivalent to the upper Windsor and lower Mabou groups, or potentially younger strata of the Cumberland Group that were partly accommodated by displacing lower Windsor salt prior to compression as is documented in the Cumberland Basin by Waldron et al. (2013).

The Ojibwa Basin probably underwent compression during the final assembly of Pangea, with erosion of underlying Carboniferous strata following soon thereafter prior to rifting (to form the Tr250 unconformity). As lithospheric extension began between Nova Scotia and Morocco, some compressional basement thrust faults were reactivated into extensional structures (e.g. Figure 21a), while other extensional faults appear to detach within the prerift succession, perhaps above weak basal Windsor Group salt (e.g. the thin-skinned listric faults in the landward parts of the Oneida Graben in Figure 21b).

Rift basin setting and regional structural trends

Most, if not all, of the border faults in the study area are listric at the scale of the upper crust and sole into mid-crustal detachments, indicating the study area lies entirely within the decoupled domain (*sensu* Sutra et al. 2013; i.e. deformation of brittle upper crust is decoupled from ductile mid/lower crust across shear zones). A refraction seismic profile (SMART 2 line; Wu et al. 2006), a closely coincidence deep reflection profile (Lithoprobe 88-1/1A; Keen et al. 1991), and recent unpublished regional correlation of reflection Moho and top basement (Deptuck 2018), provide information about crustal thickness beneath rift basins in the study area. Moderately stretched continental crust (25 to 30 km thick) underlies the landward rift basins in the study area (Mushaboom, East Emerald, Emerald, Kingsburg, Naskapi, East Naskapi, and Oneida), and thinner continental crust (15-20 km thick) underlies the seaward rift basin segments that plunge off the platform (western parts of Mohican, Acadia, and eastern parts of Abenaki). As such, using the terminology of Sutra et al. (2013) and Chenin et al. (2017) for magma poor margins, rift basins mapped in the landward study area developed in the "proximal domain" and those mapped in the seaward study area developed in the "necking domain" where Moho abruptly shallows and the top basement surface abruptly deepens beneath the modern slope (Table 1; e.g. Figure 33).

That the Middle to Upper Jurassic carbonate bank preferentially developed above and landward of the Moheida, Acadia, and East Moheida ridges is not a coincidence, as these basement elements are located at the transition from the proximal to the necking domains. The carbonate bank preferentially aggraded above thicker crust that experienced less overall and probably more gradual postrift thermal subsidence, while the steep carbonate foreslope preferentially developed above thinner tapered crust that experience more overall and probably more abrupt initial postrift thermal subsidence. As such, the carbonate bank edge/reef margin that separates the early postrift platform from the foreslope (Figure 11) forms a useful proxy for the boundary between these underlying crustal domains.

In terms of their dimensions, the Mohican and Oneida grabens, located in the seaward most proximal domain, are notably wider than both inboard and outboard grabens, but otherwise no obvious patterns emerge regarding rift basin size. A number of other general structural trends, however, do emerge from this study. With a few exceptions (Table 1), the most important border faults in the study area flank the seaward margins of rift basins and dip dominantly in the *landward* direction (to the northwest). Seaward-dipping faults do offset the hinged margins of some grabens (or graben segments), but in most cases these faults are steep and subordinate. Seaward of the Acadia and East Moheida ridges, however, there is a notable change in basement

fault polarity, with clear seaward-dipping border faults preferentially developing in thinner crust of the necking domain (Figures 5, 20). These faults show a substantial amount of later synrift offset (e.g. the top of the lower synrift succession is offset by more than 2 km across one such fault on the right side of Figure 20).

The structure of positive-relief basement elements also varies spatially. Basement elements flanking the more proximal East Emerald, Emerald, and Naskapi grabens are generally flat-topped and heavily eroded/ peneplained (e.g. Emerald, Sambro, and Naskapi ridges). Brittle upper crust here is generally between 7 and 12 km thick (assuming p-wave velocity of 5.5 km/s), separated from ductile middle to lower crust by topographically undulating shear zones. In contrast, seaward basement highs are more heavily fragmented and their relief is generally more irregular (e.g. Moheida, East Moheida, and Acadia ridges). Faulted intervals of synrift strata also commonly veneer seaward basement highs. These observations in part reflect a general seaward decrease in the degree of unroofing of basement and synrift strata beneath the postrift unconformity, but probably also reflect more complicated development of basement highs in areas of increasingly thinned crust (across the necking domain and into the hyperextended domain).

The presence of deformed and faulted synrift strata above distal basement elements like the Moheida, East Moheida, and Acadia ridges may reflect the increased tendency for border faults to migrate towards the hangingwall as rifting progressed in areas underpinned by thinner and weaker crust (e.g. basinward migration of footwall margins described by Dart et al. 1995). Alternatively, it is possible that some of the topographic expression of distal basement ridges was attained during later periods of lithospheric extension, with early synrift strata aggrading above more subdued early rift topography in the more distal axial parts of the rift system (with accumulation here resembling "pre-kinematic" or sag basin intervals, perhaps resembling the large-scale architecture depicted in figure 12b of Leleu et al. 2016).

Evidence for late synrift or early postrift inversion structures also increases in the seaward direction, for example above and adjacent to the Moheida and East Moheida ridges (e.g. Figures 10, 11, 17, 22). This observation is perhaps related to the increased susceptibility of thinner/weaker lithosphere to compressive deformation as noted by Lundin and Dore (2011). Brittle upper crust is generally < 7 km thick seaward of the Acadia and East Moheida ridges (assuming p-wave velocity of 5.5 km/s) and is increasingly fragmented. In some cases heavily faulted reflective intervals of lower synrift strata appear to directly veneer core complexes composed of ductile middle to lower crust (where brittle crust is absent; e.g. Figure 33). Here, middle to lower crustal flow appears to play an increasingly important role for distal extensional and compressional structures. Further, some distal basement faults appear to have remained active well into what has traditionally been considered the postrift period, supposedly dominated by thermal subsidence. Together, these observations reflect the increased structural complexity of basement elements within and seaward of the Mohican and Oneida grabens. It is, however, also increasingly difficult to distinguish late reactivation of basement-involved structures from salt related deformation moving in the seaward direction (e.g. Deptuck et al. 2009). A more comprehensive assessment of total crustal thickness, the distribution and character of brittle versus ductile crust, the structure of mid-crustal shear zones and reflection Moho, as well as the timing of deformation in the proximal, necking and hyperextended domains along the Scotian margin is beyond the scope of this report, but is currently underway (e.g. Deptuck 2018). The results should provide a clearer picture of how and when crust along the Scotian margin accommodated lithospheric extension.

In addition to early Mesozoic structural trends, this study also shows that a number of northeast-trending border faults were recently reactivated (post-Late Cretaceous) on the middle shelf, with their fault tips nearly reaching the seabed. Offset of seismic markers and local folds within Upper Cretaceous or younger hangingwall strata took place across the southern border faults of the Naskapi, the northern border fault of the Abenaki, and the southern border fault of the Erie grabens (Figures 7, 12; the latter is located in the easternmost study area, see also Kendell et al. 2013). Along-strike alignment of these faults and associated deformation indicates that a component of recent (post-Late Cretaceous) strike slip or reverse slip motion took place. What caused this late period of slip to nucleate along these northeast-trending

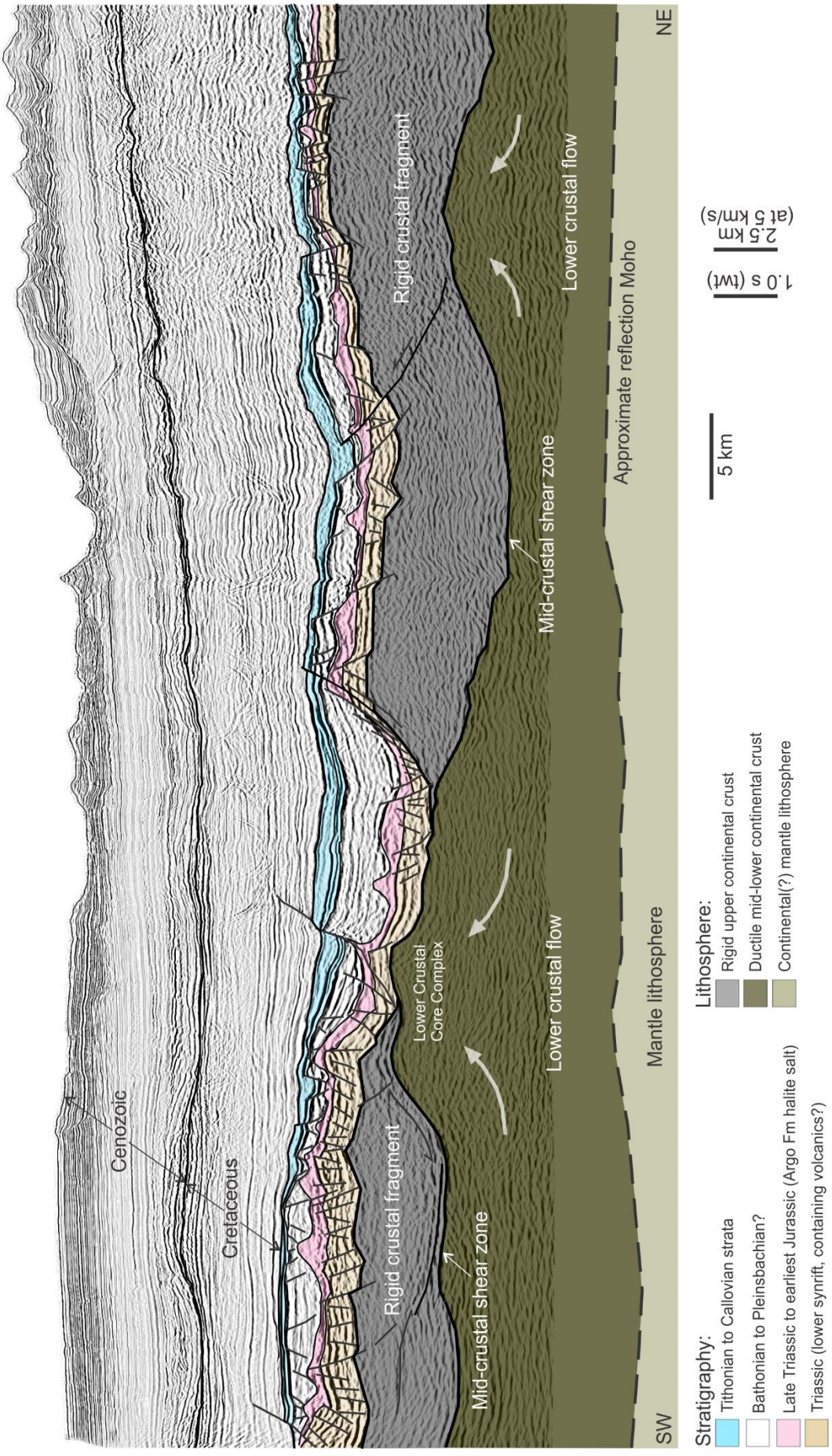

Figure 33 Composite strike line through the Thrumcap 3D seismic volume located seaward of the East Moheida Ridge (necking domain). Clear separation of brittle upper crustal fragments from ductile middle to lower crust indicates the crust in this distal transect is 'decoupled' across a mid-crustal shear zone (*sensu* Sutra et al. 2013). The pre-salt synrift interval is highly reflective, heavily faulted, and locally directly overlies ductile lower crust (forming lower crust core complexes).

basin-bounding faults is not known, but we note that a young period of compressional deformation is also recognized in the Orpheus Graben to the northeast (Figure 1) that Pe-Piper and Piper (2004) attributed to Oligocene reactivation of the Cobequid-Chedabucto fault system. If these events are synchronous, it increases the breadth of this young period of deformation to at least the eastern 500 km of the Scotian shelf.

Regional patterns in rift basin fill

Postrift erosion, variable seismic coverage and poor imaging in the study area commonly prevent direct correlation of seismic markers from one rift basin to another. Differences in vintage and acquisition/ processing parameters coupled with variations in vectorization results, and the presence of volcanics and mobile salt, also strongly affect seismic imaging and further hinder correlation efforts. Despite these challenges, several rift basins on the platform appear to show common vertical and in some cases lateral changes in seismic facies.

For example, in the eastern part of the Naskapi Graben, the deeper synrift succession below the Tr225 marker has a mixed but distinctly higher amplitude reflection character, and faults, sometimes densely spaced, are common (e.g. Figure 17). In contrast, later synrift strata between Tr225 and J200 produce a lower amplitude reflection response, and are capped by the very bright J200 basalt marker. The succession is commonly folded, less heavily faulted (except across border faults), and in some areas can be shown to pass laterally into a more reflective 'layered' successions (e.g. Figure 26) that at Glooscap C-63 correspond to halite interbedded with dolomitic shale. The fill of the Kingsburg, Emerald, and East Emerald grabens further landward is broadly similar to that of the Naskapi Graben (compare Figures 14, 15, and 16). Likewise, a similar succession is recognized in the adjacent Oneida and Abenaki grabens, and the Acadia Graben further seaward (though perhaps with a slightly dimmer character in the lower fill) (e.g. Figures 18 to 22, 25-27).

The thickness and reflection character of the lower synrift interval is quite variable. The succession is thickest above the platform, where it contains clusters of both high and low amplitude reflections (e.g. Figures 14ab, 15, 17ab). Sambro I-29 demonstrates that some of the elevated reflection amplitudes are produced by higher net:gross clastic intervals. Moving seaward of the Mohican and Oneida grabens there are fewer distinct high amplitude reflections, making it increasingly difficult to distinguish the early synrift succession from generally transparent brittle basement blocks (e.g. Figure 20). Further seaward still (seaward of the Acadia and East Moheida ridges), the lower synrift succession is comparatively thin and comprises a series of highly faulted reflective markers that directly veneer basement, and immediately underlie the primary salt layer (Figure 33; see also figure 8 of Deptuck and Kendell 2017). Some of these brighter reflections resemble volcanics (e.g. Figure 27c), but unlike the post-salt basalts at Glooscap C-63, these bright markers underlie the primary salt layer. Some of these complex markers could be products of post-salt intrusive igneous bodies, or pre-salt volcanic activity in areas underpin by the thinnest, most attenuated crust. It is also possible that some of these distal reflective intervals were produced by pre-salt carbonates, or more brittle mixed intervals of evaporites and non-evaporites.

The transition from the lower synrift to upper synrift units described in this study may coincide with the diachronous "fluvial to lacustrine transition" documented by Leleu et al. (2016) in a number of rift basins along the central Atlantic margin. The late synrift halite-bearing layered seismic facies in the Mohican Graben is also recognized in parts of the Naskapi, Emerald, and East Emerald grabens. This indicates that the landward limit of primary salt deposition is located further inland than recently suggested by Deptuck and Kendell (2017), who interpreted the Naskapi Ridge to have controlled the landward limit of the primary salt basin. Rather than a distinct salt basin edge, it appears that subtle changes in late synrift accommodation controlled facies development, particularly within the inboard-most grabens, with areas of increased accommodation accumulating thicker intervals of halite (perhaps where late synrift hypersaline lakes preferentially formed).

In contrast to the lower synrift succession, salt thickness in the upper synrift succession appears to increase in the seaward direction (Deptuck 2011). The increase in tall salt bodies (mostly stocks) above the seaward parts of the rift zone attests to the increase in salt thickness here,

consistent with the thickness distribution of late synrift salt documented in numerical models (Allen and Beaumont 2015). It is not clear if this reflects (i) increased accommodation approaching the axial zone of the rift system, (ii) a longer period of salt accumulation laterally equivalent to more proximal evaporitic and non-evaporitic facies, or (iii) salt flow towards the rift axis during the synrift or earliest postrift (Albertz et al. 2010; Goteti et al. 2011).

The separation of early, late, and latest synrift strata in the study area hinges on two main assumptions the reader should be aware of: (i) First, that the bright amplitude J200 volcanic marker calibrated at Glooscap C-63 is the same age everywhere, representing *extrusive* CAMP volcanics near the Triassic-Jurassic boundary. The volcanics are only preserved in areas where there was sufficient post-emplacement rift-related accommodation; they are eroded by the postrift unconformity elsewhere (for example above the hinged margin of most grabens). Nowhere can the volcanics from one rift basin be correlated directly into another; jump correlations were needed. (ii) Second, that where jump correlations of the base salt surface (Tr220) were necessary, that the start of salt deposition happened at roughly the same time throughout the study area. Comparing the late synrift interval penetrated at Glooscap C-63 and Moheida P-15 shows that abrupt lateral changes between evaporite and non-evaparite facies are present even within a single rift basin, so we know this assumption is incorrect. Dense seismic coverage provides constraints on marker correlation in the Mohican and Oneida grabens, but stepping seaward or to the northeast into the Abenaki Graben, for example, correlation of Tr220 was based largely on the recognition of the overlying autochthonous salt layer. If the interface between non-evaporite and evaporite facies is strongly diachronous (i.e. salt deposition began much earlier in Mohican Graben then in Abenaki Graben, or seaward, for example), the correlation into these areas will be erroneous. Nonetheless, at the moment no alternative regional approach is possible. We acknowledge the limitations caused by potential diachroneity in the base salt surface. Likewise, salt probably continued to accumulate in some areas (seaward? Orpheus Graben?) after it ceased in other areas (landward?), producing diachroneity in the top salt surface as well.

Although the boundaries between different seismic packages may be somewhat diachronous, that this succession is recognized in several rift basins implies their seismic stratigraphy and corresponding depositional systems are broadly controlled by processes at least at the scale of the LaHave Platform (e.g. climate or tectonics). See Olsen (1986; 1990; 1997), Leleu and Hartley (2010), and Leleu et al. (2016) for a more thorough discussion about potential broad-scale stratigraphic controls on Atlantic margin rift basins.

Exploration potential

Much of our understanding and perception of the synrift succession's exploration potential in Maritimes Canada comes from widely exposed synrift strata along the margins of the Fundy Basin (Figure 1), and a handful of offshore well penetrations. In addition to being the largest, the Fundy Basin is by far the best-studied rift basin off eastern Canada, containing up to 10 km of broadly fining-upward continental red-beds deposited in alluvial, fluvial, eolian, and playa-lacustrine settings (e.g. Wade et al. 1996; Olsen 1997; Leleu et al. 2009). Sedimentation was interrupted at 201 Ma when basaltic lava flows associated with the Central Atlantic Magmatic Province (CAMP) were emplaced (McHone 1996; Marzoli et al. 1999). The reservoir quality of Triassic and Lower Jurassic alluvial to fluvial deposits along its margins is mixed, and in some cases these deposits are heavily cemented (Wade et al. 1996; Redfern et al. 2010; Kettanah et al. 2013). In addition, the paleolatitude of the Fundy Basin would infer that much of its fill took place during periods of high aridity that were not conducive to synrift lacustrine source rock development (Olsen 1985; Kent et al. 1995; Kent and Tauxe 2005). If true, significant exploration challenges exist for the Fundy Basin and the rift basins that underpin the LaHave Platform described in this study.

However, the Fundy Basin is located more than 400 km from where the crust ruptured as the Atlantic Ocean opened, making it the most "continental" of the known eastern Canadian rift basins. Combined with the 100 km wide and topographically elevated landmass to its southeast (that today forms mainland Nova Scotia), the Fundy Basin was probably quite isolated from the poorly sampled rift basins on the central LaHave Platform. Further, most of its exposed rocks are along the edges of the basin, representing only 10% of the total buried

succession, and are probably not representative of deposits in basinal settings in the Fundy Basin itself (Wade et al. 1996), or more regionally in the severely under-sampled rift basins located up to 350 km further seaward.

It is difficult to evaluate the exploration potential of the rift basins beneath the LaHave Platform because so few wells penetrate the succession. Most potential hydrocarbon traps here consist of rotated basement blocks overlain by synrift fluvial (and possibly eolian) reservoirs deposited during rift extension and later sealed by latest Triassic salt (e.g. Figures 16, 18, 19). Inversion structures provide additional trap potential (Figures 18bc). This study has shown that there is a reasonable expectation that late synrift salt was more widely deposited across the central LaHave Platform rift zone than previously assumed (based on similarity of seismic facies to salt penetrated at Glooscap C-63), and thus could provide an effective regional seal in either of the above trapping scenarios. These plays, however, require either synrift lacustrine or prerift source rock intervals, neither of which is proven on the LaHave Platform.

In Mesozoic rift basins exposed in the northeastern United States, good quality oil-prone lacustrine source rocks are known in basins that formed in what have been interpreted as more favourable paleo-latitudes (Olsen 1985; Post and Coleman 2015). Brown (2014, 2015) interpreted lacustrine successions in deeper unsampled parts of the Fundy Basin, laterally equivalent to the early synrift fluvial succession exposed along the basins margins (Wolfville Formation). If correct, their older Carnian age places the region within or immediately adjacent to the tropic belt at that time, where wet climatic conditions would be more favourable for the creation (and preservation) of organic matter in long lived lakes (Brown, 2014). The absence of source rock intervals in Sambro I-29 (the only well to test the pre-salt synrift succession west of Orpheus Graben), however, makes this interpretation challenging for the early synrift strata on the LaHave Platform, unless the red beds it encountered are not representative of basinal early synrift depositional environments. We should note that the well did not reach basement, so the composition of earliest synrift successions remain unknown.

Other source rock intervals may be more likely. A number of oil, condensate, and gas discoveries have been made in similar rift basins in Morocco (e.g. Meskala field; Morabet et al. 1998; Mader et al. 2017), which was contiguous with the LaHave Platform before the Atlantic Ocean formed. In these basins, pre-rift successions (Silurian or Carboniferous) are the most likely source intervals for hydrocarbons now trapped in Triassic synrift fluvial reservoirs rotated above basement blocks, in turn sealed by late synrift salt (Tari et al. 2017). Carboniferous basins with known source rock intervals are present above both Meguma and Avalon basement in onshore areas of Nova Scotia and New Brunswick (see Langdon and Hall 1994, and Dietrich et al. 2011, and references therein). Source intervals include Upper Devonian or Mississippian black lacustrine shales and marine carbonates, as well as Pennsylvanian coal measures.

This study demonstrates the potential for prerift basins to underpin parts of the LaHave Platform (e.g. Ojibwa Basin), opening up new source rock or reservoir possibilities that could improve the regions perceived hydrocarbon potential and risk profile. Ultimately, however, this study demonstrates that acquisition of new modern seismic with substantially improved imaging is needed before either the synrift or prerift successions beneath the LaHave Platform can be properly evaluated.

Conclusions

1. Ten separate rift basins and one candidate prerift basin were identified and mapped on the central Lahave Platform. Rift basins range from <45 to >160 km long and up to 40 km wide, containing as much as 6 km of strata.

2. Changes in basement topography, along with changes in bulk sediment thickness beneath the postrift unconformity, mark the transition from one rift basin to another. Basins are commonly interconnected across accommodation zones marked by intricate fault arrays, flexures (relay zones), and less commonly more sharply defined transfer faults (e.g. eastern limit of Emerald Graben).

3. The Mushaboom, East Emerald, Emerald, Kingsburg, East Naskapi and Naskapi grabens are restricted to the platform (proximal domain), whereas the axes of the Mohican, Acadia, and Abenaki grabens plunge off the platform either to the southwest or to the northeast,

where the underlying continental crust abruptly thins in the necking domain.

4. Eight of the ten rift basins are classified as predominantly half graben structures. Their hinged (flexural) margins are heavily eroded, with the opposing border fault margin having increased accommodation and preserving the thickest and youngest graben fill. Landward-dipping (antithetic; towards the northwest) border faults flank five basins (East Emerald, Naskapi, Mohican, Acadia, and Oneida), with a seaward-dipping fault (synthetic; towards the southeast) flanking just one (Mushaboom). Two form hybrids (Kingsburg and Emerald) with border faults (and opposing eroded hinged margins) switching from the landward to the seaward side in the same rift basin. Only two of the basins (Abenaki and East Naskapi) are classified as true grabens with opposing border fault margins over most of their lengths.

5. Most rift basins show similar patterns in their fill – a lower more reflective and heavily faulted early synrift succession is overlain by a generally lower amplitude late synrift succession that is cut by fewer faults and is commonly folded along border faults. Sambro I-29 penetrating a sharply truncated and incomplete lower synrift succession in the Emerald Graben, composed mainly of poorly dated mixed-grade red beds. Glooscap C-63, Moheida P-15, and Mohican I-100 penetrate an incomplete upper synrift succession in the Mohican Graben composed mainly of late Norian to Rhaetian (Weston et al. 2012) halite or red fine-grained dolomitic siliciclastics, or some combination of the two. No other wells calibrate synrift strata in the study area.

6. Seismic facies consistent with the Late Triassic salt penetrated at Glooscap C-63 (Mohican Graben) were identified in segments of seven rift basins, three of which (Mohican, Acadia, and Abenaki) also contain salt diapirs along their seaward-plunging peripheries. Salt stocks are increasingly common towards the distal necking domain and in areas underpin by hyperextended crust just seaward of the study area.

7. CAMP-related volcanics (also calibrated at Glooscap C-63) were correlated into six grabens (on the basis of reflection seismic character and stratigraphic position), where they are best preserved on the hanging walls adjacent to border faults and large displacement secondary faults where accommodation was greatest.

8. Four rift basins (Naskapi, Mohican, Acadia, and Abenaki) contain significantly expanded intervals of latest synrift to earliest postrift fill (accommodated at least in part by salt expulsion). The lower part of this succession probably accumulated in the Lower Jurassic, after the CAMP event, but the interval has not been calibrated by any wells in the study area.

Acknowledgements – John Martin and Anita Nicoll are thanked for helping assemble the seismic database and Shaun Rhyno is thanked for editing petrophysical logs and calculating effective porosity and permeability in the Sambro I-29 well. Carl Makrides and Troy MacDonald helped keep this project on course; Kris Kendell and Brent Smith interpreted the easternmost parts of the J150 and K130 seismic markers in the Sable Subbasin and are thanked for helpful discussions. My appreciation also goes to John Waldron for helpful early discussions about the Ojibwa Basin. Reviews by Kris Kendell and David Brown sharpen the final version.

Recommended citation

Deptuck, M.E. and Altheim, B. (2018) Rift basins of the central LaHave Platform, offshore Nova Scotia. CNSOPB Geoscience Open File Report 2018-001MF, 54 p. https://www.cnsopb.ns.ca/geoscience-publications/geoscience-reports

References

Albertz, M., Beaumont, C., Shimeld, J. W., Ings, S. J. and Gradmann, S. (2010) An investigation of salt tectonic structural styles in the Scotian Basin, offshore Atlantic Canada: 1. Comparison of observations with geometrically simple numerical models. Tectonics, 29, TC4017. doi:10.1029/2009TC002539

Allen, J. and Beaumont, C. (2015) Continental margin syn-rift salt tectonics at intermediate width margins, Basin Research, p. 1–36, doi: 10.1111/bre.12123

Boehner, R.C. (1984) Stratigraphy and depositional history of marine evaporites in the Windsor Group, Shubenacadie and Musquodoboit structural basins, Nova Scotia, Canada. Ninth International Congress on Carboniferous Stratigraphy and Geology, 1979 Compte Rendu, v. 3, p. 163-178.

Brown, D.E. (2015) Lacustrine source rock potential in the Middle Triassic – Early Jurassic Chignecto Subbasin, offshore Eastern Canada. In: P.J. Post, J.L. Coleman Jr., N.C. Rosen, D.E. Brown, T. Roberts-Ashby, P. Kahn and M. Rowan (eds) Petroleum Systems in "Rift Basins", 34th Annual Gulf Coast Society – Society of Economic Paleontologists and Mineralogists Perkins-Rosen Research Conference, Houston Texas, December 13-16, 2015, p.8.

Brown, D.E. (2014) Lacustrine source rock potential in the Middle Triassic – Early Jurassic Chignecto Subbasin, offshore Eastern Canada. Geological Association of Canada/ Mineralogical Association of Canada Annual Meeting, University of New Brunswick, Fredericton, New Brunswick, May 21-23, 2014.

Chenin, P., Manatschal, G., Picazo, S., Muntener, O., Karner, G., Johnson, C., and Ulrich, M. (2017) Influence of the architecture of magma-poor hyperextended rifted margin on orogens produced by the closure of narrow versus wide oceans, Geosphere, v. 13 p. 559-576.

Cummings, D.C., and Arnott, R.W.C. (2005) Growth-faulted shelf-margin deltas: a new (but old) play type, offshore Nova Scotia. Bulletin of Canadian Petroleum Geology, v. 53, p. 211-236.

Cummings, D.C., Hart, B.S., and Arnott, R.W.C. (2006) Sedimentology and stratigraphy of a thick, areally extensive fluvial-marine transition, Missisauga Formation, offshore Nova Scotia and its correlation with shelf margin and slope strata. Bulletin of Canadian Petroleum Geology, v. 54, p. 152-174.

Dart, C., Cohen, H.A., Akyuz, H.S., and Barka, A. (1995) Basinward migration of rift-border faults: Implication for facies distribution and preservation potential, Geology, v. 23, p. 69-72.

Dehler, S.A. and Roest, W.R. (1998) Gravity anomaly map, Atlantic Region, Canada. Geological Survey of Canada Open File 3658, Scale 1:3,000,000

Deptuck, M.E. (2008) NS08-2 Call for Bids – Sub-regional geology and exploration potential for Parcels 1 and 2, Central Scotian Slope. 40 p. https://www.cnsopb.ns.ca/geoscience-publications/geoscience-reports

Deptuck, M.E. (2011) Proximal to distal postrift structural provinces on the western Scotian Margin, offshore Eastern Canada: Geological context and parcel prospectivity for Call-for-Bids NS11-1, Canada-Nova Scotia Offshore Petroleum Board, Geoscience Open File Report (GOFR) 2011-001MF, 42p. https://www.cnsopb.ns.ca/geoscience-publications/geoscience-reports

Deptuck, M.E. (2018) Insights into crustal structure and rift basin development off central and western Nova Scotia – a reflection seismic perspective, Conjugate Margins Conference, Halifax, Nova Scotia, Atlantic Geology, v.54, p. 421.

Deptuck, M.E., Kendell, K. and Smith, B. (2009) Complex deepwater fold-belts in the SW Sable Subbasin, offshore Nova Scotia, Extended Abstract, 2009 CSPG CSEG CWLS Convention, Calgary, Alberta, 4 p. https://www.cnsopb.ns.ca/geoscience-publications/presentations-abstracts

Deptuck, M.E. and Campbell, D.C. (2012) Widespread erosion and mass failure from the ~51 Ma Montagnais marine bolide impact off southwestern Nova Scotia, Canada. Canadian Journal of Earth Sciences, v. 49(12), p. 1567-1594.

Deptuck, M.E., Kendell, K., Brown, D. and Smith, B. (2014) Seismic stratigraphic framework and structural evolution of the eastern Scotian Slope: geological context for the NS14-1 Call for Bids area, offshore Nova Scotia. CNSOPB Geoscience Open File Report 2014-001MF, 58 p. https://www.cnsopb.ns.ca/geoscience-publications/geoscience-reports

Deptuck, M.E., Brown, D.E. and Altheim, B. (2015). Call for Bids NS15-1 – Exploration history, geologic setting, and exploration potential: Western and Central regions. CNSOPB Geoscience Open File Report 2015-001MF, 49 p. https://www.cnsopb.ns.ca/geoscience-publications/geoscience-reports

Deptuck, M.E. and Kendell, K.L. (2017) Chapter 13: A review of Mesozoic salt tectonics along the Scotian margin, eastern Canada, In: J. Soto, J. Flinch, and G. Tari, (Eds), Permo-Triassic Salt Provinces of Europe, North Africa and Central Atlantic: Tectonics and Hydrocarbon Potential, Elsevier, p. 287-312.

Eliuk, L.S. (1978) The Abenaki Formation, Nova Scotia Shelf, Canada - A depostional and diagenetic model for a Mesozoic carbonate platform. Bulletin of Canadian Petroleum Geology, v. 26, p.424-514.

Fensome, R.A., Crux, J.A., Gard, I.G., MacRae, R.A., Williams, G.L., Thomas, F.C., Fiorini, F., and Wach, G.

(2008) The last 100 million years on the Scotian Margin, offshore eastern Canada: an event-stratigraphic scheme emphasizing biostratigraphic data. Atlantic Geology, v. 44, p. 93-126.

Giles, P.S. (1981) The Windsor Group of the Mahone Bay Area, Nova Scotia. Nova Scotia Department of Mines and Energy Paper 81-3, 59p.

Given, M.M. (1977) Mesozoic and Early Cenozoic geology of offshore Nova Scotia, Bulletin of Canadian Petroleum Geology, v. 25, p. 63-91

Goteti, R., Beaumont, C., Ings, S.J. (2013) Factors controlling early stage salt tectonics at rifted continental margins and their thermal consequences, J. Geophys. Res. Solid Earth, 118, doi:10.1002/jgrb.50201

Jansa, L.F., and Wade, J.A. (1975) Geology of the continental margin off Nova Scotia and Newfoundland. In W.J.M. Van Der Linden and J.A. Wade (eds), Offshore Geology of Eastern Canada, Geological Survey of Canada Paper 74-30, v. 2, p. 51-105.

Kendell, K.L., Smith, B.M. and Brown, D.E. (2013) Geological context and parcel prospectivity for Call for Bids NS13-1: Seismic interpretation, source rocks and maturation, exploration history and potential play types of the central and eastern Scotian Shelf. CNSOPB Call for Bids Summary Document, 64p. https://www.cnsopb.ns.ca/geoscience-publications/geoscience-reports

Kent, D.V. and Tauxe, L. (2005) Corrected Late Triassic latitudes for continents adjacent to the North Atlantic. Science, v. 307, p. 240-244.

Kent, D.V., Olsen, P.E., and Witte, W.K., (1995) Late Triassic-earliest Jurassic geomagnetic polarity sequence and paleolatitudes from drill cores in the Newark rift basin, eastern North America. Journal of Geophysical Research – Solid Earth, 100 (B8), p. 14,965-014,998.

Kettanah, Y.A., Kettanah, M.Y., and Wach, G.D. (2013) Provenance, diagenesis and reservoir quality of the Upper Triassic Wolfville Formation, Bay of Fundy, Nova Scotia, Canada. In: R.A. Scott, H.R. Smyth, A.C. Morton, and N. Richardson (eds), Sediment Provenance Studies in Hydrocarbon Exploration and Production. Geological Society of London Special Publication 386, 37 p.

Kidston, A.G., Brown, D.E., Smith, B.M., and Altheim, B. (2005) The Upper Jurassic Abenaki Formation, offshore Nova Scotia: A seismic and geologic perspective, Canada Nova Scotia Offshore Petroleum Board, Halifax, Nova Scotia, 168 p. https://www.cnsopb.ns.ca/geoscience-publications/geoscience-reports

Kontak, D.J. and Archibald, D.A. (2003) $^{40}Ar/^{39}Ar$ age of the Jurassic North Mountain Basalt, southwestern Nova Scotia, Atlantic Geology, v. 39, p. 47-53

Leleu, S., Hartley, A.J. and Williams, B.P.J. (2009) Large-scale alluvial architecture and correlation in a Triassic pebbly braided river system, lower Wolfville Formation (Fundy Basin, Nova Scotia, Canada). Journal of Sedimentary Research, v. 79, p. 266-286.

Leleu, S. and Hartley, A.J. (2010) Controls on the stratigraphic development of the Triassic Fundy Basin, Nova Scotia: implications for the tectonostratigraphic evolution of Triassic Atlantic rift basins. Journal of the Geological Society, London, v. 167 p. 437-454.

Leleu, S., Hartley, A.J., van Oosterhout, C., Kennan, L., Ruckwied, K., and Gerdes, K. (2016) Structural, stratigraphic and sedimentological characterisation of a wise rift system: The Triassic rift system of the Central Atlantic Domain, Earth-Science Reviews, v.158, p. 89-124.

MacLean, B.C. and Wade, J.A. (1992) Petroleum geology of the continental margin south of the islands of St. Pierre and Miquelon, Offshore Eastern Canada, Bulletin of Canadian Petroleum Geology, v. 40, p. 222-253.

Mader, N.K., Redfern, J., and Ouataoui, M.U. (2017) Sedimentology of the Essaouira Basin (Meskala Field) in context of regional sediment distribution patterns during upper Triassic pluvial events. Journal of African Earth Sciences, v. 130, p. 293-318.

MacDonald, L.A., Barr, S.M., White, C.E., and Ketchum, J.W.F., (2002) Petrology, age, and tectonic setting of the White Rock Formation, Meguma terrane, Nova Scotia: evidence for Silurian continental rifting. Canadian Journal of Earth Sciences, v. 39, p. 259-277.

Marzoli, A., Renne, P.R., Piccirillo, E.M., Ernesto, M., Bellieni, G. & De Min, A. (1999) Extensive 200-million-year-old continental flood basalts of the Central Atlantic magmatic province. Science, v. 284, p. 616–618.

McHone, J. G. (1996) Broad-terrane Jurassic flood basalts across northeastern North America. Geology, v. 24, p. 319-322.

McIver, N.L., (1972) Cenozoic and Mesozoic Stratigraphy of the Nova Scotia Shelf. Canadian Journal of Earth Sciences, v. 9, p 54-70

Morabet, A.M., Bouchta, R. and Jabour, H. (1998) An overview the petroleum systems of Morocco. In: D.S. MacGregor, R.T.J. Moody, and D.D. Clark-Lowes (eds) Geological Society of London Special Publication, 132, p. 283-296.

Morley, C.K., Nelson, R.A., Patton, T.L., and Munn, S.G., (1990) Transfer zones in the East African Rift System and their relevance to hydrocarbon exploration in rifts. AAPG Bulletin v. 74, p. 1234-1253.

Oakey, G.N. and Dehler, S.A. (2004) Magnetic anomaly map, Atlantic Canada region, Atlantic Canada. Geological Survey of Canada Open File 1813, Scale 1:3,000,000

OETR (2011) Play Fairway Analysis Atlas - Offshore Nova Scotia, Nova Scotia Department of Energy Report, NSDOE Records Storage File No. 88-11-0004-01, 347p. http://www.offshoreenergyresearch.ca/OETR/OETRPlayFairwayProgramMainPage/tabid/402/Default.aspx

Olsen, P.E. (1985) Distribution of organic-matter-rich lacustrine rocks in the early Mesozoic Newark Supergroup. In: G.R. Robinson Jr. and A.J. Froelich (eds), Proceedings of the 2nd USGS Workshop on the Early Mesozoic Basins of Eastern United States, United States Geological Survey, Bulletin 946, p. 61-64.

Olsen, P.E. (1986) A 40-million year lake record of early Mesozoic climate forcing. Science, v. 234, p. 842-848

Olsen, P.E. (1990) Tectonic, climatic and biological modulation of lacustrine ecosystems: examples from the Newark Supergroup of eastern North America. In: B. Katz (ed), Lacustrine Basin Exploration, American Association of Petroleum Geologists, Memoir 50, p. 209-229.

Olsen, P.E. (1997) Stratigraphic record of the early Mesozoic breakup of Pangea in the Laurasia-Gondwana rift system. Annual Reviews of Earth and Planetary Science, v. 25, p. 337-401.

Pascucci, V. Gilbing, M.R., and Williamson, M.A. (1999) Seismic stratigraphic analysis of Carboniferous strata on the Burin Platform, offshore Eastern Canada. Bulletin of Canadian Petroleum Geology, v. 47, p. 298-316.

Paul, D. and Mitra, S. (2013) Experimental models of transfer zones in rift systems. AAPG Bulletin, v. 97, p. 759-780.

Pe-Piper, G. and Jansa, L.F. (1999) Pre-Mesozoic basement rocks offshore Nova Scotia, Canada: new constraints on the origin and Paleozoic accretionary history of the Meguma terrane, Bulletin of the Geological Society of America, v. 111, p. 1773-1791

Pe-Piper, G. and Piper, D.J.W. (2004) The effects of strike-slip motion along the Cobequid-Chedabucto-southwest Grand Banks fault system on the Cretaceous-Tertiary evolution of Atlantic Canada, Canadian Journal of Earth Sciences, v. 41, p. 799-808

Piper, D.J.W., Pe-Piper, G. and Ingram, S.C. (2004) Early Cretaceous sediment failure in the southwestern Sable Subbasin, offshore Nova Scotia. Bulletin of American Association of Petroleum Geologists v. 88, p. 991-1006.

Piper, D.J.W., Pe-Piper, G., Tubrett, M., Triantafyllidis, S. and Strathdee, G. (2012) Detrital Zircon geochronology and polycyclic sediment sources, Upper Jurassic – Lower Cretaceous of the Scotian Basin, southeastern Canada. Canadian Journal of Earth Sciences, v. 49, n. 12, p. 1540-1557.

Pollock, J.C., Hibbard, J.P., and van Staal, C.R. (2012) A paleogeographical review of the peri-Gondwanan realm of the Appalachian orogen. Canadian Journal of Earth Sciences, v. 49: p. 259-288.

Post, P. J. and Coleman, J.L. (2015) Mesozoic rift basins of the U.S. central Atlantic offshore: comparisons with onshore basins, analysis, and potential petroleum prospectivity, In: P.J. Post, J.L. Coleman, N.C. Rosen et al (Eds) Petroleum Systems in "Rift" Basins, 34th Annual GCSSEPM Foundation Perkins-Rosen Research Conference, p. 1-68.

Qayyum, F., Catuneanu, O. and Bouanga, C.E., (2015) Sequence stratigraphy of a mixed siliciclastic-carbonate setting, Scotian Shelf, Canada. Interpretation, v. 3 (May 2015), p.SN21-SN37.

Redfern, J., Shannon, P.M., William, B.P.J., Tyrrell, S., Leleu, S., Fabuel Perez, I., Baudon, C., Štolfová, K., Hodgetts, D., Van Lanen, X., Speksnijder, A., Haughton, P.D.W., and Daly, J.S. (2010) An integrated study of Permo-Triassic basins along the North Atlantic passive margin: implication for future exploration. In: B.A. Vining and S.C. Pickering (eds) Petroleum Geology: From Mature Basins to New Frontiers – Proceedings of the 7th Petroleum Geology Conference, London, March 2017, p. 921–936.

Ryan, R.J., and Giles, P.S. (2017) Preliminary Report on the Revised Paleontology of the Windsor Group and its Stratigraphic Implications. Geoscience and Mines Branch

Report of Activities 2016-17, Nova Scotia Department of Natural Resources, Report ME 2017-001, p. 79-84.

Sutra, E. Manatschal, G., Mohn, G., and Unternehr, P. (2013) Quantification and restoration of extensional deformation along the Western Iberia and Newfoundland rifted margins, AGU Geochemistry Geophysics Geosystems v. 14, p. 2575-2597.

Tari, G., Flinch, J.F., Soto, J.I. Chapter 6: Petroleum systems and play types associated with Permo-Triassic salt in Europe, North African, and the Atlantic region, In: J. Soto, J. Flinch, and G. Tari, (Eds), Permo-Triassic Salt Provinces of Europe, North Africa and Central Atlantic: Tectonics and Hydrocarbon Potential, Elsevier, p. 129-156.

Wade, J.A. and MacLean, B.C. (1990) The geology of the Southeastern Margin of Canada, Chapter 5, In: M.J. Keen and G.L. Williams (eds), Geology of the Continental Margin of Eastern Canada, Geological Survey of Canada, The Geology of Canada, p. 224-225.

Wade, J.A., Brown, D.E., Fensome, R.A. and Traverse, A. (1996) The Triassic-Jurassic Fundy Basin, Eastern Canada: regional setting, stratigraphy and hydrocarbon potential. Atlantic Geology, v. 32, n. 3, p. 189-231.

Waldron, J.W.F., Roselli, C.G., Utting, J., and Johnston, S.K., (2010) Kennetcook thrust system: Late Paleozoic transpression near the southern margin of the Maritimes Basin, Nova Scotia. Canadian Journal of Earth Sciences, vol. 47, p.137-159.

Waldron, J.W.F., Rygel, M.C., Gibling, M.R., and Calder, J.H. (2013) Evaporite tectonics and the late Paleozoic stratigraphic development of the Cumberland basin, Appalachians of Atlantic Canada. G

Waldron, J.W.F., Barr, S.M., Park, A.F., White, C.E., and Hibbard, J., (2015) Late Paleozoic strike-slip faults in Maritime Canada and their role in the reconfiguration of the northern Appalachian orogen. Tectonics, vol. 34, no. 8, p.1661-1684, eological Society of America Bulletin, v. 125, p. 945-960.

Welsink., H.J., Dwyer, J.D. and Knight, R.J. (1989) Tectono-stratigraphy of the passive margin off Nova Scotia, Chapter 14, In: A.J. Tankard and H.R. Balkwill (eds) Extensional Tectonics and Stratigraphy of the North Atlantic Margins, AAPG Memoir 46, p. 215-231.

Weston, J.F., MacRae, R.A., Ascoli, P., Cooper, M.K.E., Fensome, R.A., Shaw, D. and Williams, G.L. (2012) A revised biostratigraphic and well-log sequence stratigraphic framework for the Scotian Margin, offshore eastern Canada, Canadian Journal of Earth Sciences, v. 49, p. 1417-1462.

Wierzbicki, R., Harland, N, and Eliuk, L., (2002) Deep Panuke and Demascota core from the Jurassic Abenaki Formation, Nova Scotia: Facies Model, Deep Panuke, Abenaki Formation In: Diamond Jubilee Convention, Canadian Society of Petroleum Geologists Annual Convention, Calgary, Alberta, Conference CD-ROM disc: Abstracts of Technical Talks, Posters and Coder Displays, Paper No.12345678, 31 pages with figures.